UNIVERSIDAD DE CONCEPCIÓN
FACULTAD DE CIENCIAS FÍSICAS Y MATEMÁTICAS

"Signatures of weak gravitational fields in quantum systems"

Por: Francisco Andrés Jara Lobo

Tesis presentada a la Facultad de Ciencias Físicas y Matemáticas de la Universidad de Concepción para optar al grado académico de Magíster en Ciencias con Mención en Física

Julio 2025
Concepción, Chile

Profesor guía : Dr. Aldo Delgado

A mis abuelitos, a mi madre y a mi tía por supuesto

Agradecimientos

Recordar con una sonrisa es agradecer en silencio. Con este texto espero que dos años de sonrisas de camino a casa se manifiesten en el lector.

¿A qué hora me pasas a buscar?, es el mensaje que envió la Coni innumerables veces mientras yo dormía. Atrasado a la U, veo a Marco que me recibe con un: ¿Hola, cómo está Francisco?, ¿quiere un cafecito? Bueno Marco, muchas gracias, de verdad, muchas gracias. Hola Daniel, disculpe que lo venga a molestar.

Lunes y reunión de grupo, ¿quién presenta? Después, almuerzo con música de fondo que puso el profe Aldo. ¿Tendrá un minuto para conversar, profe, más ratito? Sí, claro. Muchas gracias por escuchar mis ideas y apoyarme, aunque sean raras.

Ya en la oficina, Jorgito y Katherine cantan. Daniel, espero esté bien.

La reunión con Juanito, María José, Mauricio, es decir, los pollitos, y Marco es en el MIRO. ¿Hola Calu, cómo está? Muchas gracias.

Por afuera de la Phys imagino a mis amigos Genio, Feñita, Dani, Borjita, Wilson y Stivi, pero no me miran. Las oficinas de los profes se abren al pasar y el tiempo se ralentiza al llegar donde el profe Rubi (GR). ¿Nos reunimos, profe? Muchas gracias.

Hola Don Juan Carlos, ¿y los quesos? A la oficina otra vez. Antes, algo dulce quizá.

Hace rato no llamo a mis abuelos, mi tía, a mi mamá y a mi tío. Ellos saben que estoy bien. ¿Qué estarán haciendo mis hermanitos? Otra buena pregunta surge: ¿qué estarán pensando mis perritos?

De camino a casa, dos hallullas. ¿Ya llegó el Leito a la casa?
Es tarde, un café.

Agradecer también a mis compañeros de la carrera: Alejandro S., Adheris C., Luis U.; a los integrantes del grupo MIRO Concepción, a Agustín y Paulina. A mis amigos Jonathan, Edson, Dilan, Pablito, Sebita, Osito y Joaquín, muchas gracias. Al profe Omar J. por su buena disposición. Finalmente, agradecer al Instituto Milenio de Investigación en Óptica (MIRO) por su apoyo financiero.

Resumen

Esta tesis explora dos enfoques distintos dentro del contexto de los efectos de la gravedad en sistemas cuánticos en una aproximación semiclásica. La primera investigación se centra en la posibilidad de distinguir entre diferentes teorías métricas dentro del formalismo post-Newtoniano, empleando diversas estrategias de discriminación de estados cuánticos no ortogonales. Se analiza la evolución temporal de un reloj cuántico masivo, demostrando cómo las diferencias en los parámetros post-Newtonianos inducen estados cuánticos distinguibles. Se proponen esquemas basados en mediciones de von Neumann, discriminación con error mínimo y discriminación no ambigua, derivando las longitudes de propagación óptimas para maximizar la probabilidad de éxito en la identificación de la teoría métrica correcta. La segunda investigación explora cómo la rotación de fase de Wigner, inducida por un campo gravitacional en la polarización de un fotón, puede utilizarse como una herramienta para la metrología cuántica en el límite de campo débil y rotación lenta de la métrica de Kerr. Se analiza un interferómetro geodésico tipo Mach-Zehnder, considerando la dilatación temporal relativa y la rotación de la polarización del fotón como recursos para la estimación del parámetro de rotación. Los resultados teóricos sugieren el potencial de los sistemas cuánticos para sondear aspectos fundamentales de la gravedad y realizar mediciones de alta precisión de parámetros de algún espaciotiempo en partícular.

Keywords – Quantum discrimination theory, Weak gravitational fields, PPN Formalism, Kerr metric, Quantum clocks, Interferometry .

Abstract

This thesis explores two distinct approaches within the context of the effects of gravity on quantum systems in a semiclassical approximation. The first investigation focuses on the possibility of distinguishing between different metric theories within the post-Newtonian formalism, employing various strategies for discriminating non-orthogonal quantum states. The temporal evolution of a massive quantum clock is analyzed, demonstrating how differences in post-Newtonian parameters induce distinguishable quantum states. Schemes based on von Neumann measurements, minimum-error discrimination, and unambiguous state discrimination are proposed, deriving the optimal propagation lengths to maximize the success probability in identifying the correct metric theory. The second investigation explores how the Wigner phase rotation, induced by a gravitational field on photon polarization, can be used as a tool for quantum sensing in the weak field and slow rotation limit of the Kerr metric. A geodesic Mach-Zehnder type interferometer is analyzed, considering relative time dilation and photon polarization rotation as resources for estimating the rotation parameter. The theoretical results suggest the potential of quantum systems to probe fundamental aspects of gravity and perform high-precision measurements of parameters of some particular spacetime.

Keywords – Quantum discrimination theory, Weak gravitational fields, PPN Foralism, Kerr metric, Quantum clocks, Interferometry.

Contents

List of Tables

List of Figures

Chapter 1

Introduction

Relativistic Quantum Information (RQI) is an emerging field of investigation that applies the framework of quantum information theory to the study of relativistic effects on quantum systems. Its scope encompasses phenomena ranging from high-energy settings, such as those involving black holes, to low-energy regimes, including weak gravitational fields. A key line of inquiry investigates how entanglement is modified by non-inertial motion, a topic intrinsically linked to the Unruh effect [1]. In the low-energy domain, research has also explored how quantum interference is affected by proper time differences for massive particles that possess internal degrees of freedom [2]. The main aim of this research is to establish a basis for the experimental observation of purely gravitational effects on quantum systems.

An early foundational experimental demonstration of weak gravitational effects on a quantum system was the Colella–Overhauser–Werner (COW) experiment [3]. In 1975, this experiment measured a phase shift induced by the Newtonian gravitational potential with high precision using a neutron interferometer.

A key theoretical breakthrough was the work of Fuentes-Schuller and Mann, who demonstrated that entanglement is an observer-dependent quantity [4]. They showed that a state which is maximally entangled in an inertial frame becomes less entangled if the observers are in relative accelerated motion. This phenomenon is a consequence of the Unruh effect, where an accelerated observer perceives a thermal state due to the loss of information from a causally disconnected region. Futhermore, Peres and Terno [5] demonstrated that relativistic considerations impact fundamental concepts in quantum information, such as entanglement, entropy, and the definition of the reduced density matrix.

The above findings underscore the necessity of studying quantum systems under gravitational influence, as they may reveal significant conceptual and operational departures from the standard non-relativistic theory.

Building upon this context, in this thesis, we address two distinct problems within the regime of weak gravitational fields. First, we assess the distinguishability of alternative metric theories of gravity through the application of quantum state discrimination techniques. Second, we analyze the utility of gravity-induced Wigner phase rotations as a resource in quantum parameter estimation, focusing on the weak-field limit of the Kerr metric. In particular, we aim to measure the rotation parameter.

In the fist topic we study the possibility of distinguishing between metric theories within the PPN formalism using various strategies for discriminating non-orthogonal quantum states. We consider the temporal evolution of a massive quantum clock, that is, a massive particle endowed with a two-dimensional inner degree of freedom. The final quantum state of the clock is a function of the post-Newtonian parameters that characterize a metric theory. The quantum clock states of various metric theories are mutually non-orthogonal and, consequently, cannot be discriminated deterministically and with certainty at the same time. Thereby, quantum state discrimination strategies are required. We first show a simple scheme, based on a von Neumann measurement, that allows for ruling out the hypothesis that a particular metric theory describes spacetime. In the case of two competing metric theories, we use minimum-error discrimination. This makes it possible to determine which of the metric theories is verified, although with a minimal probability of error. This result can be improved using unambiguous state discrimination, which allows to distinguish between two metric theories without misidentification error, albeit resorting to a generalized quantum measurement and with a smaller success probability than using minimum-error discrimination. To obtain a high probability of success detection, our theoretical results shown the necessity of larger distance and quantum clock systems with the highest energy difference and the largest natural lifetime.

The second topic study how the Wigner phase rotation, induced by a gravitational field on photon polarization, can be employed as a tool for quantum sensing. Specifically, through solutions to the geodesic equation in the coordinate $\theta = \text{const.}$, we use this configuration with the aim of studying only the effect produced by the rotation parameter a of the Kerr metric in the Wigner

rotation, since this rotation is known to be zero in the non-rotating Schwarzschild spacetime [6]. We focus on the weak-field and slow-rotation limit of the Kerr metric. Within this framework, we analyze how time dilation and polarization rotation of a photon in a geodesic Mach-Zehnder type interferometer can be used in the estimation of a. The phase difference given by the rotation polarization effect on the detection probability is small. In future work, we will explore how to enhance this effect using quantum metrology techniques.

1.1 Thesis organization

Chapter 2 presents the fundamental concepts required to follow the developments of this thesis. It begins with the postulates of Quantum Mechanics and basic notions of Differential Geometry and General Relativity. The remainder of the chapter introduces the models used, both of which are based on a Wentzel–Kramers–Brillouin (WKB) approximation [7] for the quantum wave fuction and gravitational field interaction.

Chapter 3 explores the possibility of using quantum information tools, specifically, the quantum theory of discrimination of non-orthogonal states to test the validity of modified theories of gravity, analyzed within the framework of the parametrized post-Newtonian (PPN) formalism. To this end, we consider particles with internal degrees of freedom propagating through a curved spacetime.

In Chapter 4, the Wigner phase acquired by a photon undergoing geodesic motion in the Kerr spacetime is studied. Additionally, a geodesic Mach–Zehnder-type interferometer is proposed, and the detection probability for this setup is calculated, including the polarization degree of freedom. Thereby allowing for the estimation of the rotation parameter a.

Chapter 2

Mathematical framework

2.1 Postulates of Quantum Mechanics

In the following five sections, the postulates of Quantum Mechanics are presented, highlighting the connection between the quantum world and the mathematical framework that models it [8].

First postulate

The first postulate refers to the mathematical space in which quantum systems are described and where predictions to be observed in experimental realizations can be made: An isolated physical system is associated with a complex vector space equipped with an inner product, and called a Hilbert space $\mathcal{H}$. The system is completely described by a state vector, which is a unit vector in the Hilbert space of the system.

This postulate implies that the superposition of two states is a state of the system. If $|\psi_1\rangle$ and $|\psi_2\rangle$ are possible states of the system, then the superposition $|\psi\rangle = a_1|\psi_1\rangle + a_2|\psi_2\rangle$, where a_1 and a_2 are complex numbers, is also a state of the system if $|a_1|^2 + |a_2|^2 = 1$. Furthermore, the inner product associates a complex number to two arbitrary states.

A state vector $|\psi\rangle$ can be expressed in a discrete basis as:

$$|\psi\rangle = \sum_k a_k|k\rangle \tag{2.1.1}$$

also in a continuous basis

$$|\psi\rangle = \int dx\, \psi(x)|x\rangle,$$

where $\psi(x)$ is the wave fuction and $|x\rangle$ are the basis vectors. We can also be considered as a class of equivalence, because, $|\psi\rangle$ and $e^{i\phi}|\psi\rangle$ represent the same physical state.

Second postulate

A closed system evolves under the action of a unitary transformation. Thus, the state of a system at time t_i is related to the state of the system at time t_f through a unitary operator U, which is a function of the times t_i and t_f. In this way, the relationship between the states is given by

$$|\psi(t_f)\rangle = U(t_f, t_i)|\psi(t_i)\rangle.$$

Furthermore, the time evolution of a quantum state preserves its normalization. Quantum states obey a differential equation of the form

$$i\hbar\frac{d}{dt}|\psi(t)\rangle = H(t)|\psi(t)\rangle,$$

which is the Schrödinger equation, with H being the Hamiltonian operator. If the hamiltonian is not time depend $H(t) = H$ then the evolution operator is given by

$$U(t) = e^{-\frac{i}{\hbar}Ht}. \tag{2.1.2}$$

Third postulate: Quantum Measurement

A quantum measurement is described by a collection of measurement operators M_j, which act on the Hilbert space of the measured system. The index j refers to the number of possible outcomes in an experiment. If the quantum state of the system immediately before measurement is $|\psi\rangle$, then the probability of obtaining the outcome j is

$$p(j) = \langle\psi|M_j^\dagger M_j|\psi\rangle,$$

and the post-measurement state takes the form

$$|\psi_j\rangle = \frac{M_j|\psi\rangle}{\sqrt{\langle\psi|M_j^\dagger M_j|\psi\rangle}}.$$

The measurement operators satisfy the completeness relation

$$\sum_j M_j^\dagger M_j = I,$$

where I is the identity operator and this relation expresses the fact that probabilities must sum to one

$$\sum_j p(j) = \sum_j \langle\psi|M_j^\dagger M_j|\psi\rangle = \langle\psi| \left(\sum_j M_j^\dagger M_j\right) |\psi\rangle = 1.$$

From this postulate, we can infer another type of measurement operators, which are known as projective measurements. A projective measurement is described by an observable O, which is a Hermitian operator in the Hilbert space of the observed system. The observable has a spectral decomposition

$$O = \sum_j \lambda_j P_j,$$

where P_j is the projector in the eigenspace of O with eigenvalue λ_j, satisfies the properties of idempotency and is a rank-1 operator, since upon diagonalization it has only one non-zero eigenvalue.

$$P_k^2 = P_k\,, \tag{2.1.3}$$

$$P_i P_j = P_i \delta_{ij} \tag{2.1.4}$$

and

$$\sum_j M_j^\dagger M_j = \sum_j P_j = I. \tag{2.1.5}$$

The possible outcomes of the measurements correspond to the eigenvalues λ_j of the observable. The post-measurement state is given by

$$|\psi_j\rangle = \frac{P_j|\psi\rangle}{\sqrt{p(j)}},$$

with $p(j) = \langle\psi|P_j|\psi\rangle$, the probability of obtaining a result j when applying the projector P_j.

Fourth postulate: Composite Systems

In the previous sections, we have studied only systems consisting of a single system. In the case of multiple systems, we talk about composite systems. These are defined as:

The state space of a composite physical system is the tensor product of the state spaces of the physical components of the system. If the subsystems are numbered from 1 to m, then the state space is given by

$$\mathcal{H} = \mathcal{H}_1 \otimes \mathcal{H}_2 \otimes \cdots \otimes \mathcal{H}_m.$$

If the k-th subsystem is prepared in the states $|\psi_k\rangle$ for $k = 1, 2, \ldots, m$, then the state of the system is described by

$$|\Psi\rangle = |\psi_1\rangle \otimes |\psi_2\rangle \otimes \cdots \otimes |\psi_m\rangle. \tag{2.1.6}$$

Note that not all composite systems have a state of the form given by equation (2.1.6) . These are known as separable states. If they do not have this form, they are called entangled states. For example, consider a physical system described by the states $|u\rangle$ and $|v\rangle$. A separable composite system has the form

$$|\Psi\rangle = |u\rangle \otimes |v\rangle,$$

whereas an entangled state is described by

$$|\Psi\rangle = \frac{1}{\sqrt{2}} \left(|u\rangle \otimes |v\rangle + |v\rangle \otimes |u\rangle\right).$$

Matrix Density formalism

The density matrix formalism plays a central role in the modern understanding of quantum mechanics, particularly when dealing with statistical ensembles, mixed states, or systems entangled with inaccessible environments. While the state of a quantum system is traditionally described by a state $|\psi\rangle$, this description assumes complete knowledge of the system and is thus limited to *pure states*. However,

many physical situations involve incomplete information, requiring a more general framework.

Pure and Mixed States

A *pure state* is described by a normalized vector $|\psi\rangle$ in a Hilbert space $\mathcal{H}$, with its physical observables obtained from the expectation value

$$\langle A\rangle = \langle\psi|A|\psi\rangle,$$

for any Hermitian operator A. In contrast, a *mixed state* arises when the system is in a statistical ensemble of pure states $\{|\psi_i\rangle\}$ with associated probabilities $\{p_i\}$, such that $\sum_i p_i = 1$. The corresponding description is then given by the *density operator*

$$\rho = \sum_i p_i |\psi_i\rangle\langle\psi_i|.$$

Properties of the Density Matrix

The density matrix ρ is a positive semi-definite, Hermitian operator with unit trace:

- $\rho^\dagger = \rho$,
- $\mathrm{Tr}[\rho] = 1$,
- $\langle\phi|\rho|\phi\rangle \geq 0$ for all $|\phi\rangle \in \mathcal{H}$.

A state is *pure* if and only if $\rho^2 = \rho$, in which case $\mathrm{Tr}[\rho^2] = 1$. For mixed states, $\mathrm{Tr}[\rho^2] < 1$, and this quantity serves as a measure of the state purity [9].

2.2 Quantum state discrimination theory

According to quantum theory, non-orthogonal quantum states cannot be deterministically distinguished without error. The field of quantum state discrimination focuses on designing quantum measurements to determine the state in which a quantum system was prepared, given a set $\{\rho_j\}$ of possible states, each occurring with a priori probability η_j. However, any quantum strategy inevitably involves a nonzero probability of either erroneous or inconclusive results

[10, 11, 12]. In this scenario, we consider two discrimination strategies: minimum-error discrimination and optimal unambiguous discrimination.

2.2.1 Minimun error quantum state discrimination

The purpose of Minimum error (ME) discrimination is to minimize the average probability of misidentifying the state of a quantum system [13]. This strategy involves finding the optimal Positive Operator-Valued Measure (POVM) $\{\Pi_i\}$ that minimizes the average probability of misidentifying the state [14]. If the measurement returns the result i, then we assume that the state prior to the measurement was ρ_i. The probability of this event is given by Born's rule $P(i|\rho_i) = Tr(\rho_i\Pi_i)$. The average probability of error is $P_e(\{\Pi_i\}) = 1 - \sum_i \eta_i Tr(\rho_i\Pi_i)$. This is optimized on the set of POVMs to obtain the minimal average probability of error, that is,

$$P_H = \min_{\{\Pi_i\}} P_e(\{\Pi_i\}). \tag{2.2.1}$$

The measurement that reaches minimum is known as the Helstrom measurement [15], and the corresponding minimum average error probability is called the Helstrom bound [13]. The necessary and sufficient conditions for achieving the Helstrom bound [16, 17] are

$$\Pi_k(\eta_k\rho_k - \eta_j\rho_j)\Pi_j = 0, \quad \forall j,k, \tag{2.2.2}$$

and

$$\sum_k \eta_k\Pi_k\rho_k - \eta_j\rho_j \geq 0, \quad \forall j. \tag{2.2.3}$$

In the case of discriminating between two states, ρ_1 and ρ_2, with prior probabilities η_1 and η_2, respectively, the Helstrom bound has the simple analytical expression [13]

$$P_H = \frac{1}{2}\left(1 - \mathrm{Tr}\left(|\eta_1\rho_1 - \eta_2\rho_2|\right)\right). \tag{2.2.4}$$

For two pure states $\rho_0 = |\psi_0\rangle\langle\psi_0|$ and $\rho_1 = |\psi_1\rangle\langle\psi_1|$ the previous expression can be further simplified to

$$P_H = \frac{1}{2}\left(1 - \sqrt{1 - 4\eta_0\eta_1|\langle\psi_0|\psi_1\rangle|^2}\right). \tag{2.2.5}$$

In this case, the Helstrom measurement becomes a von Neumann, or projective, measurement.

ME discrimination has been experimentally demonstrated using two-dimensional quantum systems [18, 19, 20] and higher-dimensional quantum systems [21].

2.2.2 Unambiguous discrimination

An important feature of ME discrimination is that it minimizes the probability of a wrong identification. However, this is different from zero. Unambiguos discrimination (UD) arises as an attempt to perfectly distinguish quantum states. In general, this requires a POVM $\{\Pi_i\}$ $(i = 0, 1, \ldots, n)$ with a number of outcomes equal to $n + 1$, where n is the total number of states to be discriminated. The additional measurement outcome $i = 0$ does not convey any information about the state to be identified, that is, it is not conclusive. The remaining measurement results $i = 1, \ldots, n$ allow for a perfect identification of each state, that is, they are unambiguous.

In the case of discriminating two non-orthogonal pure states $|\psi_0\rangle$ and $|\psi_1\rangle$ with a priori probabilities η_0 and η_1, respectively, the optimal average success probability P_{UD}, which considers the conclusive events only, depends on the relationship between the a priori probabilities and the inner product $s = |\langle\psi_0|\psi_1\rangle|$ [22]. If $\eta_1 < s^2/(1 + s^2)$, then $P_{UD} = 1 - \eta_1 - \eta_2 s^2$. If $\eta_1 > 1/(1 + s^2)$, then $P_{UD} = 1 - \eta_2 - \eta_1 s^2$. If $s^2/(1 + s^2) \leq \eta_1 \leq 1/(1 + s^2)$, then $P_{UD} = 1 - 2\sqrt{\eta_1\eta_2}s$. The particular case $\eta_1 = \eta_2 = 1/2$ is known as the Ivanovic-Dieks-Peres limit [23, 24, 25], where

$$P_{UD} = 1 - s. \tag{2.2.6}$$

2.3 Differential geometry

The tangent space is a vector space geometrically defined by all tangent vectors to possible curves at a point P on the manifold M [1]. It is denoted by $T_n(P)$, where n represents the number of linearly independent components determined

[1] A differentiable manifold M is a topological space that locally resembles $\mathbb{R}^n$ and is equipped with a differentiable structure, defined by an atlas of charts whose transition maps are differentiable. For a detailed reference, see [26].

by the dimension of the manifold. Given a general coordinate transformation:

$$x^i \to \widetilde{x}^i = \widetilde{x}^i(x). \tag{2.3.1}$$

The components of the tangent vectors, known as contravariant vectors, transform according to the following rule [2]

$$\widetilde{A}^i(\widetilde{x}) = \frac{\partial \widetilde{x}^i}{\partial x^j}(x) A^j(x), \tag{2.3.2}$$

where $\partial\widetilde{x}^i/\partial x^j$ is the Jacobian matrix transformation. The cotangent space is the dual space of the tangent space and is denoted by $T_n^*(P)$. The vectors that constitute this space are referred to as covariant vectors, and under a general coordinate transformation (2.3.1), their components transform as follows

$$\widetilde{A}_i(\widetilde{x}) = \frac{\partial x^j}{\partial \widetilde{x}^i}(x) A_j(x), \tag{2.3.3}$$

where $\partial x^j/\partial\widetilde{x}^i$ is the inverse Jacobian matrix of the transformation. A tensor is defined as the result of taking tensor products between the spaces $T_n^*(P)$ y $T_n(P)$. A quantity A is said to be a tensor of rank (m, n) if

$$A \in \underbrace{\mathrm{T}_p^*(M) \otimes ..... \otimes T_p^*(M)}_{n \text{ times}} \otimes \overbrace{\mathrm{T}_p(M) \otimes ..... \otimes T_p(M)}^{m \text{ times}} \tag{2.3.4}$$

and it inherits the following transformation rule

$$\widetilde{A}^{j_1....j_n}{}_{i_1....i_m}(\widetilde{x}) = \frac{\partial x^{k_1}}{\partial \widetilde{x}^{i_1}} ... \frac{\partial x^{k_m}}{\partial \widetilde{x}^{i_m}} \frac{\partial \widetilde{x}^{j_1}}{\partial x^{l_1}} ... \frac{\partial \widetilde{x}^{j_m}}{\partial x^{l_m}} A^{l_1....l_m}{}_{k_1....k_n}(x). \tag{2.3.5}$$

2.3.1 Metric tensor

The metric tensor g_{ij} is a symmetric covariant tensor of rank $(0, 2)$, which allows the concept of distance to be introduced on a manifold M.
The line element is defined as

$$dl^2 = g_{ij}(P) dx^i dx^j. \tag{2.3.6}$$

[2] Throughout this thesis, we adopt Einstein's summation convention: repeated indices, one covariant (subscript) and one contravariant (superscript), are implicitly summed over the appropriate range.

The inverse metric is defined such that

$$g_{ij}(P)g^{jk}(P) = \delta_i^k. \tag{2.3.7}$$

Let $\mathcal{C}$ be a curve defined between points P and Q on a manifold $\mathcal{M}$, parametrized by $x^i = x^i(\lambda)$, where $\lambda \in [\lambda_P, \lambda_Q]$ is a continuous real parameter. The tangent vector to the curve $\mathcal{C}$ is given by $dx^i/d\lambda$. We define the length of a curve as the scalar

$$L = \int_P^Q dl = \int_{\lambda_0}^{\lambda_1} \sqrt{g_{ij}\frac{dx^i}{d\lambda}\frac{dx^j}{d\lambda}}d\lambda. \tag{2.3.8}$$

2.3.2 Tensor density

The need to define a tensor density arises naturally when we try to integrate a scalar A over a region Ω.

$$I = \int_\Omega A d^n x. \tag{2.3.9}$$

In (2.3.9), the integral I is not a scalar because, under a general coordinate transformation, $d^n x$ transforms according to the Riemann theorem for multiple integrals.

$$d^n\widetilde{x} = \left|\frac{\partial\widetilde{x}^i}{\partial x^j}\right| d^n x, \tag{2.3.10}$$

where $|\partial\widetilde{x}^i/\partial x^j|$ is the Jacobian determinant of the coordinate transformation. We note that, for I to be a scalar under general coordinate transformations, $Ad^n x$ must be a scalar. For that, the transformation rule of A must be[3]:

$$\widetilde{\mathcal{A}} = \left|\frac{\partial x^i}{\partial\widetilde{x}^j}\right| \mathcal{A}. \tag{2.3.11}$$

Therefore, the integral argument is a scalar under general coordinate transformations:

$$\mathcal{A}d^n x = \left|\frac{\partial\widetilde{x}^i}{\partial x^j}\right| \widetilde{\mathcal{A}} \left|\frac{\partial x^i}{\partial\widetilde{x}^j}\right| d^n\widetilde{x} = \widetilde{\mathcal{A}}\, d^n\widetilde{x}. \tag{2.3.12}$$

We define a scalar density $\mathcal{A}$ of weight p, where p is the power of the Jacobian determinant, as

$$\widetilde{\mathcal{A}} = \left|\frac{\partial x^i}{\partial\widetilde{x}^j}\right|^p \mathcal{A}. \tag{2.3.13}$$

[3]Henceforth, tensor densities will be denoted using italic letters.

According to (2.3.10), $d^n x$ is a scalar density of weight $p = -1$
Analogously, a tensor density of weight p and type (m, n), is defined as an object that transforms according to the following rule:

$$\widetilde{\mathcal{A}}^{j_1\ldots j_n}_{i_1\ldots i_m}(\widetilde{x}) = \left|\frac{\partial x^i}{\partial \widetilde{x}^j}\right| \frac{\partial x^{k_1}}{\partial \widetilde{x}^{i_1}} \ldots \frac{\partial x^{k_m}}{\partial \widetilde{x}^{i_m}} \frac{\partial \widetilde{x}^{j_1}}{\partial x^{l_1}} \ldots \frac{\partial \widetilde{x}^{j_m}}{\partial x^{l_m}} \mathcal{A}^{l_1\ldots l_m}_{k_1\ldots k_n}(x). \tag{2.3.14}$$

We know that the metric tensor transform as (2.3.5), and therefore the determinant of metric $\det(g_{ij}) = g$, is a scalar density of weight $p = 2$, since

$$\widetilde{g}(P) = \left|\frac{\partial x^k}{\partial \widetilde{x}^i}\right|^2 g(P). \tag{2.3.15}$$

Using $\sqrt{|g|}$, which a scalar density of weight $p = 1$, it is possible to define a scalar of the form

$$I = \int_\Omega \sqrt{|g|}\, d^n x. \tag{2.3.16}$$

An example of this is the Einstein-Hilbert action

$$S_{\text{E}-\text{H}} = \int R\sqrt{|g|}\, d^4 x, \tag{2.3.17}$$

where R is the Ricci scalar.
Another important application of tensor densities arises when attempting to properly define conservation laws. For instance, consider the conservation of the four-current J^μ [4]. It can be show a that the four-divergence of the four-current $\partial_\mu J^\mu$ is not a scalar

$$\begin{aligned} \widetilde{\partial}_\mu \widetilde{J}^\mu &= \frac{\partial x^\rho}{\partial \widetilde{x}^\mu} \partial_\rho \left(\frac{\partial \widetilde{x}^\mu}{\partial x^\nu} J^\nu \right) \\ &= \frac{\partial x^\rho}{\partial \widetilde{x}^\mu} \frac{\partial \widetilde{x}^\mu}{\partial x^\nu} \partial_\rho J^\nu + \frac{\partial x^\rho}{\partial \widetilde{x}^\mu} J^j \frac{\partial^2 \widetilde{x}^\nu}{\partial x^\rho \partial x^\nu}. \end{aligned} \tag{2.3.18}$$

Now, if we consider a tensor density of type $(1, 0)$ and weight $p = 1$ for the four-current as follows

$$\widetilde{\mathcal{J}}^\mu = \left|\frac{\partial x^\tau}{\partial \widetilde{x}^\lambda}\right| \frac{\partial \widetilde{x}^\mu}{\partial x^\nu} \mathcal{J}^\nu. \tag{2.3.19}$$

[4] Greek indices (e.g., μ, ν) run over spacetime coordinates (0, 1, 2, 3), and Latin indices (e.g., i, j) are used for spatial components (1, 2, 3).

It can be shown that $\partial_\mu \mathcal{J}^\mu$ is a scalar density of weight $p = 1$, that is

$$\begin{aligned}\widetilde{\partial}_\mu \widetilde{\mathcal{J}}^\mu &= \widetilde{\partial}_\mu \left(\left| \frac{\partial x^\tau}{\partial \widetilde{x}^\lambda} \right| \frac{\partial \widetilde{x}^\mu}{\partial x^\nu} \mathcal{J}^\nu \right) \\ &= \frac{\partial x^\sigma}{\partial \widetilde{x}^\mu} \partial_\sigma \left(\left| \frac{\partial x^\tau}{\partial \widetilde{x}^\lambda} \right| \frac{\partial \widetilde{x}^\mu}{\partial x^\nu} \mathcal{J}^\nu \right) \\ &= \left| \frac{\partial x^\tau}{\partial \widetilde{x}^\lambda} \right| \partial_\nu \mathcal{J}^\nu + \left| \frac{\partial x^\tau}{\partial \widetilde{x}^\lambda} \right| \mathcal{J}^\nu \frac{\partial x^\sigma}{\partial \widetilde{x}^\mu} \partial_\sigma \frac{\partial \widetilde{x}^\mu}{\partial x^\nu} + \mathcal{J}^\nu \partial_\nu \left| \frac{\partial x^\tau}{\partial \widetilde{x}^\lambda} \right|.\end{aligned} \tag{2.3.20}$$

The derivative of the Jacobian determinant is given by [27]

$$\partial_\nu \left| \frac{\partial x^\tau}{\partial \widetilde{x}^\lambda} \right| = - \left| \frac{\partial x^\tau}{\partial \widetilde{x}^\lambda} \right| \frac{\partial x^\sigma}{\partial \widetilde{x}^\mu} \partial_\nu \frac{\partial \widetilde{x}^\mu}{\partial x^\sigma}, \tag{2.3.21}$$

obtaining the following rule of transformation

$$\widetilde{\partial}_\mu \widetilde{\mathcal{J}}^\mu = \left| \frac{\partial x^\tau}{\partial \widetilde{x}^\lambda} \right| \partial_\nu \mathcal{J}^\nu, \tag{2.3.22}$$

showing that it is a scalar density under general coordinate transformation.

In Special Relativity theory the transformation of coordinates are lineal, so the conservation laws $\partial_\mu J^\mu = 0$ are satisfied under coordinate transformations as can be seen in the equation (2.3.18). But under a general coordinate transformation the conservation laws must be defined using scalar densities:

$$\partial_\mu \mathcal{J}^\mu = 0. \tag{2.3.23}$$

By integrating expression (2.3.23) over a region Σ large enough so that the current through its boundary surface is negligible, we obtain:

$$\begin{aligned}\int_\Sigma \partial_0 \mathcal{J}^0 d^3x + \int_{\partial\Sigma} \mathcal{J}^i d^2 S_i = 0. \\ \partial_0 \int_\Sigma \mathcal{J}^0 d^3x = 0.\end{aligned} \tag{2.3.24}$$

This tells us that the total quantity $\mathcal{J}^0$ in the region Σ is conserved over time.

Let J^μ a tensor of rank $(1, 0)$, it is then possible to define a tensor density as

$$\mathcal{J}^\mu = J^\mu \sqrt{|g|}. \tag{2.3.25}$$

The conservation identity involving covariant derivatives, also known as the covariant form of the continuity equation [27], is given by

$$\partial_\mu \mathcal{J}^\mu = \sqrt{|g|}\, \nabla_\mu J^\mu. \tag{2.3.26}$$

Where ∇_μ is the covariant derivative [5].

2.3.3 Tetrad formalism

This formalism allows us to define at each point of the manifold M, a local coordinate system with orthonormal basis $\{e^\mu_I\}$ where I denotes the index labeling the I-th element of the tetrad basis, and μ denotes the μ-th coordinate component of that basis element.
The metric tensor can be written as

$$g_{\mu\nu} = e^I_\mu e^J_\nu \eta_{IJ}, \tag{2.3.27}$$

where e^I_μ are four covariant vectors (rank $(0,1)$). These satisfy

$$e^I_\mu e^\nu_I = \delta^\nu_\mu \quad \text{and} \quad e^I_\mu e^\mu_J = \delta^I_J\,, \tag{2.3.28}$$

then

$$e^\mu_I e^\nu_J g_{\mu\nu} = \eta_{IJ}. \tag{2.3.29}$$

Let A^μ be a tensor of rank $(1,0)$, which corresponds to a vector. We can define

$$A^I = A^\mu e^I_\mu. \tag{2.3.30}$$

Where A^I are the components of vector in the tetrad basis. Similarly, let B_μ be the components of a covariant tensor, then we can use the inverse tetrad basis and writte:

$$B_\mu = B_I e^I_\mu\,. \tag{2.3.31}$$

[5] The covariant derivative is a generalization of the directional derivative that is compatible with the manifold's connection and metric structure. It ensures that derivatives of tensor fields are tensorial, preserving geometric relationships under parallel transport. For a rigorous treatment, see [28].

Using (2.3.28) we obtain the components of A^μ in the tetrad basis:

$$A^I = g_{\mu\sigma} A^\mu e^\sigma_J \eta^{IJ}. \tag{2.3.32}$$

The scalar product can be written as

$$A_\mu B^\mu = A_I e^I_\mu B^J e^\mu_J = A_I B^J \delta^I_J = g_{\mu\nu} A^\mu B^\nu = \eta_{IJ} A^I B^J. \tag{2.3.33}$$

This shows how the information of the spacetime is encoded in the tetrad basis. The index used for the tetrad components are upcase latin letters, and when they are evaluated we denote the corresponding index with a hat i.e, the components of a vector in some tetrad basis are given by

$$A^I = (A^{\hat{0}}, A^{\hat{1}}, A^{\hat{2}}, A^{\hat{3}}). \tag{2.3.34}$$

2.4 Brief review of General Relativity theory

General Relativity describes gravity as the curvature of spacetime caused by mass and energy. Its dynamics is governed by Einstein's field equations, whose solutions describe the geometry of spacetime under different physical conditions [29]. In this section, we present the essential concepts of General Relativity (GR) required for the development of this thesis, starting from Einstein field equations and two of its analytical solutions.

2.4.1 Einstein field equations

The theory of General Relativity is a geometric theory of gravity that arises from incorporating the principles of relativity, i.e., strong equivalence principle and the requirement that the laws of physics be covariant[6]. This implies that the laws of General Relativity must take a tensorial form.

Einstein's equations, that is, the field equations for the metric of spacetime

[6]Here, the term covariant refers to covariance in the sense of form invariance—that is, the equations retain their form under general coordinate transformations. This ensures that the physical laws expressed by such equations are independent of the particular coordinate system used.

were introduced (without cosmological constant) in 1915 [30], and are given by

$$R_{\mu\nu} - \frac{1}{2} g_{\mu\nu} R = \frac{8\pi G}{c^4} T_{\mu\nu}. \tag{2.4.1}$$

Here, the components of the Ricci tensor $R_{\mu\nu}$ are directly related to the local energy-momentum tensor $T_{\mu\nu}$ via Einstein's field equations [31]. Einstein's general theory of relativity establishes that the curvature of spacetime is determined by the distribution of matter and energy. These equations constitute a system of nonlinear differential equations for the metric. However, in certain cases, it is possible to obtain exact analytical solutions. The following sections present two such static solutions.

2.4.2 Exterior Schwarzschild metric

The first exact solution of Einstein's field equations was found by Schwarzschild in February 1916 [32]. This solution describes the gravitational field outside a spherically symmetric mass at rest and is given in quasi-spherical coordinates (ct, r, θ, φ) in mostly minus signature by

$$ds^2 = \left(1 - \frac{2m}{r}\right) c^2 dt^2 - \left(1 - \frac{2m}{r}\right)^{-1} dr^2 - r^2 \left[d\theta^2 + \sin^2\theta d\varphi^2\right], \tag{2.4.2}$$

where $m = GM/c^2$ is the mass parameter, with units of length ($[m] = L$).

The Schwarzschild solution has the following properties:

- It is spherically symmetric.
- It is static, i.e., the metric components do not depend on time.
- It is asymptotically flat, i.e; in the limit when $r \gg m$ the metric becomes the flat metric $\eta_{\mu\nu} = \text{diag}(1, -1, -1, -1)$.

2.4.2.1 Schwarzschild solution in isotropic coordinates

The equations in General Relativity are invariant under general coordinate transformations, and we have an infinite number of possible coordinate systems. A useful one is isotropic coordinates. This coordinate system allows, in the spatial

section ($t =$ constant.), the line element ds^2 to be proportional to the usual line element $dl^2 = dx^2 + dy^2 + dz^2$, i.e;

$$ds^2 = A(\rho)(cdt)^2 - B(\rho)dl^2. \tag{2.4.3}$$

For the exterior Schwarzschild solution it is possible to find a simple transformation of the radial coordinates $\rho = \rho(r)$, namely

$$r = \rho\left(1 + \frac{m}{2\rho}\right)^2, \qquad \rho > \frac{m}{2}. \tag{2.4.4}$$

Then, the line element of the exterior Schwarzschild solution in isotropic coordinates is given by

$$ds^2 = \frac{\left(1 - \frac{m}{2\rho}\right)^2}{\left(1 + \frac{m}{2\rho}\right)^2}(cdt)^2 - \left(1 + \frac{m}{2\rho}\right)^4 \left[d\rho^2 + \rho^2\left(d\theta^2 + \sin^2\theta d\varphi^2\right)\right]. \tag{2.4.5}$$

2.4.3 The Kerr metric

The Kerr solution describes the spacetime around a rotating Black Hole with mass M and angular momentum J. In the Boyer-Lindquist coordinates (ct, r, θ, φ) it is given by the following line element:

$$\begin{aligned} ds^2 =& \frac{\Delta}{\rho^2}\left(cdt - a\sin^2\theta d\varphi\right)^2 - \frac{\sin^2\theta}{\rho}\left[\left(r^2 + a^2\right)d\varphi - acdt\right]^2 \\ & - \frac{\rho^2}{\Delta}dr^2 - \rho^2 d\theta^2, \end{aligned} \tag{2.4.6}$$

where

$$a := \frac{J}{Mc}, \qquad \rho^2 := r^2 + a^2\cos^2\theta, \qquad \Delta := r^2 - 2mr + a^2. \tag{2.4.7}$$

The parameter a is called the *Kerr parameter* or *rotation parameter* and it has unit of length and $M = mc^2/G$ is the mass of the rotating body. The Kerr metric for $r \gg M$ and $r \gg a$ approaches the solution of a rotating mass in the weak field limit [33]. Comparison of the metric (2.4.6) with the solution in [34] confirms the identification of M with the total mass and J with the total angular momentum.

2.4.3.1 Killing vectors of the Kerr metric

Being stationary and axisymmetric, the Kerr metric admits two Killing vector fields

$$\vec{\xi} := \frac{\partial}{\partial ct} \qquad \text{and} \qquad \vec{m} := \frac{\partial}{\partial \varphi}. \tag{2.4.8}$$

or equivalently, in coordinates (ct, r, θ, φ),

$$\xi^\mu \equiv (1, 0, 0, 0) \qquad \text{and} \qquad m^\mu \equiv (0, 0, 0, 1), \tag{2.4.9}$$

As a consequence, there are two conserved quantities associated to the motion of test particles:

$$k_\mu \xi^\mu = k_t \equiv l \qquad \text{and} \qquad k_\mu m^\mu = k_\varphi \equiv -n. \tag{2.4.10}$$

For massless particles, we can choose the affine parameter (as we will always do in the following) such that the four-momentum coincides with the four-velocity, i.e. $P_\mu = k_\mu$; thus, for massless particles l is the energy and n the angular momentum at infinity.

2.4.4 Geodesics

A geodesic of spacetime is a curve of minimum length between two points, in a space-time equipped with a metric. The geodesic curve $x^\mu(\lambda)$ fulfills the following equation:

$$\frac{d^2 x^\mu}{d\lambda^2} + \Gamma^\mu_{\nu\sigma} \frac{dx^\nu}{d\lambda} \frac{dx^\sigma}{d\lambda} = f(\lambda) \frac{dx^\mu}{d\lambda}. \tag{2.4.11}$$

Here $\Gamma^\mu_{\nu\sigma}$ is the Christoffel connection. The fuction $f(\lambda)$ is equal to zero when λ is an affine parameter.

2.4.4.1 Geodesics in the Kerr metric

In the Schwarzschild spacetime it is possible to find radial null geodesics [27], however the Kerr spacetime does not admit the existence of these, because the spacetime does not have sphericall symmetry. Nevertheless, it is possible to find analytical solutions in the particular case where the trajectories are confined to a

cone defined by $\theta = \text{const}$. Defining the efective lagrangian.

$$\widetilde{\mathcal{L}} = \sqrt{-g_{\mu\nu}\dot{x}^\mu \dot{x}^\nu}, \tag{2.4.12}$$

where $\dot{x}^\mu = dx^\mu/d\lambda$, with λ a parameter.

If λ is an affine parameter, it is possible to obtain the geodesics equations from the following alternative lagrangian,

$$\widetilde{\mathcal{L}} = \frac{1}{2} g_{\mu\nu}\dot{x}^\mu \dot{x}^\nu. \tag{2.4.13}$$

In the case of the Kerr metric (2.4.6), we obtain

$$\begin{aligned} 2\widetilde{\mathcal{L}} &= \frac{\Delta}{\rho^2}\left(c\dot{t} - a\sin^2\theta\dot{\varphi}\right)^2 - \frac{\sin^2\theta}{\rho}\left[\left(r^2+a^2\right)d\dot{\varphi} - ac\dot{t}\right]^2 \\ &\quad -\frac{\rho^2}{\Delta}\dot{r}^2. \end{aligned} \tag{2.4.14}$$

The Euler-Lagrange equations are given by

$$\frac{\partial\widetilde{\mathcal{L}}}{\partial x^\mu} - \frac{d}{d\lambda}\left(\frac{\partial\widetilde{\mathcal{L}}}{\partial\dot{x}^\mu}\right) = 0. \tag{2.4.15}$$

For $x^0 = ct$, we have

$$\frac{d}{d\lambda}\left(\frac{\partial\widetilde{\mathcal{L}}}{\partial c\dot{t}}\right) = 0, \qquad \text{then} \qquad \frac{\partial\widetilde{\mathcal{L}}}{\partial c\dot{t}} = \text{const.} := l, \tag{2.4.16}$$

where l is an integration constant associated to the energy. Expanding the expression (2.4.16), we obtain

$$\frac{\Delta}{\rho^2}\left(c\dot{t} - a\sin^2\theta\dot{\varphi}\right) + a\frac{\sin^2\theta}{\rho^2}\left[\left(r^2+a^2\right)\dot{\varphi} - ac\dot{t}\right] = l. \tag{2.4.17}$$

Now, for $x^3 = \varphi$, the Euler-Lagrange equations becomes

$$\frac{d}{d\lambda}\left(\frac{\partial\widetilde{\mathcal{L}}}{\partial\dot{\varphi}}\right) = 0, \qquad \text{then} \qquad \frac{\partial\widetilde{\mathcal{L}}}{\partial\dot{\varphi}} = \text{const.} := -n, \tag{2.4.18}$$

where n is a constant associated to the angular momentum. Expanding the

expression (2.4.18) we have

$$a\sin^2\theta\,\frac{\Delta}{\rho^2}\left(c\dot{t}-a\sin^2\theta\dot{\varphi}\right)+\left(r^2+a^2\right)\frac{\sin^2\theta}{\rho^2}\left[\left(r^2+a^2\right)\dot{\varphi}-ac\dot{t}\right]=n. \quad (2.4.19)$$

For $x^2=\theta$, we can write

$$\begin{aligned}&a^2\frac{\Delta}{\rho^4}\left(c\dot{t}-a\sin^2\theta\dot{\varphi}\right)^2-2a\dot{\varphi}\frac{\Delta}{\rho^2}\left(c\dot{t}-a\sin^2\theta\dot{\varphi}\right)\\&+\frac{\left(r^2+a^2\right)}{\rho^4}\left[\left(r^2+a^2\right)\dot{\varphi}-ac\dot{t}\right]^2+\frac{a^2\dot{r}^2}{\Delta}=0.\end{aligned} \quad (2.4.20)$$

It can be observed that there are only three unknowns variables $(\dot{t},\dot{r},\dot{\varphi})$ and four equations. Therefore, there must exist a relation between the constants l and n. Multiplying by (r^2+a^2) the equations for l (2.4.16)

$$\begin{aligned}\left(r^2+a^2\right)\frac{\Delta}{\rho^2}\left(c\dot{t}-a\sin^2\theta\dot{\varphi}\right) \;+\; &a\left(r^2+a^2\right)\frac{\sin^2\theta}{\rho^2}\left[\left(r^2+a^2\right)\dot{\varphi}-ac\dot{t}\right]\\&=\left(r^2+a^2\right)l.\end{aligned} \quad (2.4.21)$$

We note that the second term is equal to the expression (2.4.18), and substituting in the equation (2.4.21), we obtain

$$\begin{aligned}\left(r^2+a^2\right)\frac{\Delta}{\rho^2}\left(c\dot{t}-a\sin^2\theta\dot{\varphi}\right) \;+\; &a\left[n-a\sin^2\theta\,\frac{\Delta}{\rho^2}\left(c\dot{t}-a\sin^2\theta\dot{\varphi}\right)\right]\\&=\left(r^2+a^2\right)l.\end{aligned} \quad (2.4.22)$$

We rearrange the terms:

$$\frac{\Delta}{\rho^2}\left(c\dot{t}-a\sin^2\theta\dot{\varphi}\right)\left[\left(r^2+a^2\right)-a^2\sin^2\theta\right]=\left(r^2+a^2\right)l-an. \quad (2.4.23)$$

We recall that $\rho^2:=r^2+a^2\cos^2\theta$, so the previous expression becomes:

$$\Delta\left(c\dot{t}-a\sin^2\theta\dot{\varphi}\right)=\left(r^2+a^2\right)l-an. \quad (2.4.24)$$

Multiplying the equation for l by $a\sin^2\theta$, we get:

$$\frac{\Delta a\sin^2\theta}{\rho^2}\left(c\dot{t}-a\sin^2\theta\dot{\varphi}\right)+a^2\frac{\sin^4\theta}{\rho^2}\left[\left(r^2+a^2\right)\dot{\varphi}-ac\dot{t}\right]=a\sin^2\theta l. \quad (2.4.25)$$

By substituting the equation for n, into the above expression, we obtain

$$\sin^2\theta\left[\left(r^2+a^2\right)\dot{\varphi}-ac\dot{t}\right]=n-al\sin^2\theta. \tag{2.4.26}$$

Multiplying (2.4.24) by $a\sin^2\theta$ and (2.4.26) by Δ, and adding the expressions, we obtain the equation that relates the conserved quantities l and n:

$$\left(n+a\,l\,\sin^2\theta\right)\left(n-a\,l\,\sin^2\theta\right)=0. \tag{2.4.27}$$

Considering the solution $\left(n-a\,l\,\sin^2\theta\right)=0$ in the expression (2.4.26), we obtain:

$$c\dot{t}=\dot{\varphi}\frac{(r^2+a^2)}{a}. \tag{2.4.28}$$

Substituting (2.4.28) in the equation (2.4.18), we get

$$\dot{\varphi}=\frac{n}{\Delta\sin^2\theta}. \tag{2.4.29}$$

Using the two previous results it is possible to find an equation for $c\dot{t}$ as a function of r:

$$c\dot{t}=\frac{(r^2+a^2)}{a}\frac{n}{\Delta\sin^2\theta}. \tag{2.4.30}$$

By substituting the three previous results into the equation for $ds^2=0$, we obtain

$$\dot{r}^2=\frac{n^2}{a^2}\frac{1}{\sin^4\theta}. \tag{2.4.31}$$

Therefore,
$$\dot{r}=\pm\,\frac{n}{a}\frac{1}{\sin^2\theta}. \tag{2.4.32}$$

Then

$$r(\lambda)=\pm\frac{n}{a\sin^2\theta}\,\lambda+\text{const.} \tag{2.4.33}$$

This gives the freedom to choose r as the parameter along each geodesic. In particular, by selecting the positive solution for $\dot{r}$ and using (2.4.29), we obtain:

$$\frac{d\varphi}{d\lambda}=\frac{dr}{d\lambda}\frac{d\varphi}{dr}=\frac{n}{a\sin^2\theta}\frac{d\varphi}{dr}=\frac{n}{\Delta\sin^2\theta}. \tag{2.4.34}$$

Therefore,
$$\frac{d\varphi}{dr}=\frac{a}{\Delta}. \tag{2.4.35}$$

Analogously for $dt/d\lambda$, we have that

$$c\frac{dt}{d\lambda} = \frac{dr}{d\lambda}c\frac{dt}{dr} = \frac{n}{a\sin^2\theta}c\frac{dt}{dr} = \left(r^2+a^2\right)\frac{n}{a^2\sin^2\theta}. \tag{2.4.36}$$

Therefore,
$$c\frac{dt}{dr} = \frac{(r^2+a^2)}{\Delta}. \tag{2.4.37}$$

In summary, the outgoing solutions are given after integration of (2.4.35) and (2.4.37) by:

$$\varphi_+(r) = \frac{a}{2\sqrt{m^2-a^2}}\ln\left|\frac{(r-r_+)}{(r-r_-)}\frac{(r_0-r_-)}{(r_0-r_+)}\right| + \varphi_0, \tag{2.4.38}$$

where φ_0 is the initial angular coordinate, and

$$ct_+(r) = \Delta r + m_+\ln\left|\frac{(r-r_+)}{(r_0-r_+)}\right| + m_-\ln\left|\frac{(r-r_-)}{(r_0-r_-)}\right| + ct_0. \tag{2.4.39}$$

Here $\Delta r = r - r_0$ and ct_0 is the initial temporal coordinate and

$$m_\pm = \left(m \pm \frac{m^2}{\sqrt{m^2-a^2}}\right) \quad \text{and} \quad r_\pm = m \pm \sqrt{m^2-a^2}. \tag{2.4.40}$$

In the case of incoming null geodesics, we consider $dr/dt < 0$. This result is equivalent to simultaneously changing the sign of both ct and φ:

$$\frac{dr}{dt} < 0 \qquad \longleftrightarrow \qquad ct \to -ct \quad \wedge \quad \varphi \to -\varphi. \tag{2.4.41}$$

The ingoing geodesics are

$$\varphi_-(r) = -\frac{a}{2\sqrt{m^2-a^2}}\ln\left|\frac{(r-r_+)}{(r-r_-)}\frac{(r_0-r_-)}{(r_0-r_+)}\right| + \varphi_0, \tag{2.4.42}$$

$$ct_-(r) = -\Delta r - m_+\ln\left|\frac{(r-r_+)}{(r_0-r_+)}\right| - m_-\ln\left|\frac{(r-r_-)}{(r_0-r_-)}\right| + ct_0. \tag{2.4.43}$$

2.4.5 Null vector

In the context of General Relativity, a null vector (also known as a lightlike vector) is a tangent vector k^μ for which the scalar product, calculated with the

spacetime metric $g_{\mu\nu}$, vanishes:

$$g_{\mu\nu}k^\mu k^\nu = 0. \tag{2.4.44}$$

Null vectors characterize the trajectories of massless particles, such as photons, and define the light-cone structure[7] of the spacetime.

2.4.5.1 Null vector in Kerr spacetime

We express the null vector k^μ as

$$k^\mu = \left(c\frac{dt}{d\lambda}, \frac{dr}{d\lambda}, \frac{d\theta}{d\lambda}, \frac{d\varphi}{d\lambda}\right), \tag{2.4.45}$$

where λ is an affine parameter along the trajectory. For a photon following an arbitrary geodesic in the Kerr spacetime, the null vector can be expressed as [35, 27]:

$$c\frac{dt}{d\lambda} = \frac{1}{\rho}\left[-a\left(al\sin^2\theta - n\right) + \frac{(r^2+a^2)}{\Delta}P\right], \tag{2.4.46}$$

$$\frac{dr}{d\lambda} = \epsilon\frac{1}{\rho}\sqrt{R}, \tag{2.4.47}$$

$$\frac{d\theta}{d\lambda} = \epsilon_\theta\frac{1}{\rho}\sqrt{\Theta}, \tag{2.4.48}$$

$$\frac{d\varphi}{d\lambda} = -\frac{1}{\rho}\left[\left(al - \frac{n}{\sin^2\theta}\right) + \frac{a}{\Delta}P\right]. \tag{2.4.49}$$

Where ϵ and ϵ_θ are sign indicators (i.e. $\epsilon_r = \pm 1$, $\epsilon_\theta = \pm 1$), and

$$P = l\left(r^2+a^2\right) - an, \tag{2.4.50}$$

$$R = P^2 - \Delta\left[\mathcal{K} + \left(n - al\sin^2\theta\right)^2\right], \tag{2.4.51}$$

$$\Theta = \mathcal{K} - \cos^2\theta\left[-a^2l^2 + \frac{n^2}{\sin^2\theta}\right]. \tag{2.4.52}$$

Where $\mathcal{K}$ and the separation constant of the Hamilton-Jacobi equation [35]. If the photon follows a geodesic in an arbitrary θ plane as before (2.4.38), the relationship (2.4.27) is fulfilled and the affine parameter $r = \epsilon\, l\lambda + \text{const}$, then the null vector

[7] The light-cone structure encodes the causal relationships in spacetime and is determined by the metric tensor [28].

$u^\mu = dx^\mu/dr$ is given by

$$u^0 = \epsilon \frac{a^2 + r^2}{\Delta}, \tag{2.4.53}$$

$$u^1 = 1, \tag{2.4.54}$$

$$u^2 = 0, \tag{2.4.55}$$

$$u^3 = \epsilon \frac{a}{\Delta}. \tag{2.4.56}$$

where ϵ is equal to $1\,(-1)$ if it is a outgoing (ingoing) geodesic.

2.4.6 The Parametrized Post-Newtonian formalism

The Parametrized Post-Newtonian (PPN) formalism provides a framework to study different metric theories of gravity by quantifying deviations from Newtonian gravity in the weak-field, slow-motion limit [36]. This formalism utilizes a set of parameters, each with a distinct physical interpretation [37, 38]. The PPN formalism includes parameters that assess the effects of a preferred universal rest-frame on the post-Newtonian metric, which are relevant to theories that propose such a frame. These parameters quantify how deviations from this hypothetical universal rest-frame affect gravitational interactions. Additionally, the formalism incorporates parameters that quantify potential violations of energy-momentum conservation laws. These parameters would be non-zero if, in certain theoretical frameworks, the fundamental principles of energy and momentum conservation were not strictly adhered to. In this work, we use a simple version of the parameterized post-Newtonian approximation, which depends only on the parameters γ and β (the Eddington-Robertson-Schiff parameters [39]): γ measures the curvature of space-geometry, quantifying the amount of space curvature produced by mass; β characterizes the nonlinearity of gravity, reflecting the extent to which gravity itself generates gravity. They are crucial for analyzing experimental tests of gravity, such as the classical tests of General Relativity [36] and these parameters acquires different values depending on the particular of modified theory of gravity see, Table (3.6.1). In this approximation the metric in

isotropic coordinates and in mostly plus signature is given by

$$g_{00} = -\left[1 - 2\frac{\phi}{c^2} + 2\beta\left(\frac{\phi}{c^2}\right)^2\right], \tag{2.4.57}$$

$$g_{0i} = 0, \tag{2.4.58}$$

$$g_{ij} = \left(1 + 2\gamma\frac{\phi}{c^2}\right)\delta_{ij}. \tag{2.4.59}$$

And the components of the inverse metric are given by

$$g^{00} = -\left[1 + 2\left(\frac{\phi}{c^2}\right) + 2(2-\beta)\left(\frac{\phi}{c^2}\right)^2\right], \tag{2.4.60}$$

$$g^{0i} = 0, \tag{2.4.61}$$

$$g^{ij} = \left[1 - 2\gamma\left(\frac{\phi}{c^2}\right) + 4\gamma^2\left(\frac{\phi}{c^2}\right)^2\right]\delta^{ij}. \tag{2.4.62}$$

there ϕ represents the Newtonian potential,

$$\phi(\vec{x}, t) = G\int \frac{\rho(\vec{x}', t)}{|\vec{x} - \vec{x}'|} d^3\vec{x}', \tag{2.4.63}$$

where ρ is the density of rest mass as measured in a local freely falling frame momentarily comoving with the gravitating matter.

Theory	PPN parameters	
	γ	β
General relativity	1	1
Scalar-tensor		
Brans-Dicke	$\frac{1+\omega_{BD}}{2+\omega_{BD}}$	1
General, $f(R)$	$\frac{1+\omega}{2+\omega}$	$1 + \frac{\lambda}{4+2\omega}$
Vector-tensor		
Unconstrained	γ'	β'
Einstein-Aether	1	1
Tensor-Vector-Scalar	1	1

Table 2.4.1: Metric theories and their respective values of γ and β. Table adapted from [36].

2.5 Relativistic corrections to the Schrödinger equation

In this section, we briefly discuss the modifications to the non-relativistic Schrödinger equation required to account for relativistic effects. These corrections will be considered for cases significant when the particle velocities are small with respect the speed of light or when weak gravitational fields are involved.

2.5.1 Klein-Gordon derivation of the quantum Hamiltonian

In this section, we aim to derive a Schrödinger-type equation with relativistic corrections starting from the Klein-Gordon equation in curved spacetime [40] in a semiclassical WKB approximation. The Klein-Gordon equation in mostly plus signature reads:

$$\hbar^2 g^{\mu\nu}\nabla_\mu\nabla_\nu\varphi_{KG} + m^2c^2\varphi_{KG} = 0. \tag{2.5.1}$$

Let us assume the following ansatz for the scalar field φ_{KG} (interpreted as the wave function):

$$\varphi_{\mathrm{KG}} = \exp\left[\frac{i}{\hbar}S(x,t)\right]. \tag{2.5.2}$$

We perform an expansion of the action $S(x,t)$ in powers of c^2:

$$S(x,t) = c^2 S_0(x) + S_1(x) + c^{-2}S_2 + ... \tag{2.5.3}$$

By substituting the ansatz (2.5.2) in the equation (2.5.1) we obtain:

$$0 = \hbar^2 g^{\mu\nu}\nabla_\mu\nabla_\nu\varphi_{\mathrm{KG}} + m^2c^2\varphi_{\mathrm{KG}} \tag{2.5.4}$$

$$0 = \hbar^2 g^{\mu\nu}\nabla_\mu\left(\partial_\nu\varphi_{\mathrm{KG}}\right) - m^2c^2\varphi_{\mathrm{KG}} \tag{2.5.5}$$

$$0 = \hbar^2 g^{\mu\nu}\left(\partial_\mu\partial_\nu\varphi_{\mathrm{KG}} - \Gamma^\sigma_{\mu\nu}\partial_\sigma\varphi_{\mathrm{KG}}\right) + m^2c^2\varphi_{\mathrm{KG}}. \tag{2.5.6}$$

We can rewrite the derivative of the field φ_{KG} as

$$\begin{aligned}\partial_\nu\varphi_{\mathrm{KG}} &= \partial_\nu\left(\exp\left[\frac{i}{\hbar}S(x,t)\right]\right)\\ &= \frac{i}{\hbar}\exp\left[\frac{i}{\hbar}S(x^\mu)\right]\partial_\nu\left[S(x,t)\right]\\ &= \frac{i}{\hbar}\varphi_{\mathrm{KG}}\,\partial_\nu\left[S(x,t)\right].\end{aligned} \tag{2.5.7}$$

Analogously

$$\begin{aligned}\partial_\mu\partial_\nu\varphi_{\mathrm{KG}} &= \frac{i}{\hbar}\partial_\mu\varphi_{\mathrm{KG}}\,\partial_\nu\left[S(x,t)\right]+\frac{i}{\hbar}\varphi_{\mathrm{KG}}\partial_\mu\,\partial_\nu\left[S(x,t)\right]\\ &= \frac{-1}{\hbar^2}\varphi_{KG}\,\partial_\mu\left[S(x,t)\right]\partial_\nu\left[S(x,t)\right]+\frac{i}{\hbar}\varphi_{KG}\partial_\mu\,\partial_\nu\left[S(x,t)\right]. \quad (2.5.8)\end{aligned}$$

Therefore, equation (2.5.6) becomes:

$$\begin{aligned}\hbar^2 g^{\mu\nu}\Big(&-\frac{1}{\hbar^2}\varphi_{\mathrm{KG}}\,\partial_\mu\left[S(x,t)\right]\partial_\nu\left[S(x,t)\right]+\frac{i}{\hbar}\varphi_{\mathrm{KG}}\partial_\mu\,\partial_\nu\left[S(x,t)\right]\\ &-\frac{i}{\hbar}\Gamma^\sigma_{\mu\nu}\varphi_{\mathrm{KG}}\,\partial_\sigma\left[S(x,t)\right]\Big)+m^2c^2\varphi_{\mathrm{KG}}=0. \quad (2.5.9)\end{aligned}$$

Considering the WKB approximation (2.5.3) and analyzing each power of c^2 one obtains a Hamiltonian that satisfies a Schrödinger-type equation. A transformation is then applied to both the Hamiltonian and the wavefunction in such a way that the Hamiltonian becomes Hermitian with respect to the flat inner product [41, 42], obtaining the following Hamiltonian

$$\begin{aligned}H=&mc^2+\frac{p^2}{2m}-\frac{p^4}{8m^3c^2}+m\phi(r)+\frac{(2\gamma+1)}{2mc^2}\left(\phi(r)p^2+[\vec{p}\,\phi]\cdot\vec{p}\right)\\ &-\left(\frac{1}{2}-\beta\right)m\frac{\phi^2(r)}{c^2}+\frac{3}{4}\frac{\gamma}{mc^2}\left[p^2\phi(r)\right], \quad (2.5.10)\end{aligned}$$

where $[\vec{p}\,\phi]$ and $[p^2\phi(r)]$ represent the action of the momentum operator on the potential $\phi(r)$.

2.5.2 Clock states

In our work, we employ quantum systems whose total Hilbert space $\mathcal{H}_{\mathrm{tot}}$ is the tensor product of the Hilbert spaces $\mathcal{H}_{\mathrm{cm}}$ and $\mathcal{H}_{\mathrm{clock}}$, describing the degrees of freedom of the center of mass and the internal degrees of freedom, respectively. In this work, we consider initial states of the form

$$\rho=\rho_{\mathrm{cm}}\otimes\sigma_{\mathrm{clock}}, \quad (2.5.11)$$

where ρ_{cm} is the state for the center of mass position, and σ_{clock} is the state for the internal degrees of freedom. The latter can be physically implemented, for example, in atoms or molecules with their electronic or vibrational energy levels

as the internal degrees of freedom; we describe these states as **clocks** [2].

For the following calculations, we will use a two-level **clock** state in a coherent superposition:

$$|\tau\rangle = \frac{1}{\sqrt{2}}\left(|0\rangle + |1\rangle\right). \tag{2.5.12}$$

Note that this choice is for simplicity, and there is the possibility of extending our results to a larger number of levels [43]. The Hamiltonian operator in the rest frame driving the evolution of the inner degree of freedom is

$$H_{\text{clock}} = E_0|0\rangle\langle 0| + E_1|1\rangle\langle 1|, \tag{2.5.13}$$

where $|0\rangle$ and $|1\rangle$ are eigenstates with energies E_0 and E_1, respectively.
To include the inner degree of freedom in the Hamiltonian (2.5.10), we follow ref [44] and consider the following relation:

$$Mc^2 = H_{\text{rest}} = mc^2 + \frac{H_{\text{clock}}}{c^2}. \tag{2.5.14}$$

Where M is the total mass at rest, m is the mass of the system for the state in which $\langle H_{\text{clock}}\rangle = 0$ and H_{clock} it is the Hamiltonian that describes the dynamics of the internal degrees of freedom of the (point-like) particle. Considering a first order approximation in H_{clock}/c^2, and keeping terms up to order c^{-4}, we obtain

$$\begin{aligned} H = H_{\text{cm}}^{\text{rel}} + H_{\text{clock}}\Big(1 - \frac{p^2}{2m} + \frac{3p^4}{8m^3c^4} + m\frac{\phi(r)}{c^2} - \frac{(2\gamma+1)}{2mc^4}\left(\phi(r)p^2 + [\vec{p}\,\phi]\cdot\vec{p}\right) \\ - \left(\frac{1}{2} - \beta\right) m\frac{\phi^2(r)}{c^4} - \frac{3}{4}\frac{\gamma}{mc^4}\left[p^2\phi(r)\right]\Big), \end{aligned} \tag{2.5.15}$$

where $H_{\text{cm}}^{\text{rel}}$ is the Hamiltonian of center of mass with fourth order relativistic corrections

$$\begin{aligned} H_{\text{cm}}^{\text{rel}} = mc^2 + \frac{p^2}{2m} - \frac{p^4}{8m^3c^2} + M\phi(r) + \frac{(2\gamma+1)}{2mc^2}\left(\phi(r)p^2 + [\vec{p}\,\phi]\cdot\vec{p}\right) \\ - \left(\frac{1}{2} - \beta\right) m\frac{\phi^2(r)}{c^2} + \frac{3}{4}\frac{\gamma}{mc^2}\left[p^2\phi(r)\right]. \end{aligned} \tag{2.5.16}$$

It is possible to identify the coupling between the gravitational field and the

Hamiltonian of the internal degrees of freedom, which we denote by λ, that is:

$$\lambda = \left(1 - \frac{p^2}{2m} + \frac{3p^4}{8m^3c^4} + m\frac{\phi(r)}{c^2} - \frac{(2\gamma+1)}{2mc^4}\left(\phi(r)p^2 + [\vec{p}\,\phi]\cdot\vec{p}\right)\right.$$
$$\left. - \left(\frac{1}{2} - \beta\right) m\frac{\phi^2(r)}{c^4} - \frac{3}{4}\frac{\gamma}{mc^4}\left[p^2\phi(r)\right]\right). \tag{2.5.17}$$

We rewrite the Hamiltonian in the form:

$$H = \hat{H}^{\text{rel}}_{\text{cm}} \otimes \mathbb{I}_{\text{clock}} + \hat{\lambda} \otimes \hat{H}_{\text{clock}}. \tag{2.5.18}$$

2.5.3 State evolution

In this section, we analyze the evolution of a composite quantum state under the influence of gravity, focusing on the semiclassical WKB approximation. This approximation is particularly useful when considering well-localized states. Here, we use Gaussian states, as they allow us to treat quantum operators approximately as classical variables. This is crucial for simplifying the analysis of systems in which the center-of-mass (c.m.) motion can be treated classically, while the internal degrees of freedom retain their quantum nature.

We consider an initial separable state of the form:

$$|\psi\rangle = |\gamma\rangle \otimes |\tau_0\rangle\,, \tag{2.5.19}$$

where $|\gamma\rangle$ represents the center-of-mass (c.m.) or path state, and $|\tau_0\rangle$ is the clock state defined by equation (2.5.12).

Given the WKB approximation, the state $|\psi\rangle$ satisfies a modified Schrödinger equation governed by the Hamiltonian (2.5.18). Consequently, its evolution is described by:

$$\hat{U}\,|\psi\rangle = e^{-\frac{i}{\hbar}\int dt\left[\hat{H}^{\text{rel}}_{\text{cm}}\otimes\mathbb{I}_{\text{clock}} + \hat{\lambda}\otimes\hat{H}_{\text{clock}}\right]}\,|\gamma\rangle \otimes |\tau_0\rangle\,. \tag{2.5.20}$$

We now assume $|\gamma\rangle$ to be a well-localized Gaussian wave packet [45, 46]. In the coordinate representation:

$$|\gamma\rangle = \frac{1}{(2\pi\sigma^2)^{1/4}}\int dx\, e^{-\frac{(x-x_0)^2}{4\sigma^2}}\,|x\rangle \tag{2.5.21}$$

and in the momentum representation:

$$|\gamma\rangle = \left(\frac{2\sigma^2}{\pi\hbar^2}\right)^{1/4} \int dp\, e^{-\frac{p^2\sigma^2}{\hbar^2} - i\frac{px_0}{\hbar}} |p\rangle\,, \tag{2.5.22}$$

where σ^2 is the position variance and $(\hbar/2\sigma)^2$ is the momentum variance.

In the WKB limit, quantum states become highly localized, then quantum operators can be approximated by their expectation values,

$$\hat{p}\,|p\rangle \approx \langle p\rangle\,|p\rangle\,, \tag{2.5.23}$$

leading to a nearly vanishing commutator:

$$[\hat{p}, \hat{x}] \approx 0. \tag{2.5.24}$$

We now examine the commutator between the components of the Hamiltonian acting on $|\psi\rangle$:

$$\begin{aligned}&\left[\hat{H}^{\text{rel}}_{\text{cm}} \otimes \mathbb{I}_{\text{clock}}\ ,\ \hat{\lambda} \otimes \hat{H}_{\text{clock}}\right] |\gamma\rangle \otimes |\tau_0\rangle\,,\\ &\left[\left(\hat{H}^{\text{rel}}_{\text{cm}} \otimes \mathbb{I}_{\text{clock}}\right)\left(\hat{\lambda} \otimes \hat{H}_{\text{clock}}\right) - \left(\hat{\lambda} \otimes \hat{H}_{\text{clock}}\right)\left(\hat{H}^{\text{rel}}_{\text{cm}} \otimes \mathbb{I}_{\text{clock}}\right)\right] |\gamma\rangle\,|\tau_0\rangle\,.\end{aligned} \tag{2.5.25}$$

Assuming that $\hat{H}^{\text{rel}}_{\text{cm}}$ and $\hat{\lambda}$ are functions of $\hat{p}$ and $\hat{x}$, and using the fact that $|\gamma\rangle$ is highly localized, we have:

$$\left[\hat{H}^{\text{rel}}_{\text{cm}}\,\hat{\lambda} \otimes \hat{H}_{\text{clock}} - \hat{\lambda}\,\hat{H}^{\text{rel}}_{\text{cm}} \otimes \hat{H}_{\text{clock}}\right] |\gamma\rangle\,|\tau_0\rangle\,. \tag{2.5.26}$$

Hence,

$$\left[\hat{H}^{\text{rel}}_{\text{cm}}\,\hat{\lambda} - \hat{\lambda}\,\hat{H}^{\text{rel}}_{\text{cm}}\right] |\gamma\rangle = 0. \tag{2.5.27}$$

Using the Baker-Campbell-Hausdorff formula, we eliminate the commutator terms in the time evolution operator, allowing us to factorize the evolution:

$$e^{-\frac{i}{\hbar}\int dt\left[\hat{H}^{\text{rel}}_{\text{cm}}\otimes\mathbb{I}_{\text{clock}} + \hat{\lambda}\otimes\hat{H}_{\text{clock}}\right]} |\gamma\rangle\,|\tau_0\rangle = e^{-\frac{i}{\hbar}\int dt \hat{H}^{\text{rel}}_{\text{cm}}\otimes\mathbb{I}_{\text{clock}}} e^{-\frac{i}{\hbar}\int dt \hat{\lambda}\otimes\hat{H}_{\text{clock}}} |\gamma\rangle\,|\tau_0\rangle\,.$$

This leads to the following explicit evolution:

$$\begin{aligned}\hat{U}\,|\gamma\rangle\,|\tau_0\rangle =& e^{-\frac{i}{\hbar}H_{\mathrm{cm}}^{\mathrm{rel}}}\,|\gamma\rangle\,\frac{1}{\sqrt{2}}\left[e^{-\frac{i}{\hbar}\lambda E_0}\,|0\rangle + e^{-\frac{i}{\hbar}\lambda E_1}\,|1\rangle\right]\\ =& e^{-\frac{i}{\hbar}H_{\mathrm{cm}}^{\mathrm{rel}}}\,|\gamma\rangle\,\frac{1}{\sqrt{2}}e^{-\frac{i}{\hbar}\lambda E_0}\left[|0\rangle + e^{-\frac{i}{\hbar}\lambda\,\Delta E}\,|1\rangle\right]\end{aligned} \tag{2.5.28}$$

To analyze the clock state evolution, we trace over the center-of-mass degrees of freedom. Since $\exp\{-\frac{i}{\hbar}H_{\mathrm{cm}}^{\mathrm{rel}}\}$ is a the global phase, we focus on the internal degrees of freedom and their gravitational interaction.

2.6 Maxwell equations in curved spacetimes

For spacetimes without torsion[8], the Faraday tensor becomes:

$$\begin{aligned}F_{\mu\nu} &:= \nabla_\mu A_\nu - \nabla_\nu A_\mu\\ &:= \partial_\mu A_\nu - \Gamma^\rho_{\mu\nu}A_\rho - \partial_\mu A_\nu + \Gamma^\rho_{\nu\mu}A_\rho\\ &:= \partial_\mu A_\nu - \partial_\nu A_\mu.\end{aligned} \tag{2.6.1}$$

The Maxwell equations in curved spaces [48] are given by:

$$\nabla_\mu F^\mu_\nu = g^{\mu\rho}\nabla_\rho\left(\partial_\mu A_\nu - \partial_\nu A_\mu\right) = \frac{1}{\varepsilon_0}J_\nu. \tag{2.6.2}$$

2.6.1 Gauge freedom

The gauge transformations in electrodynamics arise naturally, since the scalar potential ϕ and the vector potential $\vec{A}$ are fields introduced in such a way that the electric and magnetic fields satisfy the homogeneous Maxwell equations. From Gauss's law for the magnetic field, we have:

$$\vec{B} = \nabla \times \vec{A}. \tag{2.6.3}$$

[8] Torsion is a geometric property that quantifies the antisymmetric part of the affine connection. The standard General Relativity assumes a torsion-free Levi-Civita connection [47].

By substituting in the Faraday-Lenz law

$$\begin{aligned} \nabla \times \vec{E} + \partial_t \left(\nabla \times \vec{A} \right) &= 0 \\ 0 &= \nabla \times \left(\vec{E} + \partial_t \vec{A} \right). \\ \text{Then} \quad \vec{E} &= -\partial_t \vec{A} - \nabla \phi. \end{aligned} \tag{2.6.4}$$

This is manifested in the invariance of the electric and magnetic fields under a gauge transformation of the form:

$$\phi' = \phi + \partial_t \lambda \ \ , \ \ \vec{A}' = \vec{A} - \nabla \lambda. \tag{2.6.5}$$

In special relativity, the potentials are components of a four-potential

$$A^\mu = (\phi/c, \vec{A}). \tag{2.6.6}$$

A gauge transformation takes the form:

$$A'_\mu = A_\mu + \partial_\mu \xi. \tag{2.6.7}$$

The Faraday tensor defined by $F_{\mu\nu} = \partial_\mu A_\nu - \partial_\nu A_\mu$, is invariant under a gauge transformation (2.6.7):

$$\begin{aligned} F'_{\mu\nu} &= \partial_\mu A'_\nu - \partial_\nu A_\mu \\ &= \partial_\mu \left(A_\nu + \partial_\nu \xi \right) - \partial_\nu \left(A_\mu + \partial_\mu \xi \right) \\ &= \partial_\mu A_\nu - \partial_\nu A_\mu + \partial_\mu \partial_\nu \xi - \partial_\nu \partial_\mu \xi \\ &= F_{\mu\nu}. \end{aligned} \tag{2.6.8}$$

The Lorenz gauge [49], in the covariant form (under Lorentz transformations) is given by:

$$\begin{aligned} \frac{1}{c^2} \partial_t \phi + \partial_i A^i &= 0 \\ \partial_\mu A^\mu &= 0. \end{aligned} \tag{2.6.9}$$

2.7 Polarization in curved spacetimes

We now discuss how polarization is affected by spacetime curvature, based on [46]. In that work, a parallel transport equation was derived for the complex polarization vector. To achieve this, the following ansatz was considered for the four-potential of the wave

$$A_\mu = Re\left\{\phi_\mu e^{i\vartheta/\epsilon}\right\}. \tag{2.7.1}$$

In this approximation, the phase ϑ varies rapidly compared to the complex amplitude ϕ_μ— that is, we consider the WKB approximation.
We will use a gauge transformation $A_\mu \to A_\mu + \nabla_\mu\lambda$ in such a way that it preserves the form of equation (2.7.1).
A function λ of the form $\lambda = \zeta e^{i\vartheta/\epsilon}$ is proposed, where ζ is a slowly varying function.

$$A_\mu \to A_\mu + \nabla_\mu\left(\zeta e^{i\vartheta/\epsilon}\right) = \left(\phi_\mu + \nabla_\mu\zeta + \frac{i}{\epsilon}k_\mu\zeta\right)e^{i\vartheta/\epsilon}, \tag{2.7.2}$$

where

$$\nabla_\mu\vartheta = \partial_\mu\vartheta = k_\mu, \tag{2.7.3}$$

and ϑ depends on the spacetime parameters — for example, for a plane wave, $\vartheta = \omega t - \vec{k}\cdot\vec{x}$. This yields the gauge transformation for the complex polarization vector.

$$\phi_\mu \to \phi_\mu + \nabla_\mu\zeta + \frac{i}{\epsilon}k_\mu\zeta. \tag{2.7.4}$$

Since this gauge transformation diverges in the limit $\epsilon \to 0$, it is necessary to impose an additional restriction on the family of allowed gauge transformations, specifically in the way the function ζ is chosen. We consider only functions of the form $\zeta = -i\epsilon\xi$. Then, the gauge transformation for the complex polarization vector becomes

$$\phi_\mu \to \phi_\mu - i\epsilon\nabla_\mu\xi + k_\mu\xi. \tag{2.7.5}$$

We will also consider the ansatz,

$$\phi_\mu k^\mu = i\epsilon\alpha(x^\mu). \tag{2.7.6}$$

which implies that the wave vector and the polarization vector are orthogonal to first order, with α an arbitrary function.
Substituting the ansatz (2.7.1) in the inhomogeneous Maxwell equations (2.7.7),

and considering a source-free region.

$$\begin{aligned}\nabla_\mu F^\mu_\nu &= g^\rho \nabla_\rho \left(\nabla_\mu A_\nu - \nabla_\nu A_\mu\right) \\ &= \nabla^\mu \left(\nabla_\mu \phi_\nu e^{i\vartheta/\epsilon} - \nabla_\nu \phi_\mu e^{i\vartheta/\epsilon}\right) \\ &= 0. \end{aligned} \tag{2.7.7}$$

Expanding the terms, we can write

$$\nabla_\mu F^\mu_\nu = \underbrace{\nabla^\mu \left(\left(\nabla_\mu \phi_\nu\right) e^{i\vartheta/\epsilon}\right)}_{(1)} + \underbrace{\nabla^\mu \left(\phi_\nu k_\mu \tfrac{i}{\epsilon} e^{i\vartheta/\epsilon}\right)}_{(2)} \tag{2.7.8}$$

$$\underbrace{- \nabla^\mu \left(\left(\nabla_\nu \phi_\mu\right) e^{i\vartheta/\epsilon}\right)}_{(3)} \underbrace{- \nabla^\mu \left(\phi_\mu k_\nu \tfrac{i}{\epsilon} e^{i\vartheta/\epsilon}\right)}_{(4)}. \tag{2.7.9}$$

Now, expanding each contribution of the previous expression, we obtain

$$\begin{aligned}\nabla_\mu F^\mu_\nu = [\ &\Box \phi_\nu - \nabla^\mu \nabla_\nu \phi_\mu - \frac{1}{\epsilon^2}\phi_\nu k_\mu k^\mu + \frac{1}{\epsilon^2}\phi_\mu k_\nu k^\mu \\ &+ \frac{i}{\epsilon}\left(\ \nabla_\mu \phi_\nu k^\mu + \left(\nabla^2 \phi_\nu\right) k_\mu + \phi_\nu \nabla^\mu k_\mu - \left(\nabla_\nu \phi_\mu\right) k^\mu \right. \\ &\left. - \left(\nabla^\mu \phi_\mu\right) k_\nu - \phi_\mu \nabla^\mu k_\nu\ \right)\ ] e^{i\vartheta/\epsilon}. \end{aligned} \tag{2.7.10}$$

We know that

$$\begin{aligned} k^\mu \nabla_\mu \phi_\nu &= g^{\mu\rho} k_\rho \nabla_\mu \phi_\nu = k_\rho g^{\rho\mu} \nabla_\mu \phi_\nu \\ &= k_\rho \nabla^\rho \phi_\nu = k_\mu \nabla^\mu \phi_\nu, \end{aligned} \tag{2.7.11}$$

and

$$\begin{aligned} \nabla_\mu k_\nu = \nabla_\mu \nabla_\nu \vartheta &= \nabla_\mu \left(\partial_\nu \vartheta\right) = \nabla_\nu k_\mu \\ &= \partial_\mu \partial_\nu \vartheta - \Gamma^\lambda_{\mu\nu} \partial_\lambda \vartheta = \partial_\nu \partial_\mu \vartheta - \Gamma^\lambda_{\nu\mu} \partial_\lambda \vartheta. \end{aligned} \tag{2.7.12}$$

Substituting in the expression (2.7.10), we have

$$\begin{aligned}\nabla_\mu F^\mu_\nu = [\ &\Box \phi_\nu - \nabla^\mu \nabla_\nu \phi_\mu - \frac{1}{\epsilon^2}\phi_\nu k_\mu k^\mu + \frac{1}{\epsilon^2}\phi_\mu k_\nu k^\mu \\ &+ \frac{i}{\epsilon}\left(\ 2k_\mu \left(\nabla^\mu \phi_\nu\right) + \phi_\nu \nabla^\mu k_\mu - \nabla_\nu \left(\phi_\mu k^\mu\right) \right. \\ &\left. - \left(\nabla^\mu \phi_\mu\right) k_\nu\ \right)\ ] e^{i\vartheta/\epsilon}. \end{aligned} \tag{2.7.13}$$

Using the gauge condition (2.7.6) in the previous equation we obtain

$$\begin{aligned}\nabla_\mu F^\mu_\nu = [\, &\Box\phi_\nu - \nabla^\mu\nabla_\nu\phi_\mu - \frac{1}{\epsilon^2}\phi_\nu k_\mu k^\mu + \frac{1}{\epsilon^2}k_\nu\,(i\epsilon\alpha) \\ &+ \frac{i}{\epsilon}\,(\,2k_\mu\,(\nabla^\mu\phi_\nu) + \phi_\nu\nabla^\mu k_\mu - \nabla_\nu\,(i\epsilon\alpha) \\ &- (\nabla^\mu\phi_\mu)\,k_\nu\,)\,]\,e^{i\vartheta/\epsilon}.\end{aligned} \tag{2.7.14}$$

Then

$$\begin{aligned}\nabla_\mu F^\mu_\nu = [\, &\Box\phi_\nu - \nabla^\mu\nabla_\nu\phi_\mu + \nabla_\nu\,(\alpha(x^\mu)) \\ &+ \frac{i}{\epsilon}\,(\,2k_\mu\,(\nabla^\mu\phi_\nu) + \phi_\nu\nabla^\mu k_\mu + k_\nu\alpha(x^\mu) \\ &- (\nabla^\mu\phi_\mu)\,k_\nu\,) - \frac{1}{\epsilon^2}\phi_\nu k_\mu k^\mu\,]\,e^{i\vartheta/\epsilon}.\end{aligned} \tag{2.7.15}$$

Next, we require that the field ϕ_μ does not depend on the parameter ϵ. Physically, this means that in the high-frequency limit, the solutions of equation (2.7.15) must be independent of the frequency (encoded in ϵ, as introduced in the ansatz). Therefore, all terms of order $1/\epsilon$ must vanish [50].

$$2k^\mu\nabla_\mu\phi_\nu + \phi_\nu\nabla_\mu k^\mu - k_\nu\,(\nabla_\mu\phi^\mu - \alpha) = 0, \tag{2.7.16}$$

$$k^\mu k_\mu = 0. \tag{2.7.17}$$

We easily notice that the second expression is gauge invariant. This indicates that the wave vector k^μ is a null vector. By taking the covariant derivative, we obtain:

$$\nabla_\nu\,(k^\mu k_\mu) = 2k^\mu\nabla_\nu k_\mu = 2k^\mu\nabla_\mu k_\nu = 0. \tag{2.7.18}$$

This corresponds to the geodesic equation under the assumption that the trajectory is parameterized by an affine parameter. Now, applying the gauge transformation (2.7.5) to the expression (2.7.16), we obtain:

$$0 = 2k^\mu\nabla_\mu\,(\phi_\nu - i\epsilon\nabla_\nu\xi + k_\nu\xi) + (\phi_\nu - i\epsilon\nabla_\nu\xi + k_\nu\xi)\,\nabla_\mu k^\mu \tag{2.7.19}$$

$$- k_\nu\nabla_\mu\,(\phi^\mu - i\epsilon\nabla^\mu\xi + k^\mu\xi) + k_\nu\alpha \tag{2.7.20}$$

$$0 = 2k^\mu\nabla_\mu\phi_\nu + \phi_\nu\nabla_\mu k^\mu - k_\nu\,(\nabla_\mu\phi^\mu - \alpha) - i\epsilon 2k^\mu\nabla_\mu\nabla_\nu\xi + 2k^\mu\nabla_\mu\,(k_\nu\xi) \tag{2.7.21}$$

$$- i\epsilon\nabla_\nu\xi\nabla_\mu k^\mu + k_\nu\xi\nabla_\mu k^\mu + i\epsilon k_\nu\nabla_\mu\nabla^\mu\xi - k_\nu\nabla_\mu\,(k^\mu\xi)\,. \tag{2.7.22}$$

For convenience we define $B_\nu := 2k^\mu\nabla_\mu\phi_\nu + \phi_\nu\nabla_\mu k^\mu - k_\nu\nabla_\mu\phi^\mu$, then

$$\begin{aligned} 0 = {} & B_\nu + k_\nu\alpha - 2i\epsilon k^\mu\nabla_\mu\nabla_\nu\xi + 2\xi k^\mu\nabla_\mu k_\nu + 2k_\nu k^\mu\nabla_\mu\xi \\ & - i\epsilon\nabla_\nu\xi\nabla_\mu k^\mu + k_\nu\xi\nabla_\mu k^\mu + i\epsilon k_\nu\nabla_\mu\nabla^\mu\xi - k_\nu k^\mu\nabla_\mu\xi - \xi k_\nu\nabla_\mu k^\mu. \end{aligned} \tag{2.7.23}$$

$$\begin{aligned} 0 = {} & B_\nu + k_\nu\alpha - 2i\epsilon k^\mu\nabla_\mu\nabla_\nu\xi + 2\xi k^\mu\nabla_\mu k_\nu + k_\nu k^\mu\nabla_\mu\xi \\ & - i\epsilon\nabla_\nu\xi\nabla_\mu k^\mu + i\epsilon k_\nu\nabla_\mu\nabla^\mu\xi. \end{aligned} \tag{2.7.24}$$

We note that the fourth term in (2.7.24) vanishes due to the result obtained in (2.7.18). Completing the derivative of the penultimate terms, we have:

$$\begin{aligned} -i\epsilon\nabla_\nu\xi\nabla_\mu k^\mu &= -i\epsilon\nabla_\mu\left(k^\mu\nabla_\nu\xi\right) + i\epsilon k^\mu\nabla_\mu\nabla_\nu\xi \\ &= i\epsilon\nabla_\mu\left(k^\mu\nabla_\nu\xi\right) + i\epsilon k^\mu\nabla_\nu\nabla_\mu\xi, \end{aligned} \tag{2.7.25}$$

and

$$\begin{aligned} i\epsilon k_\nu\nabla_\mu\nabla^\mu\xi &= i\epsilon\nabla_\mu\left(k_\nu\nabla^\mu\xi\right) - i\epsilon\nabla^\mu\xi\nabla_\mu k_\nu \\ &= i\epsilon\nabla_\mu\left(k_\nu\nabla^\mu\xi\right) - i\epsilon\nabla_\nu\left(k_\mu\nabla^\mu\xi\right) + i\epsilon k_\mu\nabla_\nu\nabla^\mu\xi \\ &= i\epsilon\nabla_\mu\left(k_\nu\nabla^\mu\xi\right) + i\epsilon k^\mu\nabla_\nu\nabla_\mu\xi. \end{aligned} \tag{2.7.26}$$

By substituting in the expression (2.7.24) we obtain:

$$B_\nu + k_\nu\alpha + k_\nu k^\mu\nabla_\mu\xi = 0. \tag{2.7.27}$$

Then, expression (2.7.16) is gauge invariant, just if we consider an additional transformation given by

$$\alpha \to \alpha - k^\mu\nabla_\mu\xi. \tag{2.7.28}$$

2.7.0.1 Conserved current

If we contract the expression (2.7.16) with the complex conjugate of the polarization vector $\bar{\phi}_\nu$, we obtain:

$$2\bar{\phi}^\nu k^\mu\nabla_\mu\phi_\nu + \bar{\phi}^\nu\phi_\nu\nabla_\mu k^\mu - \bar{\phi}^\nu k_\nu\left(\nabla_\mu\phi^\mu - \alpha\right) = 0. \tag{2.7.29}$$

The complex conjugate of the gauge condition (2.7.6), with α a real function, is

$$\bar{\phi}_\mu k^\mu = -i\epsilon\bar{\alpha}(x^\mu). \tag{2.7.30}$$

Then, the expression (2.7.29) becomes

$$2\bar{\phi}^\nu k^\mu \nabla_\mu \phi_\nu + \bar{\phi}^\nu \phi_\nu \nabla_\mu k^\mu - i\epsilon\bar{\alpha}\bar{\phi}^\nu k_\nu \nabla_\mu \phi^\mu + i\epsilon\bar{\phi}^\nu k_\nu \bar{\alpha}\alpha = 0. \tag{2.7.31}$$

By adding its complex conjugate to the expression and considering the limit $\epsilon \to 0$, the continuity equation is obtained:

$$\begin{aligned} 0 &= 2\bar{\phi}^\nu k^\mu \nabla_\mu \phi_\nu + 2\bar{\phi}^\nu \phi_\nu \nabla_\mu k^\mu + 2\phi^\nu k^\mu \nabla_\mu \bar{\phi}_\nu && (2.7.32)\\ &= 2k^\mu \nabla_\mu \left(\bar{\phi}^\nu \phi_\nu\right) + 2\bar{\phi}^\nu \phi_\nu \nabla_\mu k^\mu && (2.7.33)\\ &= 2\nabla_\mu \left(\bar{\phi}^\nu \phi_\nu k^\mu\right) = -2\nabla_\mu \left(\phi^2 k^\mu\right) = -2\partial_\mu \left(\sqrt{g}\phi^2 k^\mu\right). && (2.7.34) \end{aligned}$$

where $\phi^2 := -g^{\mu\nu}\bar{\phi}_\mu \phi_\nu$, it can be shown it is gauge invariant to leading order in ϵ, by performing a gauge transformation

$$\begin{aligned} \phi^2 \to & -g^{\mu\nu}\left(\bar{\phi}_\mu + k_\mu \xi\right)\left(\phi_\nu + k_\nu \xi\right) \\ & -g^{\mu\nu}\left(\bar{\phi}_\mu \phi_\nu + \xi k_\mu \phi_\nu + \xi k_\mu k_\nu \xi + \xi \bar{\phi}_\mu k_\nu\right) \\ & -g^{\mu\nu}\bar{\phi}_\mu \phi_\nu - i\epsilon\alpha\xi + i\epsilon\alpha\xi \\ \phi^2 \to & -g^{\mu\nu}\bar{\phi}_\mu \phi_\nu := \phi^2 + \mathcal{O}(\epsilon). \end{aligned} \tag{2.7.35}$$

Thus, $\mathcal{J}^\mu := \sqrt{g}\phi^2 k^\mu$ is a vector density that is gauge invariant. We can interpret $\mathcal{J}^\mu$ as a conserved current, i.e.

$$\partial_\mu \mathcal{J}^\mu = 0. \tag{2.7.36}$$

2.7.0.2 Parallel transport

It is possible to rewrite expression (2.7.32) as:

$$\begin{aligned} 2\bar{\phi}^\nu k^\mu \nabla_\mu \phi_\nu + 2\bar{\phi}^\nu \phi_\nu \nabla_\mu k^\mu + 2g^{\nu\sigma}\phi_\sigma k^\mu \nabla_\mu \bar{\phi}_\nu &= 0, \\ 2\bar{\phi}^\nu k^\mu \nabla_\mu \phi_\nu - 2\phi^2 \nabla_\mu k^\mu + 2\phi_\sigma k^\mu \nabla_\mu \bar{\phi}^\sigma &= 0, \\ -2k^\mu \nabla_\mu \phi^2 - 2\phi^2 \nabla_\mu k^\mu &= 0, \\ -4\phi k^\mu \nabla_\mu \phi - 2\phi^2 \nabla_\mu k^\mu &= 0, \end{aligned} \tag{2.7.37}$$

and the following relation is obtained:

$$\nabla_\mu k^\mu = -\frac{2}{\phi} k^\mu \nabla_\mu \phi, \tag{2.7.38}$$

where $\phi = +\sqrt{\phi^2}$. By substituting the expression (2.7.38) into (2.7.16), we find

$$2k^\mu \nabla_\mu \phi_\nu + \phi_\nu \left(-\frac{2}{\phi} k^\mu \nabla_\mu \phi \right) - k_\nu \left(\nabla_\mu \phi^\mu - \alpha \right) = 0. \tag{2.7.39}$$

Defining the polarization vector ψ_ν as

$$\phi_\nu := \phi \psi_\nu = \phi(x) \psi_\nu, \tag{2.7.40}$$

Then, expression (2.7.39) can be rewritten as

$$\begin{aligned} 2k^\mu \nabla_\mu \left(\phi \psi_\nu \right) + \phi \psi_\nu \left(-\frac{2}{\phi} k^\mu \nabla_\mu \phi \right) - k_\nu \left(\nabla_\mu \left(\phi \psi^\mu \right) - \alpha \right) = 0 \\ 2\phi k^\mu \nabla_\mu \psi_\nu + 2\psi_\nu k^\mu \nabla_\mu \phi - 2\psi_\nu k^\mu \nabla_\mu \phi - k_\nu \left(\nabla_\mu \left(\phi \psi^\mu \right) - \alpha \right) = 0 \\ 2\phi k^\mu \nabla_\mu \psi_\nu - k_\nu \left(\nabla_\mu \left(\phi \psi^\mu \right) - \alpha \right) = 0. \end{aligned} \tag{2.7.41}$$

Thus, we obtain

$$k^\mu \nabla_\mu \psi_\nu = \left(\frac{k_\nu \left(\nabla_\mu \left(\phi \psi^\mu \right) - \alpha \right)}{2\phi} \right) k_\nu. \tag{2.7.42}$$

Since α is an arbitrary parameter, we can write

$$k^\mu \nabla_\mu \psi_\nu = \beta k_\nu. \tag{2.7.43}$$

In this way, we obtain an expression for the transport of the polarization vector along a null geodesic. We note that on the right-hand side of the equation there remains a residual gauge freedom. However, it can be shown that the form of this expression is invariant: indeed, the polarization vector inherits the following gauge transformation

$$\psi_\nu \to \psi_\nu + k_\nu \frac{\xi}{\phi}. \tag{2.7.44}$$

Applying this transformation, together with the gauge transformation for α given by (2.7.28), to the equation (2.7.42), we have

$$k^\mu \nabla_\mu \left(\psi_\nu + k_\nu \frac{\xi}{\phi} \right) = \beta' k_\nu \tag{2.7.45}$$

$$k^\mu \nabla_\mu \psi_\nu + k^\mu \nabla_\mu \left(k_\nu \frac{\xi}{\phi} \right) = \beta' k_\nu \tag{2.7.46}$$

$$k^\mu \nabla_\mu \psi_\nu + \frac{\xi}{\phi} k^\mu \nabla_\mu k_\nu + k_\nu k^\mu \nabla_\mu \left(\frac{\xi}{\phi} \right) = \beta' k_\nu. \tag{2.7.47}$$

The second term vanishes due to (2.7.18), thus we obtain

$$k^\mu \nabla_\mu \psi_\nu = \left(\beta' - k^\mu \nabla_\mu \left(\frac{\xi}{\phi} \right) \right) k_\nu. \tag{2.7.48}$$

By introducing the integral curves of $u^\mu = k^\mu / E$ given by $dx^\mu / d\lambda = u^\mu$ where E is an arbitrary constant with units of energy, we can write equation (2.7.42) in the form

$$\frac{D\psi_\mu}{D\lambda} = \beta u_\mu, \tag{2.7.49}$$

where $D\psi^\mu / D\lambda \equiv d/d\lambda + (dx^\nu / d\lambda) \Gamma^\mu_{\nu\rho} \psi^\rho$. In this way, the transport of the polarization vector is given by parallel transport along the null geodesics of u^μ, with an arbitrary gauge transformation.

2.7.1 Localization

The WKB approximation is not sufficient to guarantee that the wave packet is localized or that it remains localized under evolution. To ensure a good localization of the wave packet, it is necessary to consider the following:

- The photon must exhibit non-vanishing sub-exponential tails when propagating through curved spacetimes [51], which we will neglect [52], and we treat the wavepacket as effectively having compact support within a small region much smaller than the typical curvature scale.

- The envelope ϕ must be rigidly transported along the trajectory. The continuity equation $\nabla_\mu (\phi^2 u^\mu) = 0$, allows the rigid evolution under the assumption that $\nabla_\mu u^\mu = 0$. The quantity $\nabla_\mu u^\mu$ quantifies the change of cross-sectional area element A transverse to u^μ in an arbitrary reference

frame given by the following identity [53]:

$$\nabla_\mu u^\mu = \frac{1}{A}\frac{dA}{d\lambda}. \tag{2.7.50}$$

Hence, if we consider $\nabla_\mu u^\mu \approx 0$ the continuity equation (2.7.38) becomes:

$$\nabla_\mu u^\mu = -\frac{2}{\phi} u^\mu \nabla_\mu \phi = 0. \tag{2.7.51}$$

The envelope ϕ does not vary as it moves along the trajectory, therefore, the wave packet is transported rigidly along the trajectory. Furthermore, assuming that the polarization vector ψ^I does not vary spatially within the wave packet, we can effectively describe the system as a polarization vector $\psi^\mu(\lambda)$.

In this way, a photonic qubit can be characterized by a position $x^\mu(\lambda)$, a wave vector $k^\mu(\lambda)$, and a complex polarization vector ψ_μ [46].

2.7.2 Qubit localization as Photon Polarization

In the tetrad basis and for $\epsilon = 0$, the orthogonality condition (2.7.6) can be written as:

$$\begin{aligned} u_\mu \psi^\mu &= i\epsilon\alpha = 0 \\ u_I e^I_\mu \psi^J e^\mu_J &= 0. \end{aligned} \tag{2.7.52}$$

The remaining gauge freedom (2.7.44) in the tetrad basis is given by:

$$\begin{aligned} \psi_\mu &\to \psi_\mu + u_\mu \frac{\xi}{\phi} E = \psi_\mu + u_\mu v \qquad , v = \frac{\xi}{\phi} \\ \psi_I e^I_\mu &\to \psi_I e^I_\mu + u_I e^I_\mu v. \end{aligned} \tag{2.7.53}$$

By contracting both sides with e^J_μ, we obtain

$$\psi_J \to \psi_J + u_J v. \tag{2.7.54}$$

It can be shown that given (2.7.53), the following holds:

$$u_I \left(\psi^I + u^I v\right) = 0, \tag{2.7.55}$$

since $u_\mu u^\mu = u_I u^I = 0$. Now, we can choose the more suitable v for our proposals. We can see the effect of the gauge transformation on the polarization vector if we adapt the tetrad reference frame e^μ_I to the movement of the photon, such that $u^\mu \propto e^\mu_{\hat{0}} + e^\mu_{\hat{3}}$. It is easy note that

$$u^\mu u_\mu \propto g_{\mu\nu}\left(e^\mu_{\hat{0}} + e^\mu_{\hat{3}}\right)\left(e^\nu_{\hat{0}} + e^\nu_{\hat{3}}\right) \tag{2.7.56}$$

$$\propto g_{\mu\nu}\left(e^\mu_{\hat{0}} e^\mu_{\hat{0}} + 2e^\mu_{\hat{3}} e^\mu_{\hat{0}} + e^\mu_{\hat{3}} e^\mu_{\hat{3}}\right) \tag{2.7.57}$$

$$\propto (\eta_{\hat{0}\hat{0}} + \eta_{\hat{3}\hat{3}}) = 0. \tag{2.7.58}$$

Notice that this choice of the tetrad is not unique.
It is possible to write $\bar{u}^\mu = e^\mu_{\hat{0}} + e^\mu_{\hat{3}}$, defining a suitable rescaling of wave vector u^μ, such that $e^{\hat{0}}(dx^\mu/d\lambda) = 1$. In the tetrad components $\bar{u}^I = (1, 0, 0, 1)$. If $\bar{u}_I \psi^I = 0 = \psi^{\hat{0}} - \psi^{\hat{3}}$, then $\psi^{\hat{0}} = \psi^{\hat{3}} = \nu$. The polarization vector in tetrad components is

$$\psi = \begin{pmatrix} \nu \\ \psi^1 \\ \psi^2 \\ \nu \end{pmatrix}. \tag{2.7.59}$$

If we apply a gauge transformation

$$\psi^I = \begin{pmatrix} \nu \\ \psi^{\hat{1}} \\ \psi^{\hat{2}} \\ \nu \end{pmatrix} \qquad \rightarrow \qquad \psi^I + v\bar{u}^I = \begin{pmatrix} \nu + v \\ \psi^{\hat{1}} \\ \psi^{\hat{2}} \\ \nu + v \end{pmatrix}. \tag{2.7.60}$$

The two complex components ψ^1 and ψ^2 are the components in the tetrad frame of the quantum state in the linear polarization basis:

$$|1\rangle \sim \begin{pmatrix} 0 \\ 1 \\ 0 \\ 0 \end{pmatrix}, \qquad \text{and} \qquad |2\rangle \sim \begin{pmatrix} 0 \\ 0 \\ 1 \\ 0 \end{pmatrix}. \tag{2.7.61}$$

The quantum state of light can be written in polarization basis or Jones vector using the diad formalism[9] $\psi^I = f^I_B \psi^B$:

$$\begin{aligned} |\psi\rangle \sim \psi^A &= f^A_I \psi^I \\ &= \begin{pmatrix} \psi^1 \\ \psi^2 \end{pmatrix}. \end{aligned} \tag{2.7.62}$$

2.7.3 Wigner rotation

Using the tetrad formalism in the transport equation (2.7.49), we obtain

$$\frac{D}{D\lambda}\left(\psi^I e^\mu_I\right) = \beta\, u^J e^\mu_J. \tag{2.7.63}$$

Expanding and multiplying by e^J_μ we obtain

$$\left(\frac{D\psi^J}{D\lambda}\right) + \psi^I \left(\frac{De^\mu_I}{D\lambda}\right) e^J_\mu = \beta u^J. \tag{2.7.64}$$

Where $D(e^\mu_I)/D\lambda = (dx^\sigma/d\lambda)\nabla_\sigma e^\mu_I = u^\sigma \nabla_\sigma e^\mu_I$, then

$$\frac{D(e^\mu_I)}{D\lambda} e^J_\mu = u^\sigma \left(\nabla_\sigma e^\mu_I\right) e^J_\mu = u^\sigma \omega_{\sigma\ I}^{\ J}. \tag{2.7.65}$$

By substituting (2.7.65) in (2.7.64) we obtain

$$\left(\frac{D\psi^J}{D\lambda}\right) + u^\sigma \omega_{\sigma\ I}^{\ J} \psi^I = \beta u^J. \tag{2.7.66}$$

Where $\omega_{\mu\ I}^{\ J}$ is the spin connection (for more details see A), given by

$$\omega_{\mu\ J}^{\ I} = e^I_\rho \partial_\mu e^\rho_J + \Gamma^\sigma_{\mu\rho} e^I_\sigma e_J^{\ \rho}. \tag{2.7.67}$$

Using the diad formalism $\psi^I = f^I_B \psi^B$ in the equation (2.7.66) we obtain

$$\frac{D(\psi^B)}{D\lambda} f^I_B + \psi^B \frac{D(f^I_B)}{D\lambda} + u^\mu \omega_{\mu\ J}^{\ I} f^J_C \psi^C = \beta\, u^I. \tag{2.7.68}$$

[9] A diad frame $f^I_A \equiv (f^I_1, f^I_2)$ defines a spacelike two-dimensional space.

Multiplying by f^A_I and reordering, we obtain

$$\frac{D\psi^A}{D\lambda} = -\left(u^\mu f^A_I\, \omega_{\mu\ J}^{\ I} f^J_B + f^A_I \frac{D f^I_B}{D\lambda}\right)\psi^B + \beta f^A_I u^I. \tag{2.7.69}$$

As f^A_I is the diad frame, which is defined to be orthogonal to u^I, the term $f^A_I u^I$ vanishes and in a adapted tetrad $f^A_I = \delta^a_I$ so that $Df^A_I/D\lambda = 0$. Therefore the equation (2.7.69) becomes

$$\frac{D\psi^A}{D\lambda} = -u^\mu f^A_I \omega_{\mu\ J}^{\ I} f^J_B \psi^B. \tag{2.7.70}$$

Since the spin connection is antisymmetric ($\omega_{\nu\ JI} = -\omega_{\nu\ IJ}$), then

$$\begin{aligned}
\frac{D\psi^A}{D\lambda} &= -u^\mu f^A_I \omega^R_{\mu\ J}\, \delta^I_R\, f^J_B \psi^B \\
&= -u^\mu f^A_I \omega^R_{\mu\ J}\, \eta_{RL}\eta^{LI}\, f^J_B \psi^B \\
&= -u^\mu f^A_I f^J_B\, \omega_{\mu LJ}\, \eta^{LI}\, \psi^B \\
&= -u^\mu \left(\omega_{\mu L1} f^A_I \eta^{LI}\psi^1 + \omega_{\mu L2} f^A_I \eta^{LI}\psi^2\right).
\end{aligned} \tag{2.7.71}$$

Therefore, for values of the index A, we obtain the following:

$$\begin{aligned}
A = 1, &\qquad f^1_I f^J_B\, \omega_{\mu LJ}\, \eta^{LI}\, \psi^B = -\omega_{\mu 12}\psi^2. \\
A = 2, &\qquad f^2_I f^J_B\, \omega_{\mu LJ}\, \eta^{LI}\, \psi^B = \omega_{\mu 12}\psi^1.
\end{aligned} \tag{2.7.72}$$

Then

$$\frac{D}{D\lambda}\begin{pmatrix}\psi^1\\ \psi^2\end{pmatrix} = u^\mu\omega_{\mu 12}\begin{pmatrix}\psi^2\\ -\psi^1\end{pmatrix} = u^\mu\omega_{\mu 12}\begin{pmatrix}0 & 1\\ -1 & 0\end{pmatrix}\begin{pmatrix}\psi^1\\ \psi^2\end{pmatrix} \tag{2.7.73}$$

$$= iu^\mu\omega_{\mu 12}\begin{pmatrix}0 & -i\\ i & 0\end{pmatrix}\begin{pmatrix}\psi^1\\ \psi^2\end{pmatrix}. \tag{2.7.74}$$

Finally, we can write

$$\frac{D\psi^A}{D\lambda} = iu^\mu\omega_{\mu 12}(\sigma_y)^A_{\ B}\psi^B. \tag{2.7.75}$$

We can now readily identify the infinitesimal Wigner rotation in an adapted tetrad as $W^A_{\ B} = iu^\mu\omega_{\mu 12}(\sigma_y)^A_{\ B}$ where $A, B \in \{1, 2\}$ denotes the components of a photon in the linear polarization basis. Then, we have two coupling differentials equation

that describe the polarization rotation of a photon given by

$$\frac{D\psi^{\hat{1}}}{D\lambda} - W_2^1\psi^{\hat{2}} = 0 \qquad \text{and} \qquad \frac{D\psi^{\hat{2}}}{D\lambda} + W_2^1\psi^{\hat{1}} = 0, \tag{2.7.76}$$

where $W_2^1 = u^\mu\omega_{\mu 12} = -u^\mu\omega_{\mu 21}$ is the Wigner rotation.

2.7.4 Wigner phase and helicity states

The evolution of the polarization state must be given by a unitary operation:

$$\psi^A(\lambda) = U(\lambda)^A_{\ B}\psi^B(0). \tag{2.7.77}$$

To find the form of the unitary operator, we must solve the differential equation given in (2.7.75). We start by differentiating the expressions (2.7.76) with respect to the parameter λ, then

$$\frac{d^2\psi^{\hat{1}}}{d\lambda^2} - \frac{dW_2^1}{d\lambda}\psi^{\hat{2}} - W_2^1\frac{d\psi^{\hat{2}}}{d\lambda} = 0. \tag{2.7.78}$$

Now, by substituting from the equation (2.7.76), it is possible to write the previous expression in terms of $\psi^{\hat{1}}$, that is,

$$\frac{d^2\psi^{\hat{1}}}{d\lambda^2} - \frac{1}{W_2^1}\frac{dW_2^1}{d\lambda}\frac{d\psi^{\hat{1}}}{d\lambda} + (W_2^1)^2\psi^{\hat{1}} = 0. \tag{2.7.79}$$

If we consider $\vartheta(\lambda)$ as the accumulated angle up to the parameter λ, it is interpreted as a geometric phase.

$$\vartheta(\lambda) = \int_0^\lambda W_2^1(\lambda')d\lambda'. \tag{2.7.80}$$

And the following change of variable:

$$\frac{d}{d\lambda} = \frac{d\vartheta}{d\lambda}\frac{d}{d\vartheta} = W_2^1(\lambda)\frac{d}{d\vartheta}. \tag{2.7.81}$$

The equation (2.7.79) becomes

$$\frac{d^2\psi^{\hat{1}}}{d\vartheta^2} + \psi^{\hat{1}} = 0, \tag{2.7.82}$$

which has the general solution:

$$\psi^{\hat{1}}(\lambda) = A\cos(\vartheta(\lambda)) + B\sin(\vartheta(\lambda)). \tag{2.7.83}$$

Using (2.7.76), we find the solution for $\psi^{\hat{2}}$:

$$\psi^{\hat{2}}(\lambda) = \frac{d\psi^{\hat{1}}}{d\vartheta} = -A\sin(\vartheta) + B\cos(\vartheta). \tag{2.7.84}$$

With this, and imposing the initial conditions, we obtain the following unitary operator:

$$\begin{pmatrix} \psi^{\hat{1}}(\lambda) \\ \psi^{\hat{2}}(\lambda) \end{pmatrix} = \begin{pmatrix} \cos(\vartheta) & \sin(\vartheta) \\ -\sin(\vartheta) & \cos(\vartheta) \end{pmatrix} \begin{pmatrix} \psi^{\hat{1}}(0) \\ \psi^{\hat{2}}(0) \end{pmatrix}. \tag{2.7.85}$$

We can write the expresion (2.7.85) as $\psi^I = R^I_{\ J}(\vartheta)\psi^J$, where $R^I_{\ J}(\vartheta)$ can be recognized as a rotation matrix. When considering the helicity states given by

$$\psi^s(0) = \frac{1}{\sqrt{2}}\left(\psi^{\hat{1}}(0) - s\, i\psi^{\hat{2}}(0)\right), \tag{2.7.86}$$

where $s = \pm 1$, the unitary operation in the helicity basis becomes

$$\begin{pmatrix} \psi^{-1}(\lambda) \\ \psi^{+1}(\lambda) \end{pmatrix} = \begin{pmatrix} e^{-i\vartheta} & 0 \\ 0 & e^{i\vartheta} \end{pmatrix} \begin{pmatrix} \psi^{-1}(0) \\ \psi^{+1}(0) \end{pmatrix}. \tag{2.7.87}$$

From now on, to simplify the notation we will use Dirac notation $\psi^s \to |s\rangle$. In this way, the action of the unitary operator on a helicity state can be written as:

$$U(\vartheta)\,|s\rangle = e^{si\vartheta}\,|s\rangle\,. \tag{2.7.88}$$

Where ϑ is the Wigner phase (2.7.80).

2.7.5 Phases and Interference in WKB approximation

In the previous sections, we obtained the phase acquired by a wave packet in the WKB approximation as it is transported through a curved spacetime. However, not all contributions to the global phase are accounted for in the transport equations

(2.7.49). Considering a wave packet within this approximation,

$$\mathbf{\Psi}_\sigma(x^\mu) = \varphi(x^\mu)\psi_\sigma(x^\mu)e^{i\vartheta^\tau(x^\mu)}, \tag{2.7.89}$$

where $\vartheta^\tau(x^\mu)$ is a phase that is not included in $\psi_\sigma(x^\mu)$. If we consider a wave packet that is transported through a spacetime in the helicity basis, it is easy to note that the total phase is given by

$$\vartheta_{\text{Total}} = \vartheta^\tau + \vartheta, \tag{2.7.90}$$

which corresponds to the phase of the wave packet obtained from the inner product of the wave vector obtained in the WKB approximation (2.7.17) and the other due to the rotation of the polarization (2.7.88), respectively.

The total phase enters as a global phase in the wave packet, which cannot be observed if we only consider a single photon moving along one trajectory. However, in Quantum Mechanics, it is possible to consider experiments where a single photon is in spatial superposition and travels along different trajectories simultaneously, recombining at a point afterwards, which will produce interference. In this way, it is possible to obtain the phase difference between the states in superposition and how this directly affects the detection probabilities. The states in spatial superposition are transported along two different paths in the metric $g_{\mu\nu}$; this suggests that the phase acquired along each path will be different.

2.7.5.1 Phase difference in spacetime interferometry

We want to generate interference of a state in spatial superposition. To this end, we will consider a Mach-Zehnder type interferometer that produces this spatial superposition using a beam-splitter [54, 55]. The state in superposition travels through spacetime along different paths Γ_1 and Γ_2, to then interfere at another beamsplitter, producing two possible output states which are measured by detectors D_1 and D_2, see figure 2.7.1.

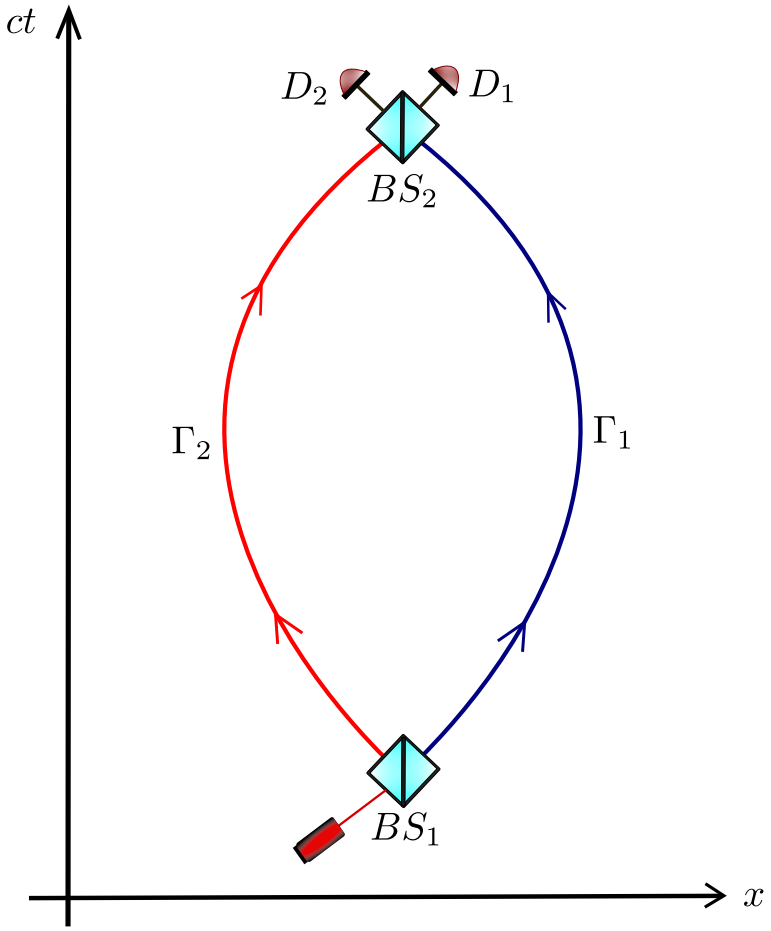

Figure 2.7.1: Geodesic Interferometer: A particle propagates in a superposition of two geodesic paths, Γ_1 and Γ_2, which subsequently interfere at the beam splitter BS_2. Adapted from [46].

The wave packet after the second beamsplitter at detector D_1 will be given by:

$$\Psi = a\Psi_\sigma^{\Gamma_1} + b\Psi_\sigma^{\Gamma_2}. \tag{2.7.91}$$

We will ignore for now any global phase and any phase due to reflections.

With the intention of finding the phase difference due to a Mach-Zehnder type interference, we will make use of the equations in the WKB approximation and the localization assumptions. We will see that the components in the superposition, $a\Psi_\sigma^{\Gamma_1}$ and $b\Psi_\sigma^{\Gamma_2}$ differ in the accumulated phase due to the rigid transport of the envelope. So, the wave packet at detector D_1 written explicitly in some local frame is given by

$$\Psi = aA^I_{\Gamma_1}(x) + bA^I_{\Gamma_2}(x) = a\varphi_1(x)\psi^I_{\Gamma_1}(x)e^{i\vartheta_1^\tau(x)} + b\varphi_2(x)\psi^I_{\Gamma_2}(x)e^{i\vartheta_2^\tau(x)}. \tag{2.7.92}$$

Given the localization assumptions, the envelopes are rigidly transported along the trajectories. Therefore, we have that $\varphi_1(x) \approx \varphi_2(x)$, and the recombined state (2.7.93) becomes

$$\Psi \approx \varphi_1(x) e^{i\vartheta_1^\tau(x)} \left(a\psi_{\Gamma_1}^I(x) + b\psi_{\Gamma_2}^I(x) e^{i\Delta\vartheta^\tau(x)} \right), \tag{2.7.93}$$

where $\Delta\vartheta^\tau(x) = \vartheta_2^\tau(x) - \vartheta_1^\tau(x)$. As is known in (2.7.90), $\Delta\vartheta^\tau$ is not the only phase difference obtained in the Mach-Zehnder type interferometer, since the polarization states, as they are transported through spacetime, can contain a phase given by the transport equation of the polarization vector (2.7.80). This phase difference due to the rotation of the polarization state can be determined by [56]:

$$e^{i\Delta\vartheta} = \frac{\langle \psi_{\Gamma_1} | \psi_{\Gamma_2} \rangle}{| \langle \psi_{\Gamma_1} | \psi_{\Gamma_2} \rangle |}. \tag{2.7.94}$$

Then the total phase difference measured in a Mach-Zehnder interferometer is given by:

$$\Delta\vartheta_{\text{Total}} = \Delta\vartheta^\tau + \Delta\vartheta. \tag{2.7.95}$$

2.8 Photon state

Considering a photonic wave packet with distribution in frequency [57] and for each frequency state corresponding a helicity state in superposition of positive and negative helicity eigenstate, then we have the momentum-helicity eigenstate $|\mathbf{k}, s\rangle$ [6]. In the case of a coherent superposition of the helicity state, the initial pure quantum state is

$$|\psi\rangle = \frac{1}{\sqrt{2}} \sum_{s=\pm 1} \int d\mathbf{k} f(\mathbf{k}) |\mathbf{k}, s\rangle, \tag{2.8.1}$$

where $\mathbf{k} = (k^0, k^1, k^2, k^3)$. When the momentum state acquires a phase given by:

$$|\psi\rangle = \frac{1}{\sqrt{2}} \sum_{s=\pm 1} \int d\mathbf{k} f(\mathbf{k}) e^{-i\vartheta^\tau(\mathbf{k})} |\mathbf{k}, s\rangle, \tag{2.8.2}$$

the state in the local frame [6] is given by

$$|\psi\rangle = \frac{1}{\sqrt{2}} \sum_{s=\pm 1} \int d\hat{\mathbf{k}} f(\hat{\mathbf{k}}) \left| \hat{\mathbf{k}}, s \right\rangle, \tag{2.8.3}$$

where $\hat{\mathbf{k}} = (k^{\hat{0}}, k^{\hat{1}}, k^{\hat{2}}, k^{\hat{3}})$ is the null vector components in the tetrad adapted basis. In the local frame the state becomes

$$|\psi\rangle = \frac{1}{\sqrt{2}} \sum_{s=\pm 1} \int d\hat{\mathbf{k}} f(\hat{\mathbf{k}}) e^{-i\vartheta^{\tau}(\hat{\mathbf{k}})} \left|\hat{\mathbf{k}}, s\right\rangle . \tag{2.8.4}$$

Where $\vartheta^{\tau}(\hat{\mathbf{k}})$ is the transport phase measured in the local frame.

2.8.1 Wigner phase in terms of the local frame

The Wigner phase is obtained by integration of Wigner rotation along the photon's null geodesic follows the equations (2.7.76), i.e

$$\vartheta(\hat{\mathbf{k}}) = \int_{\lambda_i}^{\lambda_f} W_2^1 d\lambda. \tag{2.8.5}$$

Then, the evolution of momentum-helicity state

$$U \left|\hat{\mathbf{k}}, s\right\rangle = e^{is\vartheta(\hat{\mathbf{k}})} \left|\hat{\mathbf{k}}_f, s\right\rangle . \tag{2.8.6}$$

With $\hat{\mathbf{k}}_f$ is the local frame momentum at the end point λ_f. Note that each state adquires a different Wigner phase factor given by the helicity s, for more details see [46].

Chapter 3

Testing alternative metric theories using Quantum state discrimination theory

3.1 Abstract

Here, we study the possibility of distinguishing between metric theories within the PPN formalism using various strategies for discriminating non-orthogonal quantum states. We consider the temporal evolution of a massive quantum clock, that is, a massive particle endowed with a two-dimensional inner degree of freedom. The final quantum state of the clock is a function of the post-Newtonian parameters that characterize a metric theory. The quantum clock states of various metric theories are mutually non-orthogonal and, consequently, cannot be discriminated deterministically and with certainty at the same time. Thereby, quantum state discrimination strategies are required. We first show a simple scheme, based on a von Neumann measurement, that allows for ruling out the hypothesis that a particular metric theory describes spacetime. In the case of two competing metric theories, we use minimum-error discrimination. This makes it possible to determine which of the metric theories is verified, although with a minimal probability of error. This result can be improved using unambiguous state discrimination, which allows to distinguish between two metric theories without misidentification error, albeit resorting to a generalized quantum measurement and with a smaller success probability than using minimum-error discrimination. The success probability of each one of these three approaches is an harmonic function of the difference of the

proper time corresponding to each quantum clock state. Thus, it is possible to optimize the probability of success to reach 1. However, this requires a particular propagation length, which turns out to be independent of the mass of the quantum clock and inversely proportional to the energy difference of the energy eigenstates of the quantum clock. This favors the choice of atoms as quantum clocks, leading to typical lengths in the order 10^4 (m).

3.2 State evolution

Assuming that the quantum system travels a proper distance L, then we have $\Delta t = L/v$, where v is the constant speed of the quantum system. Defining $\bar{\lambda} = (L/v)\lambda$ the final state of the quantum system is

$$\hat{U}\,|\Psi\rangle = e^{-\frac{i}{\hbar}\Delta t H_{\rm cm}^{\rm rel}}\,|\gamma\rangle \otimes \frac{e^{-\frac{i}{\hbar}\bar{\lambda}E_0}}{\sqrt{2}}(|0\rangle + e^{-\frac{i}{\hbar}\bar{\lambda}\Delta E}\,|1\rangle), \tag{3.2.1}$$

where $\Delta E = E_1 - E_0$. The previous expression shows that the center-of-mass motion and the inner degree of freedom are in a separable state. Since the measurements we will study do not involve the center-of-mass motion, this degree of freedom can be traced out while the quantum clock stays in the pure state given by

$$|\psi\rangle = \frac{1}{\sqrt{2}}(|0\rangle + e^{-\frac{i}{\hbar}\bar{\lambda}\Delta E}\,|1\rangle), \tag{3.2.2}$$

where we have omitted a global phase. This state depends on the post-Newtonian parameters γ and β through the function $\bar{\lambda}$. Thus, the final state of a quantum clock becomes a signature of a metric theory. For two of these states

$$|\psi_1\rangle = \frac{1}{\sqrt{2}}(|0\rangle + e^{-\frac{i}{\hbar}\bar{\lambda}_1\Delta E}\,|1\rangle) \tag{3.2.3}$$

and

$$|\psi_2\rangle = \frac{1}{\sqrt{2}}(|0\rangle + e^{-\frac{i}{\hbar}\bar{\lambda}_2\Delta E}\,|1\rangle) \tag{3.2.4}$$

the inner product is

$$\langle\psi_1|\psi_2\rangle = \frac{1}{2}(1 + e^{\frac{i}{\hbar}\Delta E(\bar{\lambda}_1 - \bar{\lambda}_2)}), \tag{3.2.5}$$

which in general does not vanish.

3.3 Simple discrimination scheme

According to the results of the previous subsection, there are as many quantum clock final states as there are conceivable metric theories. This makes the problem of discrimination among metric theories especially difficult. However, a simple picture can be obtained if one tries to rule out or refute a given metric theory with $\gamma = \gamma_1$ and $\beta = \beta_1$ from any other metric theory.

For this purpose, we start by noting that the Hilbert space of the quantum clock is two-dimensional. Thus, if the state $|\psi_1\rangle$ corresponds to a metric theory with γ_1 and β_1 and the state $\left|\psi_1^{\perp}\right\rangle$ is orthogonal to $|\psi_1\rangle$, the two-dimensional identity operator can be represented as

$$\mathbb{I} = |\psi_1\rangle \langle\psi_1| + \left|\psi_1^{\perp}\right\rangle \left\langle\psi_1^{\perp}\right| . \tag{3.3.1}$$

Therefore, we can cast the final quantum clock state $|\psi_2\rangle$ of any other metric theory with $\gamma = \gamma_2$ and $\beta = \beta_2$ as

$$|\psi_2\rangle = \langle\psi_1|\,\psi_2\rangle\,|\psi_1\rangle + \left\langle\psi_1^{\perp}\right|\psi_2\rangle\left|\psi_1^{\perp}\right\rangle . \tag{3.3.2}$$

This suggest to measure the observable (see Fig. 3.3.1)

$$O = \kappa\Pi + \kappa^{\perp}\Pi^{\perp}, \tag{3.3.3}$$

with $\Pi = |\psi_1\rangle \langle\psi_1|$ and $\Pi^{\perp} = \left|\psi_1^{\perp}\right\rangle \left\langle\psi_1^{\perp}\right|$. A measurement of this observable leads to the detection of the eigenvalue $\kappa^{\perp}$ with probability $P(\kappa^{\perp}) = |\left\langle\psi_1^{\perp}\right|\psi_2\rangle|^2 = 1 - |\langle\psi_1|\,\psi_2\rangle|^2$, which generally does not vanish. Thus, a single detection of $\kappa^{\perp}$ would lead to the conclusion that spacetime is described by a metric theory with $\gamma \neq \gamma_1$ or $\beta \neq \beta_1$. The detection of the eigenvalue κ does not allow us to conclude that spacetime is described by a metric theory with γ_1 and β_1, since both states $|\psi_1\rangle$ and $|\psi_2\rangle$ have a component in state $|\psi_1\rangle$.

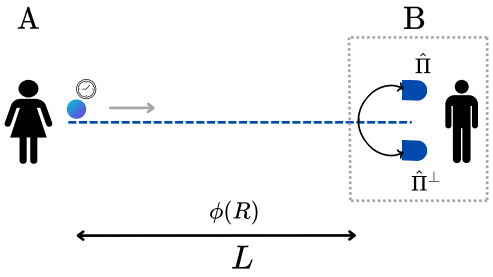

Figure 3.3.1: Scheme to discriminate between two metric theories: (A) Alice prepares a massive particle with internal degrees of freedom and sends it to Bob (B). Bob receives the particle and performs a measurement using the Positive Operator-Valued Measures (Π and $\Pi^{\perp}$). If he has a detection in Π, he concludes that $\gamma = \gamma_1$ and $\beta = \beta_1$ are the corresponding values of the theory. If he has a detection in $\Pi^{\perp}$, then γ and β have different values.

The probability of detecting the eigenvalue $\kappa^{\perp}$ is

$$P(\kappa^{\perp}) = \frac{1}{2}\left(1 - \cos\left(\frac{\Delta E}{\hbar}\Delta\bar{\lambda}\right)\right), \tag{3.3.4}$$

where $\Delta\bar{\lambda} = \bar{\lambda}_1 - \bar{\lambda}_2$ is the difference of arrival times given by

$$\Delta\bar{\lambda} = \frac{L}{v}\frac{\phi(R)}{c^2}\left((\gamma_1 - \gamma_2)\frac{p^2}{m^2c^2} - (\beta_1 - \beta_2)\frac{\phi(R)}{c^2}\right), \tag{3.3.5}$$

which is the difference of proper times between both metric theories. This quantity turns out to be independent of the mass m of the quantum system. Let us now consider a quantum system that follows a trajectory with speed $v = 10$ (m/s) in a constant gravitational field equivalent to that generated by the Earth at a radius $R = 7 \times 10^6$ (m). In this case, we have $v^2/c^2 \approx 10^{-15}$ and $\phi(R)/c^2 \approx 6.35 \times 10^{-10}$. For $\gamma_1 - \gamma_2$ and $\beta_1 - \beta_2$ in the order of 10 we can neglect the term proportional to $\gamma_1 - \gamma_2$. Thereby, we have that

$$\frac{\Delta E}{\hbar}\Delta\bar{\lambda} \approx 6 \times 10^{13}\Delta E L(\beta_1 - \beta_2). \tag{3.3.6}$$

Thus, for an atom with energy difference $\Delta E = 6.62 \times 10^{-19}$ (J), the probability $P(\kappa^{\perp})$ presents values other than zero for L values of the order of 10^4 (m). This is analyzed in more detail in Fig. 3.3.2(a) which shows the behavior of $P(\kappa^{\perp})$ as a function of L for $\gamma_1 = \beta_1 = 1$ and $\gamma_2 = \beta_2 = 0, 1, 3$ for an atom. As we can see, $P(\kappa^{\perp})$ provides a distinctive signature for a departure from a metric theory with

$\gamma_1 = \beta_1 = 1$, where the oscillation period decreases as $\beta_2 = \gamma_2$ increases. Thus, it is possible to find a suitable value of L such that if the metric theory with $\gamma_1 = \beta_1 = 1$ does not describe spacetime, then $P(\kappa^\perp)$ is different from zero.

Figures 3.3.2(b), 3.3.2(c) and 3.3.2(d) illustrates the probability $P(\kappa^\perp)$ for an electron, neutron, and molecule, respectively, where the energy difference ΔE decreases rapidly. In this case, the probability $P(\kappa^\perp)$ can be approximated as

$$P(\kappa^\perp) \approx \frac{1}{4}[6 \times 10^{13} \Delta E L(\beta_1 - \beta_2)]^2, \tag{3.3.7}$$

which leads to extremely small probability values.

The value of $P(\kappa^\perp)$ can be further reduced when $\beta_1 - \beta_2$ is small. This occurs when metric theories have very close post-Newtonian parameters, for example, when trying to rule out a metric theory whose parameters are within the innacuracy of a metric that we suspect describes spacetime. This is shown in Fig. 3.3.3, where our aim is to distinguish a metric theory with $\gamma_1 = \beta_1 = 1$ from a theory with $\gamma_2 = \beta_2 = 1 + 10^{-5}$, which leads to probabilities $P(\kappa^\perp)$ of the order of 10^{-6}. The current uncertainty in the post-Newtonian parameters for General Relativity is in the order of 10^{-5}.

The effect of the speed value v on the value of $P(\kappa^\perp)$ is shown in Fig. 3.3.4 for $\beta_1 - \beta_2 = 10^{-5}$, $L = 4 \times 10^3$ (m) and the gravitational potential of Earth at $R = 7 \times 10^6$ (m). In this case, it is evident that $P(\kappa^\perp)$ decreases rapidly with increasing values of v.

The possibility of falsifying a given metric theory can be implemented by measuring the observable O Eq. (3.3.3). However, having a sufficiently large probability of the appropriate measurement outcome depends on a careful choice of the energy difference ΔE, gravitational potential $\phi(R)$ and the velocity v, for which it is possible to find a length L such that $P(\kappa^\perp)$ does not vanish. In addition, the choice of L depends on the difference $\beta_1 - \beta_2$, which is in principle unknown. We might, however, suspect that a given metric theory describes spacetime, in which case we can find an optimal lenght $L_{\max}$ given by

$$L_{\max} = \frac{2\pi c^4 v \hbar}{\Delta E \phi(R)((\beta_1 - \beta_2)\phi(R) + (\gamma_1 - \gamma_2)v^2)}. \tag{3.3.8}$$

Placing the second observer at $L_{\max}$ ensures that we can observe a deviation from the metric theory with $\gamma = \gamma_1$ and $\beta = \beta_1$ with the highest probability.

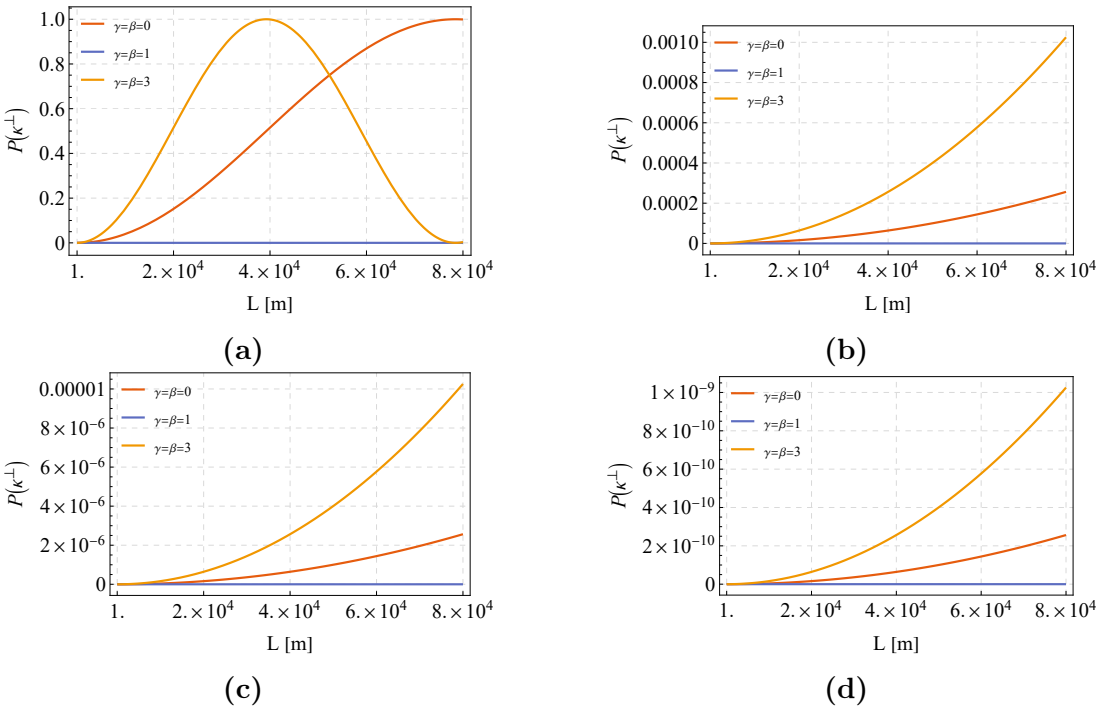

Figure 3.3.2: Detection probability $P(\kappa^{\perp})$ Eq. (3.3.4) as a function of L for (a) atom, (b) electron, (c) molecule, (d) neutron with $\Delta E = 6.61 \times 10^{-19}, 6.62 \times 10^{-21}, 6.62 \times 10^{-22}, 6.62 \times 10^{-24}$ (J), respectively, speed $v = 10$ (m/s) and a constant gravitational field equivalent to that generated by the Earth at a radius $R = 7 \times 10^{6}$ (m).

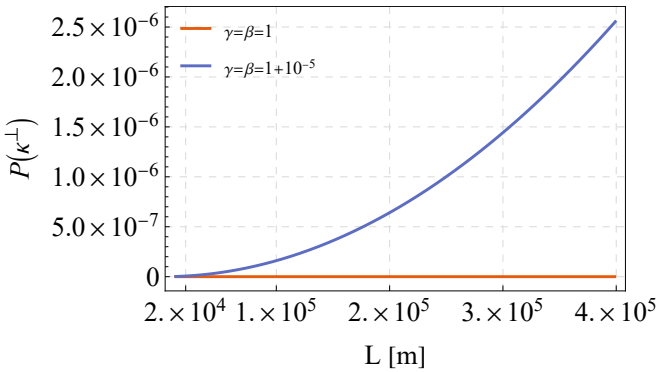

Figure 3.3.3: Probability of detection $P(\lambda^{\perp})$ Eq. (3.3.4) in case of $\gamma = \beta = 1 + 10^{-5}$ in terms of length of the arm of the array L (see Fig. 3.3.1). We have considered the Earth gravitational potential $\phi(R)$ at the radial coordinate $R = 7 \times 10^{3} km$.

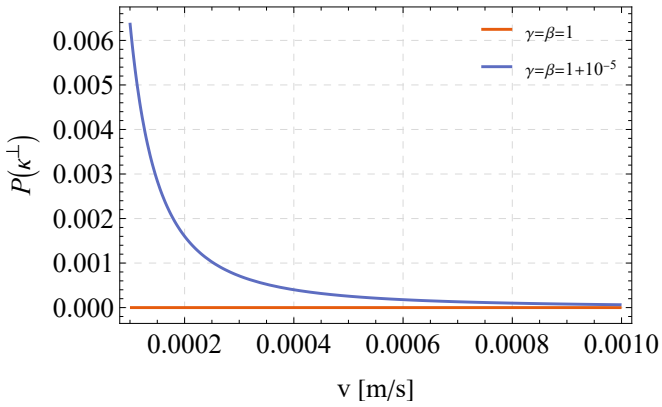

Figure 3.3.4: Probability of detection, $P(\kappa^{\perp})$, as a function of particle velocity, v, for $\gamma = \beta = 1 + 10^{-5}$, fixed proper length $L = 4\,\text{km}$, and Earth's gravitational potential at $R = 7 \times 10^3$ km. (Eq. (3.3.4)).

3.4 Minimum error discrimination

In the previous subsection, we have analyzed a simple scheme to rule out or refute a given metric theory within a set of metric theories. This is achieved by measuring the observable O Eq. (3.3.3). This contains in its spectrum the quantum state $\left|\psi_1^{\perp}\right\rangle$, whose detection can only occur if the spacetime is described by a metric theory whose corresponding quantum state is different from $|\psi_1\rangle$.

A different scenario arises when we attempt to discriminate between two different metric theories, i.e., we have two candidate metric theories to describe spacetime and we need to determine which one is correct. In this case, the measurement to be performed should have the smallest possible probability of misidentification. This is exactly the scenario where minimum error discrimination is used. This discrimination strategy allows us to incorporate a priori information in the form of probabilities that we assign to each metric theory to describe spacetime. The largest average probability of correctly distinguishing the metric theories, is given by the Helstrom bound Eq. (2.2.5), which in our case becomes

$$P_H = \frac{1}{2}(1 - \sqrt{1 - 2\eta_1\eta_2(1 + \cos\left(\frac{\Delta E}{\hbar}\Delta\bar{\lambda}\right)}), \tag{3.4.1}$$

where η_1 and $\eta_2 = 1 - \eta_1$ are the apriori probabilities asigned to each metric

theory. Assuming equal a priori probabilities, the Helstrom bound becomes

$$P_H = \frac{1}{2} - \frac{1}{2}\sqrt{\frac{1-\cos\left(\frac{\Delta E}{\hbar}\Delta\bar{\lambda}\right)}{2}}. \tag{3.4.2}$$

We can compare this strategy with the simple approach based on O Eq. (3.3.3). According to this, the detection of the eigenvalue $\kappa^{\perp}$ (κ) is interpreted as detecting the state $|\psi_2\rangle$ ($|\psi_1\rangle$). Thereby, the average error probability of identifying the state becomes

$$P_E = \frac{1}{2} - \frac{1}{2}P(\kappa^{\perp}). \tag{3.4.3}$$

This can be compared with $P_H = 1/2 - \sqrt{P(\kappa^{\perp})}/2$, which shows that the minimum error discrimination strategy provides a higher average success probability

$$P_S = \frac{1}{2} + \frac{1}{2}\sqrt{\frac{1-\cos\left(\frac{\Delta E}{\hbar}\Delta\bar{\lambda}\right)}{2}} \tag{3.4.4}$$

for all values of ΔE and $\Delta\bar{\lambda}$.

The average success probability P_S Eq. (3.4.4) provided by the minimum error discrimination strategy is shown in Fig. 3.4.1(a) as a function of length L for the case of an atom with $\Delta E = 6.61 \times 10^{-19}$, speed $v = 10$ (m/s) and a constant gravitational field equivalent to that generated by the Earth at a radius $R = 7 \times 10^6$ (m). We discriminate a metric theory with $\gamma_1 = \beta_1 = 1$ from theories with $\gamma_2 = \beta_2 = 0, 1, 3$. As this figure shows, length on the order of 10^4 (m) allows us to distinguish between metric theories, even deterministically. This occurs whenever it is possible to choose a length such that the states $|\psi_1\rangle$ and $|\psi_2\rangle$ become orthogonal. This length is given by

$$L_O = \frac{\pi c^4 v\hbar}{\Delta E\phi(R)\left((\beta_1-\beta_2)\phi(R) + (\gamma_1-\gamma_2)v^2\right)}. \tag{3.4.5}$$

Figures 3.4.1(b), 3.4.1(c) and 3.4.1(d) illustrates the probability P_S Eq. (3.4.4) for an electron, neutron, and molecule, respectively, where the energy difference decreases rapidly. These figures show a very low increase of P_S for the length scale considered, where the success probability exhibits values close to 1/2. Higher success probabilities can be achieved at the expense of increasing the propagation length. Therefore, the use of atoms favors shorter length scales and allows for optimization of the probability of success.

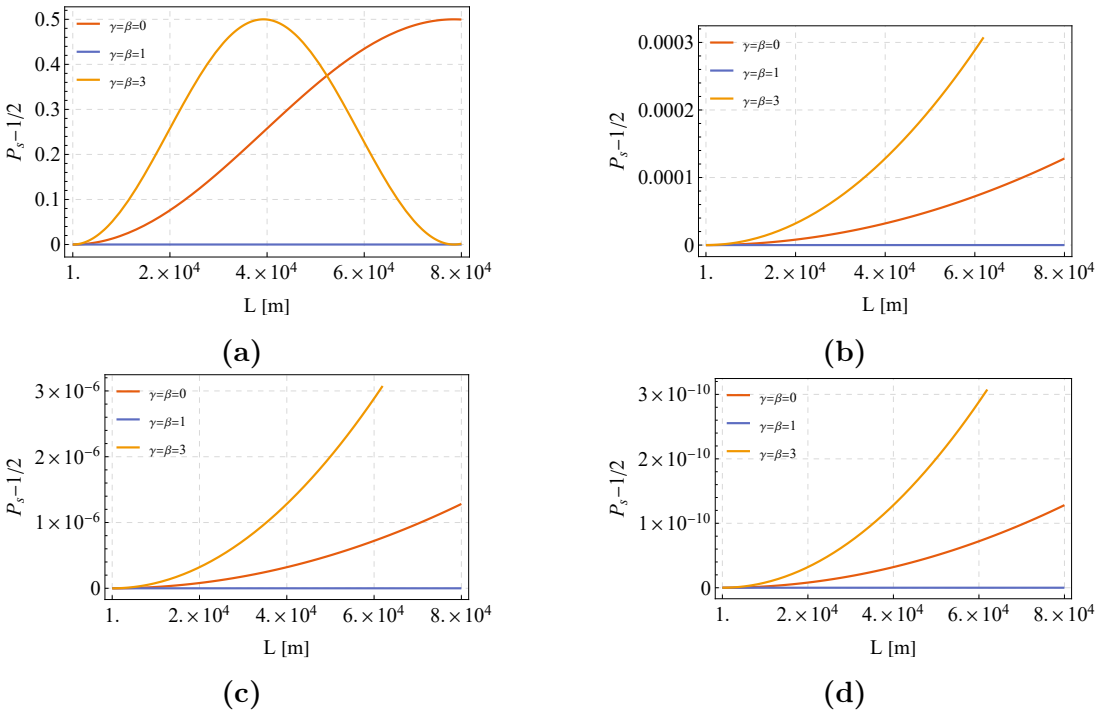

Figure 3.4.1: Success probability P_S Eq. (3.4.4) as a function of L for (a) atom, (b) electron, (c) molecule, (d) neutron with $\Delta E = 6.61 \times 10^{-19}, 6.62 \times 10^{-21}, 6.62 \times 10^{-22}, 6.62 \times 10^{-24}$ (J), respectively, speed $v = 10$ (m/s) and a constant gravitational field equivalent to that generated by the Earth at a radius $R = 7 \times 10^6$ (m).

3.5 Unambiguous discrimination

So far, we have studied two strategies for discriminating metric theories. The first and simple approach allows us to conclusively rule out or refute a given metric theory with respect to a set of possible metric theories. The second approach, based on minimum error discrimination, allows us to distinguish between any two metric theories, albeit with a minimum misidentification error. However, there exists a length L_O such that this error vanishes, making it possible for an error-free discrimination.

It is possible to discriminate between two metric theories without error, even if the length value cannot be fixed in L_O. This is achieved through unambiguous state discrimination, which allows nonorthogonal states to be detected without error at the expense of introducing an inconclusive event. This does not allow conclusions to be drawn about the states that are discriminated. Following Eq. (2.2.6), the optimal average success probability for equal a priori probabilities

is given by

$$P_{\mathrm{UD}} = 1 - \sqrt{\frac{1 + \cos\left(\frac{\Delta E}{\hbar}\Delta\bar{\lambda}\right)}{2}}. \tag{3.5.1}$$

This turns out to be less than or equal to P_S Eq. (3.4.4), but has the advantage that the measurement results associated with the states do not lead to misidentifications. Thus, a single detection allows us to determine which metric theory describes spacetime.

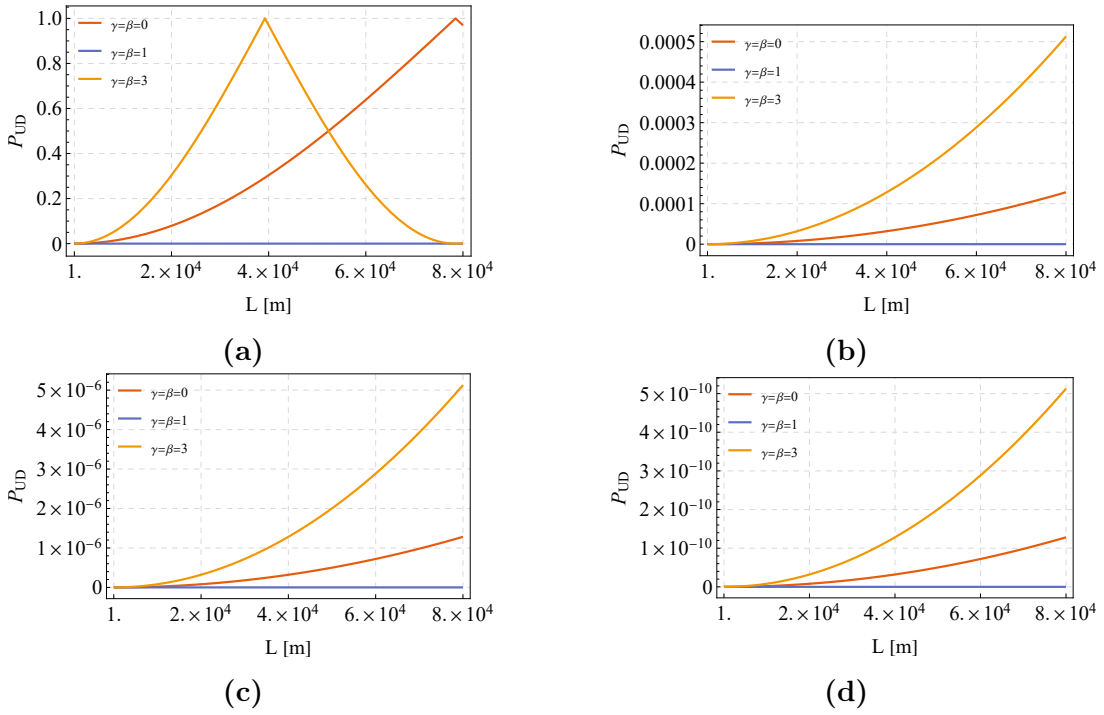

Figure 3.5.1: Success probability P_S Eq. (3.5.1) as a function of L for (a) atom, (b) electron, (c) molecule, (d) neutron with $\Delta E = 6.61 \times 10^{-19}, 6.62 \times 10^{-21}, 6.62 \times 10^{-22}, 6.62 \times 10^{-24}$ (J), respectively, speed $v = 10$ (m/s) and a constant gravitational field equivalent to that generated by the Earth at a radius $R = 7 \times 10^6$ (m).

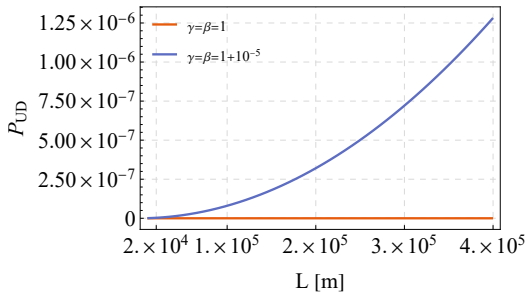

Figure 3.5.2: Probability of detection P_{UD} Eq. (3.5.1) in case of $\gamma = \beta = 1+10^{-5}$ in terms of length of the arm of the array L (see Fig. 3.3.1). We have considered the Earth gravitational potential $\phi(R)$ at the radial coordinate $R = 7 \times 10^6$ (m).

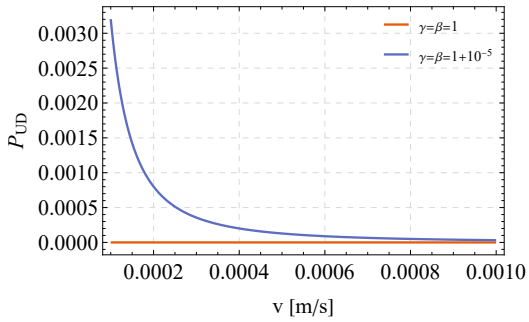

Figure 3.5.3: Probability of detection, P_{UD} Eq. (3.5.1), as a function of particle velocity, v, for $\gamma = \beta = 1 + 10^{-5}$, fixed proper length $L = 4\,\mathrm{km}$, and Earth's gravitational potential at $R = 7 \times 10^6$ (m).

3.6 Conclusion and discussion

We have studied the problem of discriminating between metric theories. We have shown that, within the post-Newtonian approach, the quantum state of a massive two-dimensional quantum clock becomes, after propagating at a low speed and in a weak gravitational field, a function of the parameters γ and β. Thus, the discrimination between metric theories becomes a discrimination between quantum states of the quantum clock. Since the number of metric theories is greater than two, the problem of discrimination becomes difficult. We have applied to this problem three different quantum state discrimination strategies. We first resorted to measuring a rank-two observable. This approach allows ruling out or refuting a particular metric theory with respect to a set of metric theories, although it is not possible to determine which theory within the set describes spacetime. A single detection event enough for this purpose, albeit its probability can become very small. A second approach, minimum-error discrimination, leads to an increase

in the average probability of a successful discrimination when dealing with only two metric theories. However, this occurs at the expense of accepting a small misidentification error. This can be improved with the help of unambiguous state discrimination, which identifies different metric theories without error but with a lower probability of success. In the first and third approach, a single detection event is enough to discard a given metric theory.

The probability of success of the three discrimination strategies is a harmonic function of the difference in proper time corresponding to each state of the quantum clock multiplied by the propagation length and the energy difference between the eigenstates of the quantum clock. This favors the use of atoms instead of molecules, neutrons, and electrons, in which cases the probability of success becomes very small. In addition, also for atoms, the length scales are on the order of 10^4 (m) to achieve a probability of success on the order of 1 for post-Newtonian parameters with values on the order of 10. Discriminating between two metric theories with very close post-Newtonian parameters, for example, by discarding a metric theory whose parameters are within the inaccuracy of a metric that we suspect describes spacetime, the probability of success becomes of the order of 10^{-6} for a length of the order of 10^4 (m). To overcome this, it is necessary to resort to a larger length scale or a large sample of atoms.

Our scheme allows us to distinguish between metric theories with distinct values of γ and β. A pertinent question then arises: can we definitively rule out alternatives to General Relativity, or distinguish General Relativity from other alternative theories? Table 3.6.1 summarizes the values of γ and β for several theories, including General Relativity, where $\gamma = \beta = 1$. However, as the table shows, other theories also predict these values. Consequently, observing $\gamma = \beta = 1$ does not uniquely identify General Relativity, but rather a family of theories sharing these parameters.

As shown in the "Status" column of Table 3.6.1, our results provide support for General Relativity, Einstein-Aether theory [58], and Tensor-Vector-Scalar theory [59]. We observe a tension with Brans-Dicke theory [60, 61] when considering only $\beta = 1$, as our protocol requires information about both γ and β to draw a definitive conclusion. Furthermore, while our findings are compatible with General Relativity, they are also compatible with Einstein-Aether theory and Tensor-Vector-Scalar theory.

Several extensions of our current results are possible. We concentrated on

the two post-Newtonian parameters γ and β, which do not fully characterize all possible metric theories. Thus, it would be interesting to extend our results to the case of a larger number of post-Newtonian parameters. However, there are some challenges along this route. A larger number of parameters probably requires a quantum clock of higher dimensions [62], which in turn might lead to a more complicated set of states that must be discriminated. Also, we have studied the case of discriminating between two quantum clock states. It is possible to discriminate among more states, but in this case general analytical results for the success probability and the optimal measurement are lacking, leading to the use of numerical techniques for solving the quantum state discrimination problem. Finally, note that other discrimination strategies can be used, such as maximum confidence [63, 64] and fixed rate of inconclusive outcome [65, 66].

Theory	PPN parameters		Our Experiment
	γ	β	Status
General relativity	1	1	Conclusive
Scalar-tensor			
Brans-Dicke	$\frac{1+\omega_{BD}}{2+\omega_{BD}}$	1	Tension
General, $f(R)$	$\frac{1+\omega}{2+\omega}$	$1+\frac{\lambda}{4+2\omega}$	Ruled out
Vector-tensor			
Unconstrained	γ'	β'	Ruled out
Einstein-Aether	1	1	Conclusive
Tensor-Vector-Scalar	1	1	Conclusive

Table 3.6.1: Metric theories and their PPN parameter values γ and β, and the status of each theory in light of our experiment. See the main text for a detailed discussion. Table adapted from [36].

Chapter 4

Using Wigner rotation as a resource in Kerr metric parameter estimation

4.1 Abstract

This chapter examines the gravitational Wigner rotation effect on photon polarization. We propose a Mach-Zehnder type interferometer operating in the weak-field, slow-rotation limit, which exploits both this effect and gravitational time dilation. The primary application explored is quantum sensing, specifically demonstrating a method to estimate the Kerr rotation parameter a.

4.2 Tetrad adapted to the geodesic motion of the photon

To obtain the phase acquired due to the rotation of the polarization in the Kerr spacetime, we will use the tetrad formalism [67]. Specifically, we will employ a tetrad basis adapted to the geodesic motion of the photon (2.4.4.1), i.e. $\bar{u}^\mu = e^\mu_{\hat{0}} + e^\mu_{\hat{3}}$, where $\bar{u}^\mu = u^\mu/N$, with u^μ the null vector for a geodesic path (2.4.53) and N the appropriate rescaling of the null vector determined by imposing $e^{\hat{0}}_\mu \bar{u}^\mu = 1$. To solve the system of equations given by (2.3.28), we choose the tetrad $e^\mu_{\hat{0}}$ to be equal to the four-velocity of a static observer (spatial coordinates remain constant for all coordinate time t) in the Kerr metric, as in [68, 6]. This is valid

for a region outside the ergosphere[1].

$$e^{\mu}_{\hat{0}} = \left(\frac{1}{\sqrt{g_{00}}}, 0, 0, 0\right) \tag{4.2.1}$$

The system of equations to be solved is given by 2.3.29

$$e^{\mu}_{I} e^{\nu}_{J} g_{\mu\nu} = \eta_{IJ}, \tag{4.2.2}$$

with

$$e^{\mu}_{\hat{3}} = e^{\mu}_{\hat{0}} - \bar{u}^{\mu}. \tag{4.2.3}$$

This reduces the system of equations to be solved. The tetrad basis that we will use is given by

$$e^{\mu}_{\hat{0}} = \left(\frac{1}{\sqrt{g_{00}}}, 0, 0, 0\right), \tag{4.2.4}$$

$$\begin{aligned} e^{\mu}_{\hat{1}} = \Bigg(& \frac{g_{03}\sqrt{g_{11}(\bar{u}^1)^2}}{\sqrt{(g_{00}g_{33}+g_{03}^2)\left(g_{00}\left(g_{11}(\bar{u}^1)^2+g_{33}(\bar{u}^3)^2\right)+g_{03}^2(\bar{u}^3)^2\right)}}, \\ & \frac{\bar{u}^1\bar{u}^3\left(g_{00}g_{33}+g_{03}^2\right)}{\sqrt{g_{11}(\bar{u}^1)^2}\sqrt{(g_{00}g_{33}+g_{03}^2)\left(g_{00}\left(g_{11}(\bar{u}^1)^2+g_{33}(\bar{u}^3)^2\right)+g_{03}^2(\bar{u}^3)^2\right)}}, \\ & 0, -\frac{g_{00}\sqrt{g_{11}(\bar{u}^1)^2}}{\sqrt{(g_{00}g_{33}+g_{03}^2)\left(g_{00}\left(g_{11}(\bar{u}^1)^2+g_{33}\bar{u}^{32}\right)+g_{03}^2(\bar{u}^3)^2\right)}}\Bigg), \end{aligned} \tag{4.2.5}$$

$$e^{\mu}_{\hat{2}} = \left(0, 0, -\frac{g_{11}\bar{u}^1}{\sqrt{g_{22}}\sqrt{g_{11}\left(g_{11}(\bar{u}^1)^2\right)}}, 0\right), \tag{4.2.6}$$

$$e^{\mu}_{\hat{3}} = \left(\bar{u}^0 - \frac{1}{\sqrt{g_{00}}}, \bar{u}^1, 0, \bar{u}^3\right). \tag{4.2.7}$$

[1] A region located outside the event horizon of a rotating (Kerr) black hole, where spacetime is dragged so strongly by the black hole rotation that no observer can remain at rest relative to infinity. Within this region, all timelike trajectories are compelled to co-rotate with the black hole, although escape to infinity is still possible [29].

If we substitute this solution back into equation (2.3.29), the following matrix is obtained

$$\eta_{IJ} = \begin{bmatrix} (e^0_{\hat{0}})^2 g_{00} = 1 & 0 & 0 & (e^0_{\hat{0}})^2 g_{00} = e^0_{\hat{0}}(g_{00}\bar{u}^0 + g_{03}\bar{u}^3) \\ 0 & 1 & 0 & 0 \\ 0 & 0 & 1 & 0 \\ (e^0_{\hat{0}})^2 g_{00} = e^0_{\hat{0}}(g_{00}\bar{u}^0 + g_{03}\bar{u}^3) & 0 & 0 & (e^0_{\hat{3}})(g_{00}(e^0_{\hat{3}}) + 2g_{03}\bar{u}^3) + 1 = g_{11}(\bar{u}^1)^2 + g_{33}(\bar{u}^3)^2 \end{bmatrix},$$

From the η_{03} and η_{30} components, it is possible to verify the rescaling N of the null vector:

$$N = \frac{g_{00}u^0 + g_{03}u^3}{\sqrt{g_{00}}} = u^{\hat{0}}. \tag{4.2.8}$$

This rescaling allows us to write the components of the null vector in the tetrad basis in the form

$$\bar{u}^I = (1, 0, 0, 1)\,. \tag{4.2.9}$$

Where $\bar{u}^I$ are the components of the rescaled null vector in the tetrad basis.

4.2.1 Transport phase in Kerr spacetime

We will now compute the phase acquired by the photon as it propagates through spacetime, in this case along a null geodesic calculated in section 2.4.4.1. To do so, we will use that in the WKB approximation we obtain the eikonal equation (2.7.17) and using the conserved quantities (2.4.16), it is possible to found a differential equation for $\vartheta^\tau(ct, r, \varphi)$and (2.4.18):

$$k^1 \frac{\partial \vartheta^\tau}{\partial r} = k^3 n - k^0 l. \tag{4.2.10}$$

Obtaining an expression for the transport phase

$$\vartheta^\tau = lct - n\varphi + \int dr \left(k^3 n - k^0 l\right)/k^1, \tag{4.2.11}$$

For convenience, we define the function $S(r, \varphi)$ so that the previous expression becomes:

$$\vartheta^\tau = lct + S(r, \varphi). \tag{4.2.12}$$

It is possible to show using, (2.3.32), that

$$k_\mu \xi^\mu = \frac{\partial \vartheta^\tau}{\partial x^0} = k^{\hat{0}}\sqrt{g_{00}} \equiv l, \tag{4.2.13}$$

where $k^{\hat{0}}$ is the component of the null vector $k^\mu = dx^\mu/d\lambda$ in the tetrad basis. The quantity $c\tau = \sqrt{g_{00}}ct = lct/k^{\hat{0}}$ corresponds to the proper time measured by a static observer at a point in spacetime. The function $S(r,\varphi)$ in (4.2.12) depends only on the spatial coordinates, so in the context of interference, the phase difference will be given by the difference in arrival times of the photon, that is,

$$\Delta\vartheta^\tau = k^{\hat{0}} c\Delta\tau = k^{\hat{0}} c\sqrt{g_{00}}\Delta t, \tag{4.2.14}$$

where all functions are evaluated at the point where the photon interferes.

4.3 Wigner phase in a geodesic path

In this section, we show the not dependence of the local four-momentum of the photon on the Wigner rotation (2.7.75) and Wigner phase (2.8.5) for a null geodesic path (2.4.4.1). We also show the explicit expression of the Wigner phase acquired by the photon polarization travelling on a geodesic path between two static observers, following the idea described in Ref. [6].

4.3.1 Wigner rotation and spin-1 connection

We write the Wigner rotation (2.7.75) in the form

$$W^A_{\ B} = ig^{\mu\nu}u_\nu\,\omega_{\mu\hat{1}\hat{2}}\,(\sigma_y)^A_{\ B} \tag{4.3.1}$$

$$= ig^{\mu 0}u_0\,\omega_{\mu\hat{1}\hat{2}}\,(\sigma_y)^A_{\ B} + ig^{\mu 1}u_1\,\omega_{\mu\hat{1}\hat{2}}\,(\sigma_y)^A_{\ B} + ig^{\mu 3}u_3\,\omega_{\mu\hat{1}\hat{2}}\,(\sigma_y)^A_{\ B}\,. \tag{4.3.2}$$

Here $\omega_{\mu\hat{1}\hat{2}}$ is the spin-1 connection computed with the tetrad basis described in Section 4.2. Using the transformation (2.3.31) to express the components of the

null vector in the tetrad basis, the Wigner rotation can be written as

$$W^A_{\ B} = i\left(k^{\hat{0}}\sqrt{g_{00}}\right) g^{\mu 0}\omega_{\mu\hat{1}\hat{2}}\,(\sigma_y)^A_{\ B} + i\left(g_{11}e^1_{\hat{3}}\,k^{\hat{3}}\right) g^{\mu 1}\omega_{\mu\hat{1}\hat{2}}\,(\sigma_y)^A_{\ B} + i\left(g_{03}\left(e^0_{\hat{0}}k^{\hat{0}} + e^0_{\hat{3}}k^{\hat{3}}\right) + g_{33}\left(e^3_{\hat{0}}k^{\hat{0}} + e^3_{\hat{3}}k^{\hat{3}}\right)\right) g^{\mu 3}\omega_{\mu\hat{1}\hat{2}}\,(\sigma_y)^A_{\ B}\,. \tag{4.3.3}$$

And remembering the conserved quantities (2.4.10) and (2.4.10) it is possible to write

$$W^A_{\ B} = ilg^{\mu 0}\omega_{\mu\hat{1}\hat{2}}\,(\sigma_y)^A_{\ B} + i\left(g_{11}e^1_{\hat{3}}\,u^{\hat{3}}\right) g^{\mu 1}\omega_{\mu\hat{1}\hat{2}}\,(\sigma_y)^A_{\ B} - ing^{\mu 3}\omega_{\mu\hat{1}\hat{2}}\,(\sigma_y)^A_{\ B}\,. \tag{4.3.4}$$

Using equations (2.3.29) and (2.3.32), it is possible to show that $e^1_{\hat{3}}\,u^{\hat{3}} = \epsilon l = u^1$. Furthermore, by applying the conserved quantities relation (2.4.27) to the expression (4.3.4), this expression becomes:

$$W^A_{\ B} = ilg^{\mu 0}\omega_{\mu\hat{1}\hat{2}}\,(\sigma_y)^A_{\ B} + i\,\epsilon l\,\omega_{1\hat{1}\hat{2}}\,(\sigma_y)^A_{\ B} - i\left(al\sin^2\theta\right) g^{\mu 3}\omega_{\mu\hat{1}\hat{2}}\,(\sigma_y)^A_{\ B}\,. \tag{4.3.5}$$

4.3.2 Wigner phase in Kerr spacetime

Recalling that the affine parameter along the photon trajectory is given by $r = \epsilon l\lambda + \text{const.}$, the Wigner phase (2.8.5) becomes

$$\vartheta(\hat{\mathbf{k}}) = \frac{1}{\epsilon l}\int_{r_i}^{r_f} W^1_2\,dr = \frac{1}{\epsilon l}\int_{r_i}^{r_f}\left[lg^{\mu 0}\omega_{\mu\hat{1}\hat{2}} + \epsilon l\omega_{1\hat{1}\hat{2}} - \left(la\sin^2\theta\right) g^{\mu 3}\omega_{\mu\hat{1}\hat{2}}\right] dr. \tag{4.3.6}$$

Finally, the Wigner phase for a photon that travels along a geodesic path (2.4.4.1) is given by

$$\vartheta = \frac{1}{\epsilon}\int_{r_i}^{r_f}\left[g^{\mu 0}\omega_{\mu\hat{1}\hat{2}} + \epsilon\,\omega_{1\hat{1}\hat{2}} - \left(a\sin^2\theta\right) g^{\mu 3}\omega_{\mu\hat{1}\hat{2}}\right] dr. \tag{4.3.7}$$

It is possible to show that in the interference context, the term $\omega_{1\hat{1}\hat{2}}$ does not contribute to the phase difference because does not depend of ϵ.

4.3.3 Wigner phase for a geodesic path between statics observers

Now we can find the Wigner phase of photons travelling between two static observers placed in a same coordinate $\theta = \text{const.}$ and difference radial coordinate r_i and r_f respectively. If we expand the argument of (4.3.7) in powers of (a/r) and (m/r), we found to fourth order a Wigner phase given by

$$\vartheta = \left[\frac{a\cos\theta}{r\epsilon} - \frac{a^3\cos\theta}{r^3\epsilon} + \frac{a^3\cos\theta}{6r^3} - \frac{a^3\cos\theta\cos 2\theta}{6r^3} - \frac{ma^3\cos\theta\sin^2\theta}{2r^4\epsilon} + \frac{ma^3\cos\theta\sin^2\theta}{2r^4} + O\left(\frac{1}{r}\right)^5 \right]_{r_i}^{r_f}. \tag{4.3.8}$$

We note that the Wigner phase vanishes for $\theta = \pi/2$.

4.4 Geodesic interferometer

To study relativistic effects on photons, we analyze their behavior in free space, specifically considering photons that propagate freely along geodesic trajectories. For a single-photon interference experiment, we consider the setup depicted in Fig. 4.4.1: A photon source is located at the radial coordinate r_2. From this source, a single photon is prepared in a superposition of states propagating along two distinct geodesic paths (γ_1' and γ_1). One path extends from r_2 to a lower radial coordinate r_1, while the other extends from r_2 to a higher radial coordinate r_3. Subsequently, upon reaching r_1 and r_3, the photon states undergo reflection. The state reflected at r_1 propagates along a geodesic path towards r_4, and the state reflected at r_3 also propagates along a geodesic path towards r_4. The photon states are then recombined at the radial coordinate r_4, where interference is measured using detectors. The radial coordinate r_4 satisfies $r_1 < r_4 < r_3$ and its value depends on the other three radial coordinates (r_1, r_2, r_3).

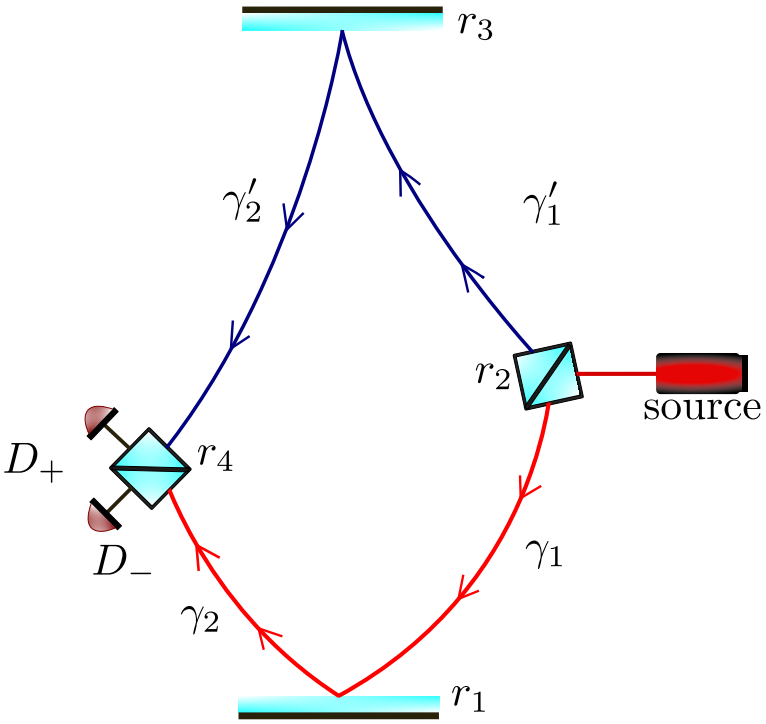

Figure 4.4.1: Geodesic Interferometer: A single photon emitted from a source at radial coordinate r_2 is prepared in a superposition of states propagating along two paths. One path component travels towards r_1 and reflects, while the other travels towards r_3 and reflects. Both reflected components subsequently propagate to the radial coordinate r_4, where they are recombined and interference is measured. The recombination point satisfies $r_1 < r_4 < r_3$.

We will now show that it is possible to find a radius r_4 where the photon trajectories recombine, as illustrated in Fig. 4.4.1; that is, $\varphi(r_4, r_0 = r_1) = \varphi(r_4, r_0 = r_3)$. To do this, we will use the solutions for the outgoing and ingoing geodesics, $\varphi_-(r)$ and $\varphi_+(r)$, given by Eqs. (2.4.38) and (2.4.42). From now on, we set $\alpha = (a/2)/\sqrt{m^2 - a^2}$.

For the path γ_1: $(r_2 \to r_1)$

$$\varphi_-(r_1) = -\alpha \ln \left| \frac{(r_1 - r_+)}{(r_1 - r_-)} \frac{(r_2 - r_-)}{(r_2 - r_+)} \right|. \tag{4.4.1}$$

For the path γ_2: $(r_1 \to r_4)$

$$\varphi_+(r_4) = \alpha \ln \left| \frac{(r_4 - r_+)}{(r_4 - r_-)} \frac{(r_1 - r_-)}{(r_1 - r_+)} \right| + \varphi_-(r_1). \tag{4.4.2}$$

Analogously, for the photon following the path γ'

For the path γ_1': $(r_2 \to r_3)$

$$\varphi_+(r_3) = \alpha \ln \left| \frac{(r_3 - r_+)}{(r_3 - r_-)} \frac{(r_2 - r_-)}{(r_2 - r_+)} \right|. \tag{4.4.3}$$

For the path γ_2': $(r_3 \to r_4)$

$$\varphi_-(r_4) = -\alpha \ln \left| \frac{(r_4 - r_+)}{(r_4 - r_-)} \frac{(r_3 - r_-)}{(r_3 - r_+)} \right| + \varphi_-(r_1). \tag{4.4.4}$$

By equating the angular coordinates at the radial coordinate r_4, i.e., we obtain

$$\varphi_+(r_4) = \varphi_-(r_4)$$
$$\alpha \ln \left| \frac{(r_4 - r_+)}{(r_4 - r_-)} \frac{(r_1 - r_-)}{(r_1 - r_+)} \right| + \varphi_-(r_1) = -\alpha \ln \left| \frac{(r_4 - r_+)}{(r_4 - r_-)} \frac{(r_3 - r_-)}{(r_3 - r_+)} \right| + \varphi_-(r_1).$$

Two possible solutions for r_4 are obtained:

$$r_4 = \frac{-a^4 + m r_1 (r_2 - 2m) r_3 + a^2(-r_1 r_2 + r_1 r_3 - r_2 r_3 + m(r_1 + r_2 + r_3))}{2m^2 r_2 + r_1 r_2 r_3 + a^2(-m + r_1 - r_2 + r_3) - m(r_1 r_2 + (r_1 + r_2) r_3)}, \tag{4.4.5}$$

and

$$r_4 = \frac{a^2(r_1 - r_2 + r_3) + r_1 r_3 (r_2 - 2m)}{a^2 - 2m r_2 + r_1 r_2 - r_1 r_3 + r_2 r_3}. \tag{4.4.6}$$

The solution (4.4.5) yields negative values for r_4, and therefore we retain the second solution (4.4.6). In this way, the setup allows us to work exclusively with the ingoing and outgoing solutions of the geodesic in the Kerr metric, thereby avoiding (potentially) non-analytic solutions of null geodesics that are not initially radial.

4.4.1 Arrival times in geodesic interferometer

First, for a static observer, the Kerr metric implies that

$$\begin{aligned} c^2 d\tau^2 &= \frac{\Delta}{\rho^2} c^2 dt^2 - \frac{a^2 \sin^2\theta}{\rho^2} c^2 dt^2 \\ &= \frac{c^2 dt^2}{\rho^2} \left(\rho^2 - 2mr \right). \end{aligned} \tag{4.4.7}$$

Then

$$\int cdt = \int cd\tau \frac{\rho}{\sqrt{\rho^2 - 2mr}}, \tag{4.4.8}$$

$$ct = c\tau \frac{\rho}{\sqrt{\rho^2 - 2mr}}. \tag{4.4.9}$$

For the detector located at the radius r_i, the four-velocity of a static observer is given by:

$$\begin{aligned} x^{\mu}_{r_i}(\tau) &= \left(ct, r_i, \varphi(r_i), \frac{\pi}{2}\right) \\ x^{\mu}_{r_i}(\tau) &= \left(c\tau \frac{\rho}{\sqrt{\rho^2 - 2mr}}, r_i, \varphi(r_i), \frac{\pi}{2}\right). \end{aligned} \tag{4.4.10}$$

Now, the worldline of the photon is given by

$$x^{\mu}_{\text{photon}}(\lambda) = \left(ct(\lambda), r, \varphi(\lambda), \frac{\pi}{2}\right). \tag{4.4.11}$$

By the affine parameter, the worldline followed by the photon, initially at $r = r_2$,will reach the mirror located at $r = r_1$ having a four-position given by:

In $\gamma_1 : (r_2 \to r_1)$

$$x^{\mu}_{\text{photon}}(r_1) = (ct_-(r_1, r_0 = r_2), r_3, \varphi_1(r_1, r_0 = r_2)). \tag{4.4.12}$$

Reflecting radially off the mirror and then reaching the detector located at r_4

In $\gamma_2 : (r_1 \to r_4)$

$$x^{\mu}_{\text{photon}}(r_4) = (ct_+(r_4, r_0 = r_1) + ct_-(r_1, r_0 = r_2), r_4, \varphi_+(r_4, r_0 = r_3) + \varphi_-(r_1, r_0 = r_2))$$

Analogously, for the other possible path γ', we have:

In $\gamma'_1 : (r_2 \to r_3)$

$$x^{\mu}_{\text{photon}}(r_3) = (ct_+(r_3, r_0 = r_2), r_3, \varphi_+(r_3, r_0 = r_2)). \tag{4.4.13}$$

reflecting radially off the mirror, reaching the detector located at r_4

In $\gamma_2' : (r_3 \to r_4)$

$$x^{\mu}_{\text{photon}}(r_4) = (ct_-(r_4, r_0 = r_3) + ct_+(r_3, r_0 = r_2), r_4, \varphi_-(r_4, r_0 = r_3) + \varphi_+(r_3, r_0 = r_2)) .$$

Difference of arrival times: First, we calculate the flight time measured by the detector located at $r = r_4$ for each possible path that the photon follows.

For the path γ

$$c\tau \frac{\rho_4}{\sqrt{\rho_4^2 - 2mr_4}} = ct_+(r_4, r_0 = r_1) + ct_-(r_1, r_0 = r_2). \tag{4.4.14}$$

For the path γ'

$$c\tau' \frac{\rho_4}{\sqrt{\rho_4^2 - 2mr_4}} = ct_-(r_4, r_0 = r_3) + ct_+(r_3, r_0 = r_2). \tag{4.4.15}$$

We define $\Pi_4 = \sqrt{\rho_4^2 - 2mr_4}/\rho_4$; then the difference in arrival times is given by

$$c\tau' - c\tau = \Pi_4 \left(ct_-(r_4, r_0 = r_3) + ct_+(r_3, r_0 = r_2) - ct_+(r_4, r_0 = r_1) - ct_-(r_1, r_0 = r_2)\right) .$$

Replacing the terms (4.4.14) and (4.4.15) we have

$$\begin{aligned} c\Delta\tau = \Pi_4 \Bigg(& \left(r_3 - r_4 - \left(m + \frac{m^2}{\sqrt{m^2 - a^2}} \right) \ln \left| \frac{(r_4 - r_+)}{(r_3 - r_+)} \right| - \left(m - \frac{m^2}{\sqrt{m^2 - a^2}} \right) \ln \left| \frac{(r_4 - r_-)}{(r_3 - r_-)} \right| \right) \\ & + \left(r_3 - r_2 + \left(m + \frac{m^2}{\sqrt{m^2 - a^2}} \right) \ln \left| \frac{(r_3 - r_+)}{(r_2 - r_+)} \right| + \left(m - \frac{m^2}{\sqrt{m^2 - a^2}} \right) \ln \left| \frac{(r_3 - r_-)}{(r_2 - r_-)} \right| \right) \\ & - \left(r_4 - r_1 + \left(m + \frac{m^2}{\sqrt{m^2 - a^2}} \right) \ln \left| \frac{(r_4 - r_+)}{(r_1 - r_+)} \right| + \left(m - \frac{m^2}{\sqrt{m^2 - a^2}} \right) \ln \left| \frac{(r_4 - r_-)}{(r_1 - r_-)} \right| \right) \\ & - \left(r_2 - r_1 - \left(m + \frac{m^2}{\sqrt{m^2 - a^2}} \right) \ln \left| \frac{(r_1 - r_+)}{(r_2 - r_+)} \right| - \left(m - \frac{m^2}{\sqrt{m^2 - a^2}} \right) \ln \left| \frac{(r_1 - r_-)}{(r_2 - r_-)} \right| \right) \Bigg) . \end{aligned} \tag{4.4.16}$$

4.4.1.1 Arrival times difference in weak gravitational field limit and slow rotation limit

As we can observe from Fig. 4.4.1, the shape of the interferometer is non-trivial, as are the expressions for the flight times and the Wigner phase in the weak-field and slow-rotation approximation. We propose a parametrization as a function of

the coordinate r_2 where the source is located, that is

$$r_3 = h + r_2 \ , \quad h > 0 \tag{4.4.17}$$

$$r_1 = r_2 - l \ , \quad l > 0 \tag{4.4.18}$$

$$r_4(r_1, r_2, r_3) = r_4(r_2 - l, r_2, h + r_2) \tag{4.4.19}$$

Then, the weak-field and slow-rotation approximation is in powers of (m/r_2) and (a/r_2). We expand the difference in arrival times (4.4.16) up to fourth order. As the induced gravitational phase-shift (4.2.14) depends on the arrival time difference in Eq. (4.4.16). In the interferometer, we define the phase ϕ_E that eliminates all contributions that does not contain information about m and a, then the phase difference by the arrival times is given by:

$$\Delta\vartheta^\tau = \frac{\omega}{c} hl \left(\frac{4a^2}{r_2^3} + \frac{4a^2 m(3 - \cos^2\theta)}{r_2^4} + \frac{3a^2 m^2 (2\cos^2\theta - 5)}{r_2^5} - \frac{4a^4}{r_2^5} \right) \tag{4.4.20}$$

Then, to see the behavior of Eq. (4.4.20), we plot the difference in the induced gravitational phase shift for different frequencies ω.

In Fig. 4.4.2 we plot $\Delta\vartheta^\tau$ in terms of the increasing distance with respect to the initial position of the photon source $r_2 = 7 \times 10^6\,\mathrm{m}$ for an geodesic interferometer with $l = 0.3\,\mathrm{m}$ and $h = 0.7\,\mathrm{m}$. As we can see, if we consider different frequencies $\omega_1 = 10^6\,\mathrm{Hz}$, $\omega_2 = 10^{10}\,\mathrm{Hz}$ and $\omega_3 = 10^{12}\,\mathrm{Hz}$, the value of $\Delta\vartheta^\tau$ decreases as we decrease the value of the frequency. This result should be useful for using this interferometer to estimate the rotation parameter.

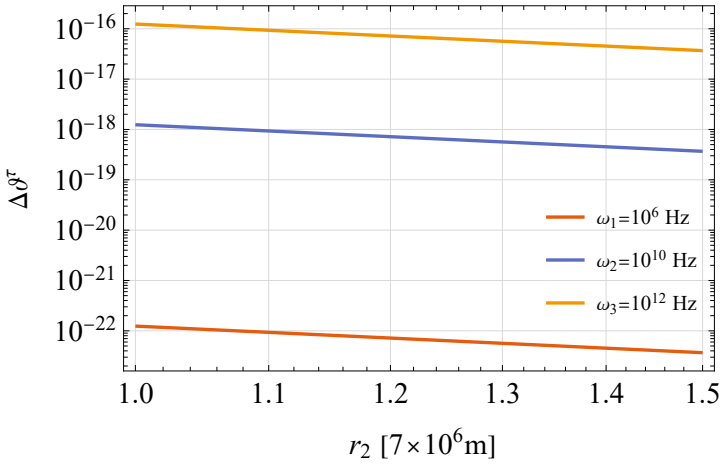

Figure 4.4.2: Difference of induced gravitational phase shift in terms of increasing distance r_2 for different frequencies ω. The red continuous line correspond to frequency $\omega_1 = 10^6$ Hz, the blue continuous line to frequency $\omega_2 = 10^{10}$ Hz and the yellow continuous line to a frequency $\omega_3 = 10^{12}$ Hz.

We plot in Fig. (4.4.3) the phase difference as a function of the increasing distance difference between r_3 and r_1, $\Delta r = r_3 - r_1$, in a geodesic interferometer with the source located at $r_2 = 1.5 \times 7 \times 10^6$.

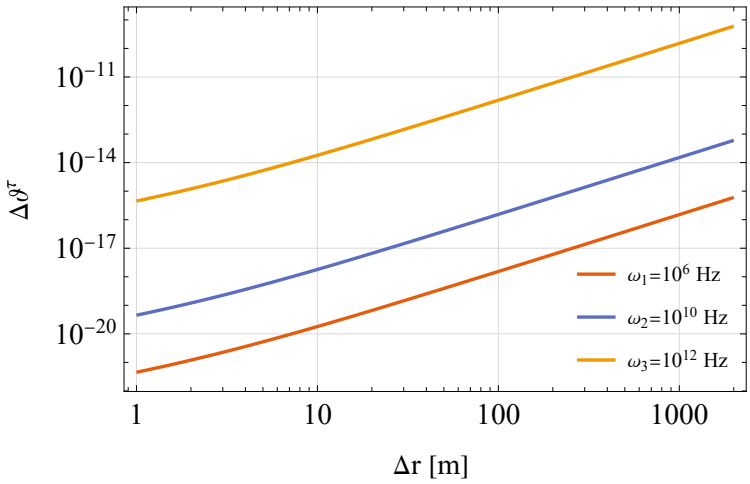

Figure 4.4.3: Difference of induced gravitational phase shift in terms of increasing distance Δr for different frequencies ω. The red continuous line correspond to frequency $\omega_1 = 10^6$ Hz, the blue continuous line to frequency $\omega_2 = 10^{10}$ Hz and the yellow continuous line to a frequency $\omega_3 = 10^{12}$ Hz.

4.4.2 Wigner phase difference in weak field limit and slow rotation limit in a geodesic interferometer

For the geodesic interferometer (see Fig. 4.4.1) we have to integrate (4.3.8) in each path of the array. The Wigner phase in the upper path $\vartheta_{\text{upper}} = \vartheta_{r_2\to r_3} + \vartheta_{r_3\to r_4}$, and the Wigner phase of lower path $\vartheta_{\text{lower}} = \vartheta_{r_2\to r_1} + \vartheta_{r_1\to r_4}$, then the phase difference of geodesic interferometer is given by

$$\Delta\vartheta = \vartheta_{\text{upper}} - \vartheta_{\text{lower}}, \tag{4.4.21}$$

we obtain

$$\begin{aligned}\Delta\vartheta = &\frac{10a^3hlm\cos\theta}{r_2^6} + \frac{6a^3hlm\cos\theta\cos 2\theta}{r_2^6} - \frac{16ahlm^3\cos\theta}{r_2^6} \\ &- \frac{8ahlm^2\cos\theta}{r_2^5} - \frac{4ahlm\cos\theta}{r_2^4}.\end{aligned} \tag{4.4.22}$$

In Fig. 4.4.4 we plot $\Delta\vartheta$ from Eq. (4.4.22) in terms of the angular coordinate θ for two different distances from Earth. As we can see, for a distance $r_2 = 2\,R_{\text{Earth}}$, with $R_{\text{Earth}} \sim 7\times10^6$ m the Wigner phase reaches a maximum value $\Delta\vartheta \sim 6\times10^{-30}$ for a size $\Delta r := r_3 - r_1 \sim 1$ m. For a bigger interferometer Fig. 4.4.5 the Wigner phase reaches a maximum value of $\Delta\vartheta \sim 6\times10^{-17}$ for a size $\Delta r \sim 10^6$ m.

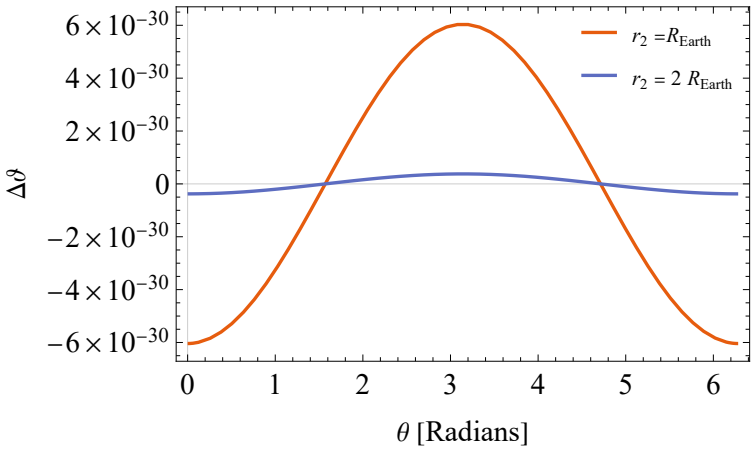

Figure 4.4.4: Wigner phase rotation Eq. (4.4.22) in terms of the angular coordinate θ. Each line represents the distance of the photon source respect to center of Earth. The red continuous line corresponds to $r_2 = R_{\text{Earth}}$ and the blue continuous line to $r_2 = 2\,R_{\text{Earth}}$. The distance between r_1 and r_3 is $\Delta r = 1$ m.

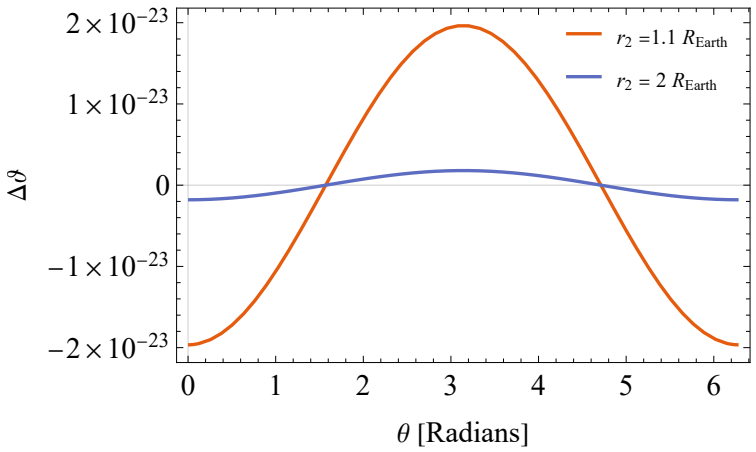

Figure 4.4.5: Wigner phase rotation Eq. (4.4.22) in terms of the angular coordinate θ. Each line represent the distance of the photon source respect to center of Earth. The red continuous line correspond to $r_2 = 1.1\,R_{\text{Earth}}$ and the blue continuous line to $r_2 = 2\,R_{\text{Earth}}$. The distance between r_1 and r_3 $\Delta r \sim 2\times10^3\,\text{m}$.

4.4.3 Probability of detection in a geodesic interferometer

In order to estimate the Kerr parameter a we calculate the probability of detection in a geodesic interferometer (see Fig.4.4.1). Then, the initial state (2.8.3) after going through the first beam-splitter, becomes

$$|\Psi\rangle = \frac{1}{2}\sum_{s=\pm1}\int d\hat{\mathbf{k}} f(\hat{\mathbf{k}})\left[e^{i\vartheta^{\tau}_{\gamma_1}}e^{is\vartheta_{\gamma_1}}\hat{a}^{\dagger}_{\hat{\mathbf{k}}}|0_{\hat{\mathbf{k}}},s\rangle + e^{-i\phi_{BS_1}}e^{is\vartheta_{\gamma_1'}}e^{i\vartheta^{\tau}_{\gamma_1'}}\hat{b}^{\dagger}_{\hat{\mathbf{k}}}|0_{\hat{\mathbf{k}}},s\rangle\right].$$

where $\vartheta^{\tau}_{\gamma_j}$ denotes the phase associated with the flight time along the path γ_j , and ϑ_{γ_j} is the Wigner phase through the path j. We consider that the beam-splitter acts on each mode. After the photon is reflected in r_1 and r_3, the state becomes

$$|\Psi\rangle = \frac{1}{2}\sum_{s=\pm1}\int d\hat{\mathbf{k}} f(\hat{\mathbf{k}})\left[e^{i(\vartheta^{\tau}_{\gamma_1}+\vartheta^{\tau}_{\gamma_2})}e^{is(\vartheta_{\gamma_1}+\vartheta_{\gamma_2})}\hat{a}^{\dagger}_{\hat{\mathbf{k}}}|0_{\hat{\mathbf{k}}},s\rangle\right.$$
$$\left. + e^{-i\phi_E}e^{is\left(\vartheta_{\gamma_1'}+\vartheta_{\gamma_2'}\right)}e^{i\left(\vartheta^{\tau}_{\gamma_1'}+\vartheta^{\tau}_{\gamma_2'}\right)}\hat{b}^{\dagger}_{\hat{\mathbf{k}}}|0_{\hat{\mathbf{k}}},s\rangle\right]. \tag{4.4.23}$$

For convenience we define

$$\Theta_{\hat{\mathbf{k}}} := \Theta(\hat{\mathbf{k}}) = \vartheta^{\tau}_{\gamma_1}(\hat{\mathbf{k}}) + \vartheta^{\tau}_{\gamma_2}(\hat{\mathbf{k}}), \tag{4.4.24}$$
$$\Omega_{\hat{\mathbf{k}}} := \Omega(\hat{\mathbf{k}}) = \vartheta_{\gamma_1}(\hat{\mathbf{k}}) + \vartheta_{\gamma_2}(\hat{\mathbf{k}}). \tag{4.4.25}$$

The state in the recombination stage reads

$$|\Psi_{\rm out}\rangle = \frac{1}{2\sqrt{2}}\sum_{s=\pm1}\int d\hat{\mathbf{k}} f(\hat{\mathbf{k}})\left[e^{i\Theta_{\hat{\mathbf{k}}}}e^{is\Omega_{\hat{\mathbf{k}}}}\left(\hat{f}^\dagger_{\hat{\mathbf{k}}}+\hat{g}^\dagger_{\hat{\mathbf{k}}}\right)|0_{\hat{\mathbf{k}}},s\rangle\right.$$
$$\left.+\, e^{-i\phi_E}e^{i\Theta'_{\hat{\mathbf{k}}}}e^{is\Omega'_{\hat{\mathbf{k}}}}\left(\hat{f}^\dagger_{\hat{\mathbf{k}}}-\hat{g}^\dagger_{\hat{\mathbf{k}}}\right)|0_{\hat{\mathbf{k}}},s\rangle\right]. \qquad (4.4.26)$$

We are considering detectors which are flat in response, therefore in this case we consider the following projectors: $\Pi_f = \int d\hat{\mathbf{k}} f^\dagger_{\hat{\mathbf{k}}}|0\rangle\langle 0|f_{\hat{\mathbf{k}}}$ and $\Pi_g = \int d\hat{\mathbf{k}} g^\dagger_{\hat{\mathbf{k}}'}|0\rangle\langle 0|g_{\hat{\mathbf{k}}'}$. The probability of detection in one port, is given by

$$\begin{aligned}
p_f &= \langle\Psi_{\rm out}|\Pi_f|\Psi_{\rm out}\rangle,\\
&= \frac{1}{8}\sum_{s=\pm1}\sum_{s'=\pm1}\int\int d\hat{\mathbf{k}} f^*(\hat{\mathbf{k}})d\hat{\mathbf{k}}' f(\hat{\mathbf{k}}')\left[\langle s',0_{\hat{\mathbf{k}}'}|\left(\hat{f}_{\hat{\mathbf{k}}'}+\hat{g}_{\hat{\mathbf{k}}'}\right)e^{-i\Theta^*_{\hat{\mathbf{k}}'}}e^{-is\Omega^*_{\hat{\mathbf{k}}'}}\right.\\
&+ \left.\langle s',0_{\hat{\mathbf{k}}'}|\left(\hat{f}_{\hat{\mathbf{k}}'}-\hat{g}_{\hat{\mathbf{k}}'}\right)e^{i\phi^*_E}e^{-i\Theta'^*_{\hat{\mathbf{k}}'}}e^{-is\Omega'^*_{\hat{\mathbf{k}}'}}\right]\int d\bar{\hat{\mathbf{k}}} f^\dagger_{\bar{\hat{\mathbf{k}}}}|0_{\bar{\hat{\mathbf{k}}}}\rangle\langle 0_{\bar{\hat{\mathbf{k}}}}|f_{\bar{\hat{\mathbf{k}}}}\left[e^{i\Theta_{\hat{\mathbf{k}}}}e^{is\Omega_{\hat{\mathbf{k}}}}\left(\hat{f}^\dagger_{\hat{\mathbf{k}}}+\hat{g}^\dagger_{\hat{\mathbf{k}}}\right)|0_{\hat{\mathbf{k}}},s\rangle\right.\\
&+ \left.e^{-i\phi_E}e^{i\Theta'_{\hat{\mathbf{k}}}}e^{is\Omega'_{\hat{\mathbf{k}}}}\left(\hat{f}^\dagger_{\hat{\mathbf{k}}}-\hat{g}^\dagger_{\hat{\mathbf{k}}}\right)|0_{\hat{\mathbf{k}}},s\rangle\right], \qquad (4.4.27)
\end{aligned}$$

$$\begin{aligned}
p_f &= \frac{1}{8}\sum_{s=\pm1}\sum_{s'=\pm1}\int\int\int d\hat{\mathbf{k}}d\bar{\hat{\mathbf{k}}}d\hat{\mathbf{k}}' f^*(\hat{\mathbf{k}})f(\hat{\mathbf{k}}')\left[\langle s',0_{\hat{\mathbf{k}}'}|\left(\hat{f}_{\hat{\mathbf{k}}'}+\hat{g}_{\hat{\mathbf{k}}'}\right)\hat{f}^\dagger_{\bar{\hat{\mathbf{k}}}}|0_{\bar{\hat{\mathbf{k}}}}\rangle e^{-i\Theta^*_{\hat{\mathbf{k}}'}}e^{-is\Omega^*_{\hat{\mathbf{k}}'}}\right.\\
&+ \left.\langle s',0_{\hat{\mathbf{k}}'}|\left(\hat{f}_{\hat{\mathbf{k}}'}-\hat{g}_{\hat{\mathbf{k}}'}\right)\hat{f}^\dagger_{\bar{\hat{\mathbf{k}}}}|0_{\bar{\hat{\mathbf{k}}}}\rangle e^{i\phi^*_E}e^{-i\Theta'^*_{\hat{\mathbf{k}}'}}e^{-si\Omega'^*_{\hat{\mathbf{k}}'}}\right]\left[e^{i\Theta_{\hat{\mathbf{k}}}}e^{is\Omega_{\hat{\mathbf{k}}}}\langle 0_{\bar{\hat{\mathbf{k}}}}|f_{\bar{\hat{\mathbf{k}}}}\left(\hat{f}^\dagger_{\hat{\mathbf{k}}}+\hat{g}^\dagger_{\hat{\mathbf{k}}}\right)|0_{\hat{\mathbf{k}}},s\rangle\right.\\
&+ \left.e^{-i\phi_E}e^{i\Theta'_{\hat{\mathbf{k}}}}e^{is\Omega'_{\hat{\mathbf{k}}}}\langle 0_{\bar{\hat{\mathbf{k}}}}|\hat{f}_{\bar{\hat{\mathbf{k}}}}\left(\hat{f}^\dagger_{\hat{\mathbf{k}}}-\hat{g}^\dagger_{\hat{\mathbf{k}}}\right)|0_{\hat{\mathbf{k}}},s\rangle\right], \qquad (4.4.28)
\end{aligned}$$

where

$$\langle 0_{\hat{\mathbf{k}}'}|\hat{f}_{\hat{\mathbf{k}}'}\hat{f}^\dagger_{\hat{\mathbf{k}}}|0_{\hat{\mathbf{k}}},s\rangle = \delta^{(3)}(\hat{\mathbf{k}}'-\hat{\mathbf{k}})|s\rangle = \delta_{\bar{\mathbf{k}}',\bar{\mathbf{k}}}|s\rangle. \qquad (4.4.29)$$

For convenience we denote $\delta^{(3)}(\bar{\mathbf{k}}'-\bar{\mathbf{k}}) \equiv \delta_{\hat{\mathbf{k}}',\hat{\mathbf{k}}}$, so that

$$\begin{aligned}
p_f =& \frac{1}{8}\sum_{s=\pm1}\sum_{s'=\pm1}\int\int\int d\hat{\mathbf{k}}d\bar{\hat{\mathbf{k}}}d\hat{\mathbf{k}}' f^*(\hat{\mathbf{k}})f(\hat{\mathbf{k}}')\left[\langle s'|e^{-i\Theta^*_{\hat{\mathbf{k}}'}}e^{-is'\Omega^*_{\hat{\mathbf{k}}'}}\delta_{\hat{\mathbf{k}}',\bar{\hat{\mathbf{k}}}}\right.\\
&\left.+\,\langle s'|e^{-i\phi^*_E}e^{-i'\Theta'^*_{\hat{\mathbf{k}}'}}e^{-is\Omega'^*_{\hat{\mathbf{k}}'}}\delta_{\hat{\mathbf{k}}',\bar{\hat{\mathbf{k}}}}\right]\left[\delta_{\hat{\mathbf{k}},\bar{\hat{\mathbf{k}}}}e^{i\Theta_{\hat{\mathbf{k}}}}e^{is\Omega_{\hat{\mathbf{k}}}}|s\rangle+\delta_{\hat{\mathbf{k}},\bar{\hat{\mathbf{k}}}}e^{i\phi_E}e^{i\Theta'_{\hat{\mathbf{k}}}}e^{is\Omega'_{\hat{\mathbf{k}}}}|s\rangle\right].
\end{aligned} \qquad (4.4.30)$$

Then,

$$p_f = \frac{1}{8}\sum_{s=\pm1}\sum_{s'=\pm1}\int\int\int d\hat{\mathbf{k}}d\bar{\hat{\mathbf{k}}}d\hat{\mathbf{k}}' f^*(\hat{\mathbf{k}})f(\hat{\mathbf{k}}')\Big[\langle s'|s\rangle e^{-i\Theta^*_{\hat{\mathbf{k}}'}}e^{-is'\Omega^*_{\hat{\mathbf{k}}'}}e^{i\Theta_{\hat{\mathbf{k}}}}e^{is\Omega_{\hat{\mathbf{k}}}}\delta_{\hat{\mathbf{k}}',\bar{\hat{\mathbf{k}}}}\delta_{\hat{\mathbf{k}},\bar{\hat{\mathbf{k}}}}$$
$$+\langle s'|s\rangle e^{i\phi^*_E}e^{-i\Theta'^*_{\hat{\mathbf{k}}'}}e^{-is'\Omega'^*_{\hat{\mathbf{k}}'}}e^{i\Theta_{\hat{\mathbf{k}}}}e^{is\Omega_{\hat{\mathbf{k}}}}\delta_{\hat{\mathbf{k}}',\bar{\hat{\mathbf{k}}}}\delta_{\hat{\mathbf{k}},\bar{\hat{\mathbf{k}}}}+\langle s'|s\rangle e^{-i\Theta^*_{\hat{\mathbf{k}}'}}e^{-is'\Omega^*_{\hat{\mathbf{k}}'}}e^{i\Theta'_{\hat{\mathbf{k}}}}e^{is\Omega'_{\hat{\mathbf{k}}}}e^{-i\phi_E}\delta_{\hat{\mathbf{k}}',\bar{\hat{\mathbf{k}}}}\delta_{\hat{\mathbf{k}},\bar{\hat{\mathbf{k}}}}$$
$$+\langle s'|s\rangle e^{i\phi^*_E}e^{-i'\Theta'^*_{\hat{\mathbf{k}}'}}e^{-is\Omega'^*_{\hat{\mathbf{k}}'}}e^{i\phi_E}e^{i\Theta'_{\hat{\mathbf{k}}}}e^{is\Omega'_{\hat{\mathbf{k}}}}\delta_{\hat{\mathbf{k}}',\bar{\hat{\mathbf{k}}}}\delta_{\hat{\mathbf{k}},\bar{\hat{\mathbf{k}}}}\Big]. \tag{4.4.31}$$

Integrating in $\bar{\hat{\mathbf{k}}}$ and $\hat{\mathbf{k}}'$

$$p_f = \frac{1}{8}\sum_{s=\pm1}\sum_{s'=\pm1}\int d\hat{\mathbf{k}}|f(\hat{\mathbf{k}})|^2\Big[\langle s'|s\rangle e^{-i(\Theta^*_{\hat{\mathbf{k}}}-\Theta_{\hat{\mathbf{k}}})}e^{-is'\Omega^*_{\hat{\mathbf{k}}}}e^{is\Omega_{\hat{\mathbf{k}}}}+\langle s'|s\rangle e^{i\phi^*_E}e^{-i(\Theta'^*_{\hat{\mathbf{k}}}-\Theta_{\hat{\mathbf{k}}})}e^{-is'\Omega'^*_{\hat{\mathbf{k}}}}e^{is\Omega_{\hat{\mathbf{k}}}}$$
$$+\langle s'|s\rangle e^{-i(\Theta^*_{\hat{\mathbf{k}}}-\Theta'_{\hat{\mathbf{k}}})}e^{-is'\Omega^*_{\hat{\mathbf{k}}}}e^{is\Omega'_{\hat{\mathbf{k}}}}e^{-i\phi_E}+\langle s'|s\rangle e^{-i(\Theta'^*_{\hat{\mathbf{k}}}-\Theta'_{\hat{\mathbf{k}}})}e^{-is'\Omega'^*_{\hat{\mathbf{k}}}}e^{is\Omega'_{\hat{\mathbf{k}}}}e^{i(\phi^*_E-\phi_E)}\Big] \tag{4.4.32}$$

The state of helicity and the respective phase is given by

$$\frac{1}{\sqrt{2}}\sum_{s=\pm1}e^{is\Omega}|s\rangle = \frac{1}{\sqrt{2}}\left(e^{i\Omega}|+1\rangle + e^{-i\Omega}|-1\rangle\right). \tag{4.4.33}$$

Then, the inner product of helicity states

$$\frac{1}{2}\sum_{s=\pm1}\sum_{s'=\pm1}\langle s'|s\rangle e^{-is'\Omega'^*_{\hat{\mathbf{k}}}}e^{is\Omega'_{\hat{\mathbf{k}}}} =$$
$$= \frac{1}{2}\left(\langle+1|e^{-i\Omega'^*}+\langle-1|e^{i\Omega'^*}\right)\left(e^{i\Omega'}|+1\rangle+e^{-i\Omega'}|-1\rangle\right)$$
$$= \frac{1}{2}\left(e^{-i(\Omega'^*-\Omega')}+e^{i(\Omega'^*-\Omega')}\right) \tag{4.4.34}$$
$$= \cos\left(\Omega'^*_{\hat{\mathbf{k}}}-\Omega'_{\hat{\mathbf{k}}}\right). \tag{4.4.35}$$

Therefore, the probability of detection (4.4.32) becomes

$$p_f = \frac{1}{4}\int d\hat{\mathbf{k}}|f(\hat{\mathbf{k}})|^2\Big[e^{-i(\Theta^*_{\hat{\mathbf{k}}}-\Theta_{\hat{\mathbf{k}}})}\cos\left(\Omega^*_{\hat{\mathbf{k}}}-\Omega_{\hat{\mathbf{k}}}\right)+e^{i\phi^*_E}e^{-i(\Theta'^*_{\hat{\mathbf{k}}}-\Theta_{\hat{\mathbf{k}}})}\cos\left(\Omega'^*_{\hat{\mathbf{k}}}-\Omega_{\hat{\mathbf{k}}}\right)$$
$$+e^{-i(\Theta^*_{\hat{\mathbf{k}}}-\Theta'_{\hat{\mathbf{k}}})}e^{-i\phi_E}\cos\left(\Omega^*_{\hat{\mathbf{k}}}-\Omega'_{\hat{\mathbf{k}}}\right)+e^{-i(\Theta'^*_{\hat{\mathbf{k}}}-\Theta'_{\hat{\mathbf{k}}})}e^{i(\phi^*_E-\phi_E)}\cos\left(\Omega'^*_{\hat{\mathbf{k}}}-\Omega'_{\hat{\mathbf{k}}}\right)\Big]. \tag{4.4.36}$$

The time delay phase and Wigner phase are real, then the probability becomes

$$p_f = \frac{1}{4}\int d\hat{\mathbf{k}}|f(\hat{\mathbf{k}})|^2 \left[1 + e^{i(\phi_E^* - \phi_E)} + e^{i\phi_E^*}e^{-i(\Theta'_{\hat{\mathbf{k}}}-\Theta_{\hat{\mathbf{k}}})}\cos\left(\Omega'_{\hat{\mathbf{k}}} - \Omega_{\hat{\mathbf{k}}}\right) + e^{-i(\Theta_{\hat{\mathbf{k}}}-\Theta'_{\hat{\mathbf{k}}})}e^{-i\phi_E}\cos\left(\Omega_{\hat{\mathbf{k}}} - \Omega'_{\hat{\mathbf{k}}}\right)\right]. \quad (4.4.37)$$

The phase ϕ_E is real, we obtain

$$p_f = \int d\hat{\mathbf{k}}|f(\hat{\mathbf{k}})|^2 \left[\frac{1}{2} + \frac{1}{4}\cos\left(\Omega'_{\hat{\mathbf{k}}} - \Omega_{\hat{\mathbf{k}}}\right)\left(e^{-i(\Theta'_{\hat{\mathbf{k}}}-\Theta_{\hat{\mathbf{k}}}+\phi_E)} + e^{i(\Theta'_{\hat{\mathbf{k}}}-\Theta_{\hat{\mathbf{k}}}+\phi_E)}\right)\right].$$

Finally, we find

$$p_f = \frac{1}{2}\left[1 + \int d\hat{\mathbf{k}}|f(\hat{\mathbf{k}})|^2 \cos\left(\Omega_{\hat{\mathbf{k}}} - \Omega'_{\hat{\mathbf{k}}}\right)\cos\left(\Theta_{\hat{\mathbf{k}}} - \Theta'_{\hat{\mathbf{k}}} + \phi_E\right)\right], \quad (4.4.38)$$

which is similar for the case of massive particles with inner degrees of freedom [69]. In this case the modulation comes from the terms $\Delta\vartheta = \Omega_{\hat{\mathbf{k}}} - \Omega'_{\hat{\mathbf{k}}}$, which correspond to the difference of the Wigner phase between the paths of the interferometer. The argument of the second cosine function is given by the difference of arrival time phase $\Delta\vartheta^\tau := \Theta_{\hat{\mathbf{k}}} - \Theta'_{\hat{\mathbf{k}}} + \phi_E$ and the accumulated phase by the action of the mirrors and controllable local phases.

If we assume that $f(\hat{\mathbf{k}})$ has a Gaussian distribution centered at ω and with spectral width σ then the probability of detection Eq. (4.4.38) becomes

$$P_\pm = \frac{1}{2} \pm \exp\left\{\left(-(\sigma/\omega)^2(\Delta\vartheta^\tau)^2\right)\right\}\cos\left(\Delta\vartheta^\tau\right)\cos\left(\Delta\vartheta\right), \quad (4.4.39)$$

As we can see from Eq. (4.4.39) if we neglect the term corresponding to the Wigner phase difference, then the probability reduces to $p = \frac{1}{2} \pm \exp\{(-(\sigma/\omega)^2(\Delta\vartheta^\tau)^2)\}\cos\left(\Delta\vartheta^\tau\right)$ which in this case is similar to the obtained by Zych *et al.* [44] where the term $\exp\{(-(\sigma/\omega)^2(\Delta\vartheta^\tau)^2)\}$ produces a damping in the probability of detection if we increase $\Delta\vartheta^\tau$ for a fixed ω and σ. Moreover, the term corresponding to the second cosine function $\cos\left(\Delta\vartheta\right)$ shows the coupling of the metric elements (such the rotation a and mass parameter m, in case of the Kerr metric) to the photon helicity, this result is similar to the obtained by Zych *et al.* [69] where the inner degrees of freedom couple to the gravitational potential and in a interferometric context there is a modulation in the probability of detection, and they produce a drop in the interferometric visibility. In our

case, Eq. (4.4.39) shows these two combined effects, that is, a damping in the probability of detection plus an induced gravitational phase shift and a damping that comes from the coupling of helicity to the gravitational source.

To see the effect of the Kerr metric in the probability of detection, we calculate the Wigner phase rotation and gravitational redshift in the slow and weak rotation limit considering Eqs. (4.4.20) and (4.4.22). For this limit, we plot the difference between the probabilities of the output ports $P_+ - P_-$ if we rigidly transport the interferometer. In Fig. 4.4.6 we can see how that difference decreases if we increase the distance between the arms of the interferometer; the effect is more notorious for a wider frequency dispersion σ. This shows that we have to consider different configurations in the photon source in order to see the effect of the Kerr rotation parameter.

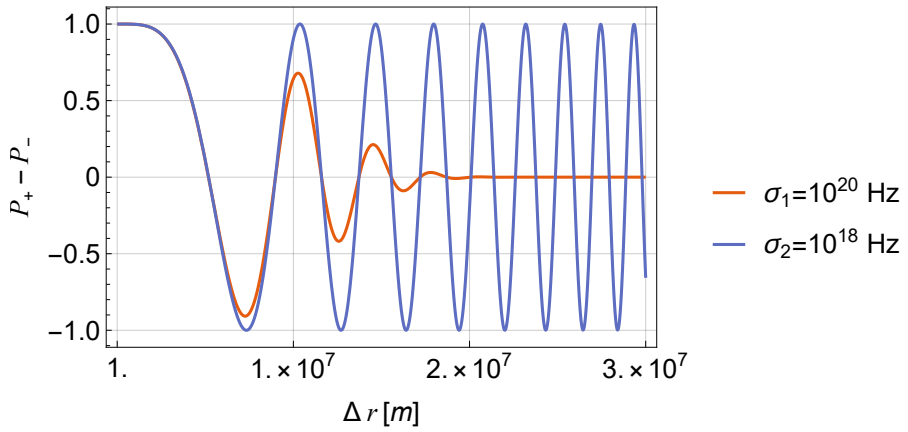

Figure 4.4.6: Plot of the probability difference between output ports, $P_+ - P_-$, versus the distance between the interferometer arms Δr [m]. The curves represent different frequency dispersions: $\sigma_1 = 10^{20}\,\text{Hz}$ (red solid line) and $\sigma_2 = 10^{18}\,\text{Hz}$ (blue solid line).

4.4.4 Estimation of the rotation parameter

In this section we consider the probability of detection Eq. (4.4.38) in order to estimate the Kerr rotation parameter. To accomplish this task, consider that the probability is given by

$$p = 1/2 \pm \exp\left\{\left(-(\sigma/\omega)^2 \Delta(\vartheta^\tau)^2\right)\right\} \cos\left(\Delta\vartheta\right) \cos\left(\Delta\vartheta^\tau + \phi_{\text{E}}\right). \tag{4.4.40}$$

Then, considering that for the contributions of the gravitational redshift Eq. (4.2.14) $\Delta\vartheta^\tau \ll 1$, the Wigner phase difference Eq. (4.4.22) $\Delta\vartheta \ll 1$ and the

product $(\sigma/\omega)\Delta\vartheta^{\tau} \ll 1$, the probability of detection becomes

$$p = ((\sigma/\omega)^2(\Delta\vartheta^{\tau})^2)/4+(\Delta\vartheta)^2/4+(\Delta\vartheta^{\tau})^2/4+O((\sigma/\omega)\Delta\vartheta^{\tau})^3)+O(\Delta\vartheta^{\tau})^3+O(\Delta\vartheta)^3. \tag{4.4.41}$$

Therefore, to estimate the a parameter in the Kerr metric in the slow rotation and weak field limit we have to consider the next experimental scenario: the photon propagates in the geodesic superposition (as was described in the above section), until obtaining an interference pattern which the probability is described by Eq. (4.4.39). Obtaining p we can obtain the value of a, in this case we have to solve the following equation

$$p = 1 - a^4\left(\frac{8h^2l^2\sigma^2}{c^4r_2^6} + \frac{4h^2l^2\omega^2}{c^4r_2^6}\right) - a^2\frac{(4m^2h^2l^2\cos^2\theta)}{r_2^8}, \tag{4.4.42}$$

where $a^2\left(4m^2h^2l^2\cos^2\theta\right)/r_2^8$ is the contribution of Wigner phase. Thus, the parameter a has the following form

$$a = \pm\frac{1}{\sqrt{2}}\sqrt{\frac{c^2\sqrt{c^4h^2l^2m^4\cos^4(\theta) - (p-1)r_2^{10}\left(2\sigma^2+\omega^2\right)}}{hlr_2^2\left(2\sigma^2+\omega^2\right)} - \frac{c^4m^2\cos^2\theta}{r_2^2\left(2\sigma^2+\omega^2\right)}}.$$

To estimate the uncertainty δa, we calculate using a simple error propagation the relative error $\delta a/a$, which in this case is a very long expression. In Fig.4.4.7, we plot the relative error $\delta a/a$ in terms of $\Delta r := r_3 - r_1$, if we increase Δr the relative error decreases until order $\sim 10^{-6}$ for $\delta p = 10^{-14}$. The radial coordinate of photon source is $r_2 = 1.5 \times 7 \times 10^6$m

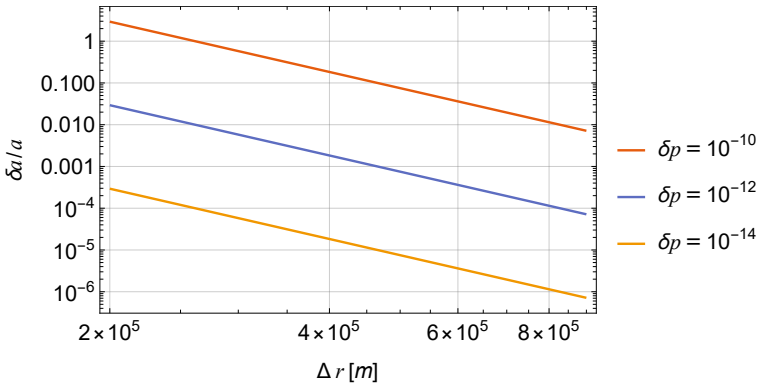

Figure 4.4.7: Relative error of the parameter a Eq. (4.4.4) in terms of distance distance between bottom and top radial coordinate Δr and for different uncertainties in the probability. The red continuous line correspond to $\delta p = 10^{-10}$, the blue continuous line to $\delta p = 10^{-12}$ and the yellow continuous line to $\delta p = 10^{-14}$.

4.5 Conclusions

This work studied the application of gravity-induced quantum phenomena, specifically relative time dilation and the Wigner rotation of photon polarization, as resources for quantum metrology in the Kerr spacetime. A model for a geodesic interferometer was developed, and the phases accumulated by a single photon traveling distinct paths in superposition were calculated. Using the adapted tetrad formalism and working within the weak-field and slow-rotation limit, analytical expressions were derived for the arrival time difference ($\Delta\vartheta^{\tau}$) and the Wigner phase difference ($\Delta\vartheta$) between the interferometer arms. The detection probability at the output ports was calculated, demonstrating the dependence of the interference on both the arrival time difference (with a damping factor dependent on the spectral width σ) and the Wigner phase, which couples the photon helicity to the metric parameters (m and a). This result highlights the system's potential for detecting subtle gravitational effects. Finally, the potential of the interferometer for estimating the Kerr rotation parameter, a, was analyzed. An expression for a as a function of the measured probability was derived, and the relative uncertainty $\delta a/a$ was evaluated through error propagation. Numerical results indicate that significant precision in estimating a is theoretically achievable, improving with decreased distance from the gravitational source, larger interferometer size, and higher precision in probability measurement.

In future work, it would be crucial to extend this analysis to explicitly include the impact of realistic noise sources and decoherence effects on the interference visibility and estimation precision. Investigating the optimization of the interferometer's geometric design to maximize sensitivity, as well as exploring regimes beyond the weak-field and slow-rotation approximation, could reveal new capabilities or limitations of the system. Furthermore, a detailed analysis of experimental feasibility, considering current technologies and the challenges inherent in manipulating and detecting single photons on controlled geodesic paths, along with a quantitative comparison with other techniques for measuring gravitational parameters, would strengthen the relevance of this proposal. Finally, considering the application of this formalism to other spacetime metrics or modified gravitational theories could open new avenues for testing fundamental physics.

Chapter 5

Conclusions

This thesis has explored two distinct approaches within the context of the effects of gravity on quantum systems in a semiclassical approximation. In the first investigation, we proposed two novel schemes to distinguish between different metric theories of gravity based on the post-Newtonian parameters γ and β. By employing quantum clock states and analyzing the Helstrom bound for discrimination, our theoretical results revealed the minimum lengths required to carry out such a distinction with different physical systems. While the optimal values obtained for discriminating between General Relativity and alternative theories with small deviations in γ and β are currently beyond experimental reach, our scheme lays the groundwork for future research and the development of more sensitive experimental methodologies. It is important to note that, while our analysis supports General Relativity, it is also compatible with other metric theories that share the same values of γ and β, underscoring the need to consider additional post-Newtonian parameters for complete discrimination.

In the second investigation, we focused on the application of gravity-induced quantum phenomena, specifically relative time dilation and the Wigner rotation of photon polarization, as resources for quantum metrology in the Kerr spacetime. The development of a model for a geodesic interferometer allowed us to calculate the phases accumulated by a single photon and demonstrate the dependence of the detection probability on the arrival time difference and the Wigner phase, the latter coupling the photon helicity with the Kerr metric parameters. Our theoretical analysis suggests that this type of interferometer has significant potential for high-precision estimation of the Kerr rotation parameter, a, with a relative uncertainty that improves with distance, interferometer size, and precision in probability

measurement.

Collectively, these two investigations highlight the growing importance of quantum physics as a fundamental tool for exploring the effects of gravity in the quantum realm within a semiclassical approximation. While the first investigation focuses on the theoretical discrimination of gravitational models through post-Newtonian parameters, the second proposes a concrete application of gravitational quantum effects for the metrology of astrophysical parameters. Future lines of research derived from both works, including the consideration of realistic experimental effects, the optimization of designs, and the extension to other gravitational scenarios for instance, in case of discrimination, extend our work to distinguish between several post-Newtonian parameters. In case of the Kerr metric, apply tools of metrology to find an optimal measurement strategy for the rotation parameter.

Appendix A

Spin-1 connection

The parallel transport of a vector V^μ to along to the curve $x^\mu(\lambda)$ given by the equation

$$\frac{DV^\mu}{D\lambda} \equiv \frac{dV^\mu}{d\lambda} + \frac{dx^\nu}{d\lambda}\Gamma^\mu_{\nu\rho}V^\rho \equiv 0. \tag{A0.1}$$

Where λ is an arbitrary parameter. The vector $V^\mu = V^I e^\mu_I$, the previous expression, we have

$$\frac{D\left(V^I e^{\mu_I}\right)}{D\lambda} \equiv \frac{d}{d\lambda}\left(V^I e^{\mu_I}\right) + \frac{dx^\mu}{d\lambda}\Gamma^\mu_{\nu\rho}V^I e^\rho_I = 0. \tag{A0.2}$$

Expanding, we have

$$\left(\frac{dV^I}{d\lambda}\right)e^\mu_I + V^I\frac{de^\mu_I}{d\lambda} + V^I\frac{dx^\nu}{d\lambda}\Gamma^\mu_{\nu\rho}e^\rho_I = 0 \tag{A0.3}$$

$$\left(\frac{dV^I}{d\lambda}\right)e^\mu_I + V^I\left(\frac{de^\mu_I}{d\lambda} + \frac{dx^\nu}{d\lambda}\Gamma^\mu_{\nu\rho}e^\rho_I\right) = 0. \tag{A0.4}$$

Using $d/d\lambda = (dx^\mu/d\lambda)\partial_\mu$ in the previous equation, we obtain

$$e^\mu_I\frac{dV^I}{d\lambda} + V^I\frac{dx^\nu}{d\lambda}\left(\partial_\nu e^\mu_I + \Gamma^\mu_{\nu\rho}e^\rho_I\right) = 0 \tag{A0.5}$$

$$e^\mu_I\frac{dV^I}{d\lambda} + V^I\frac{dx^\nu}{d\lambda}\left(\partial_\nu(e^\sigma_I\delta^\mu_\sigma) + \delta^\mu_l\Gamma^l_{\nu\rho}e^\rho_I\right) = 0. \tag{A0.6}$$

Where

$$V^I\frac{dx^\nu}{d\lambda}\left(\partial_\nu(e^\sigma_I\delta^\mu_\sigma) + \delta^\mu_l\Gamma^l_{\nu\rho}e^\rho_I\right) = V^I\frac{dx^\nu}{d\lambda}\left(\partial_\nu(e^\sigma_J\delta^\mu_\sigma\delta^J_I) + \delta^J_I\delta^\mu_l\Gamma^l_{\nu\rho}e^\rho_J\right) \tag{A0.7}$$

$$V^I\delta^J_I\delta^\mu_l\left(\partial_{nu}e^l_J + \Gamma^l_{\nu\rho}e^{rho}_J\right) = V^J e^\mu_I e^R_l\delta^I_R\left(\partial_\nu e^l_J + \Gamma^l_{\nu\rho}e^\rho_J\right) \tag{A0.8}$$

$$= e^\mu_I V^J\left(e^I_l\partial_\nu e^l_J + e^I_l\Gamma^l_{\nu\rho}e^\rho_J\right). \tag{A0.9}$$

Therefore, we can write

$$\frac{D}{D\lambda}\left(V^I e^\mu_I\right) = e^\mu_I \left[\frac{dV^I}{d\lambda} + V^J \frac{dx^\nu}{d\lambda}\left(e^I_l \partial_\nu e^l_J + e^I_l \Gamma^l_{\nu\rho} e^\rho_J\right)\right]. \tag{A0.10}$$

We define

$$\omega_\nu{}^I{}_J := e^I_l \partial_\nu e^l_J + \Gamma^l_{\nu\rho} e^I_J e^\rho_J. \tag{A0.11}$$

The transport equation for the components of V^μ in the tetrad basis is given by:

$$\frac{DV^I}{D\lambda} \equiv \frac{dV^I}{d\lambda} + \frac{dx^\mu}{d\lambda}\omega_\nu{}^I{}_J V^J = 0. \tag{A0.12}$$

The object $\omega_\nu{}^I{}_J$ is called one-form connection or spin-1 connection.

Bibliography

[1] W. G. Unruh. Notes on black-hole evaporation. *Phys. Rev. D*, 14:870–892, Aug 1976.

[2] M. Zych. *Quantum Systems under Gravitational Time Dilation*. Springer Theses. Springer International Publishing, Cham, S., 2017.

[3] R. Colella, A. W. Overhauser, and S. A. Werner. Observation of gravitationally induced quantum interference. *Phys. Rev. Lett.*, 34:1472–1474, Jun 1975.

[4] I. Fuentes-Schuller and R. B. Mann. Alice falls into a black hole: Entanglement in noninertial frames. *Phys. Rev. Lett.*, 95:120404, Sep 2005.

[5] A. Peres and D. R. Terno. Quantum information and relativity theory. *Rev. Mod. Phys.*, 76:93–123, Jan 2004.

[6] J. Kohlrus, J. Louko, I. Fuentes, and D. Edward Bruschi. Wigner phase of photonic helicity states in the spacetime of the earth. *arXiv preprint arXiv:1810.10502*, 2018.

[7] E. Manousakis. *Practical Quantum Mechanics: Modern Tools and Applications*. Oxford University Press, 11 2015.

[8] P. Shadbolt, J. C. F. M., A. Laing, and J. L. O'Brien. Testing foundations of quantum mechanics with photons. *Nature Physics*, 10:278–286, 2014.

[9] M. Kleinmann, H. Kampermann, T. Meyer, and D. Bruß. Physical purification of quantum states. *Phys. Rev. A*, 73:062309, 2006.

[10] J. Bae and Leong-Chuan K. Quantum state discrimination and its applications. *Journal of Physics A: Mathematical and Theoretical*, 48(8):083001, 2015.

[11] S. M. Barnett and S. Croke. Quantum state discrimination. *Adv. Opt. Photon.*, 1(2):238–278, 2009.

[12] J. A. Bergou. Discrimination of quantum states. *Journal of Modern Optics*, 57(3):160–180, 2010.

[13] S. M Barnett and S. Croke. Quantum state discrimination. *Advances in Optics and Photonics*, 1(2):238–278, 2009.

[14] D. Qiu and Lvjun L. Minimum-error discrimination of quantum states: New bounds and comparison. *arXiv preprint arXiv:0812.2378*, 2008.

[15] C. W. Helstrom. Quantum detection and estimation theory. *Journal of Statistical Physics*, 1:231–252, 1969.

[16] A.S Holevo. Statistical decision theory for quantum systems. *Journal of Multivariate Analysis*, 3(4):337–394, 1973.

[17] H. P Yuen, R. S Kennedy., and M. Lax. Optimum testing of multiple hypotheses in quantum detection theory. *IEEE Transactions on Information Theory*, 21(2):125–134, 1975.

[18] S. M. Barnett and E. Riis. Experimental demonstration of polarization discrimination at the helstrom bound. *Journal of Modern Optics*, 44(6):1061–1064, 1997.

[19] R. B. M. Clarke, V. M. Kendon, A. Chefles, S. M. Barnett, E. Riis, and M. Sasaki. Experimental realization of optimal detection strategies for overcomplete states. *Phys. Rev. A*, 64:012303, 2001.

[20] G. Waldherr, A. C. Dada, P. Neumann, F. Jelezko, E. Andersson, and J. Wrachtrup. Distinguishing between nonorthogonal quantum states of a single nuclear spin. *Phys. Rev. Lett.*, 109:180501, Nov 2012.

[21] M. A. Solís-Prosser, M. F. Fernandes, O. Jiménez, A. Delgado, and L. Neves. Experimental minimum-error quantum-state discrimination in high dimensions. *Phys. Rev. Lett.*, 118:100501, Mar 2017.

[22] G. Jaeger and A. Shimony. Optimal distinction between two non-orthogonal quantum states. *Physics Letters A*, 197(2):83–87, 1995.

[23] I.D. Ivanovic. How to differentiate between non-orthogonal states. *Physics Letters A*, 123(6):257–259, 1987.

[24] D. Dieks. Overlap and distinguishability of quantum states. *Physics Letters A*, 126(5):303–306, 1988.

[25] A. Peres. How to differentiate between non-orthogonal states. *Physics Letters A*, 128(1):19, 1988.

[26] J. M. Lee. *Introduction to Smooth Manifolds*. Springer, 2nd edition, 2013.

[27] Charles W. Misner, Kip S. Thorne, and John Archibald Wheeler. *Gravitation*. W. H. Freeman, 1973.

[28] R. M. Wald. *General Relativity*. University of Chicago Press, Chicago, 1984.

[29] S. M. Carroll. *Spacetime and Geometry: An Introduction to General Relativity*. Addison-Wesley, San Francisco, 2004.

[30] A. Einstein. Die grundlage der allgemeinen relativitätstheorie. *Annalen der Physik*, 354(7):769–822, 1916.

[31] J. B. Griffiths and J. Podolský. *Exact Space-Times in Einstein's General Relativity*. Cambridge University Press, Cambridge, 2009.

[32] K. Schwarzschild. Über das gravitationsfeld einer kugel aus inkompressibler flüssigkeit nach der einsteinschen theorie. *Sitzungsberichte der Königlich Preussischen Akademie der Wissenschaften*, pages 424–434, 1916.

[33] B. Mashhoon. Gravitoelectromagnetism: A brief review. *arXiv e-prints*, November 2003. 15 pages, no figures.

[34] Suvankar P. Gravitoelectromagnetism: Formulation. *ResearchGate*, 2019. Available online.

[35] F. de Felice and D. Bini. *Classical Measurements in Curved Space-Times*. Cambridge Monographs on Mathematical Physics. Cambridge University Press, 2010.

[36] C. M. Will. The confrontation between general relativity and experiment. *Living Reviews in Relativity*, 17(1):4, 2014.

[37] C. M. Will and Kenneth Nordtvedt, Jr. Conservation Laws and Preferred Frames in Relativistic Gravity. I. Preferred-Frame Theories and an Extended PPN Formalism. , 177:757, November 1972.

[38] H. Yuen, R. Kennedy, and M. Lax. Optimum testing of multiple hypotheses in quantum detection theory. *IEEE Transactions on Information Theory*, 21(2):125–134, 1975.

[39] C. Eling and T. Jacobson. Static post-newtonian equivalence of general relativity and gravity with a dynamical preferred frame. *Physical Review D*, 69(6):064005, March 2004.

[40] N. D. Birrell and P. C. W. Davies. *Quantum Fields in Curved Space*. Cambridge University Press, 1982.

[41] C. Lämmerzahl. A hamilton operator for quantum optics in gravitational fields. *Physics Letters A*, 203(1):12–17, 1995.

[42] P. K. Schwartz and D. Giulini. Post-newtonian corrections to schrödinger equations in gravitational fields. *Classical and Quantum Gravity*, 36(9):095016, 2019.

[43] Igor Pikovski, M. Zych, F. Costa, and Č. Brukner. Time dilation in quantum systems and decoherence. *New Journal of Physics*, 19(2):025011, feb 2017.

[44] M. Zych, F. Costa, I. Pikovski, T. C Ralph, and Č. Brukner. General relativistic effects in quantum interference of photons. *Classical and Quantum Gravity*, 29(22):224010, oct 2012.

[45] C. Cepollaro, F. Giacomini, and M. G.A. Paris. Gravitational time dilation as a resource in quantum sensing. *Quantum*, 7:946, March 2023.

[46] M. C. Palmer, M. Takahashi, and H. F. Westman. Localized qubits in curved spacetimes. *Annals of Physics*, 327(4):1078–1131, 2012.

[47] S. Kobayashi and K. Nomizu. *Foundations of Differential Geometry, Volume 1.* Wiley-Interscience, New York, 1963.

[48] K. S. Thorne and D. MacDonald. Electrodynamics in curved spacetime: 3 + 1 formulation. *Monthly Notices of the Royal Astronomical Society*, (2):339–343, 1982.

[49] L. Lorenz. On the identity of the vibrations of light with electrical currents. *Philosophical Magazine*, 34:287–301, 1867.

[50] M. C. Palmer. Relativistic quantum information theory and quantum reference frames. *arXiv: Quantum Physics*, 2013.

[51] I. Bialynicki-Birula. Exponential localization of photons. *Physical Review Letters*, 80:5247–5250, June 1998.

[52] E. S. C. Ching, P. T. Leung, W. M. Suen, and K. Young. Late-Time Tail of Wave Propagation on Curved Spacetime. , 1995.

[53] E. Poisson. *A Relativist's Toolkit: The Mathematics of Black-Hole Mechanics.* Cambridge University Press, Cambridge, UK, 2004.

[54] K P Zetie, S F Adams, and R M Tocknell. How does a mach-zehnder interferometer work? *Physics Education*, 35(1):46, jan 2000.

[55] Avijit Lahiri. Chapter 8 - quantum optics. In Avijit Lahiri, editor, *Basic Optics*, pages 697–899. Elsevier, Amsterdam, 2016.

[56] K. Zyczkowski I. Bengtsson, Stockholms Universitet. *Geometry of Quantum States.* Cambridge University Press, 2006.

[57] L. Adrián A. Rodríguez, A. Wolfgang Schell, and D. E. Bruschi. Introduction to gravitational redshift of quantum photons propagating in curved spacetime. *Journal of Physics: Conference Series*, 2531(1):012016, 2023.

[58] B. Z. Foster and T. Jacobson. Post-newtonian parameters and constraints on einstein-aether theory. *Phys. Rev. D*, 73:064015, Mar 2006.

[59] T. Clifton, P. G. Ferreira, A. Padilla, and C. Skordis. Modified gravity and cosmology. *Physics Reports*, 513(1):1–189, 2012. Modified Gravity and Cosmology.

[60] C. Brans and R. H. Dicke. Mach's principle and a relativistic theory of gravitation. *Phys. Rev.*, 124:925–935, Nov 1961.

[61] M. Roshan and F. Shojai. Notes on the post-newtonian limit of the massive brans–dicke theory. *Classical and Quantum Gravity*, 28(14):145012, jun 2011.

[62] J. Borregaard and I. Pikovski. Testing quantum theory on curved space-time with quantum networks, 2024.

[63] S. Croke, E. Andersson, S. M. Barnett, C. R. Gilson, and J. Jeffers. Maximum confidence quantum measurements. *Phys. Rev. Lett.*, 96:070401, Feb 2006.

[64] O. Jiménez, M. A. Solís-Prosser, A. Delgado, and L. Neves. Maximum-confidence discrimination among symmetric qudit states. *Phys. Rev. A*, 84:062315, Dec 2011.

[65] Chuan-Wei Zhang, Chuan-Feng Li, and Guang-Can Guo. General strategies for discrimination of quantum states. *Physics Letters A*, 261(1):25–29, 1999.

[66] Santiago Gómez, Esteban S. Gómez, Omar Jiménez, Aldo Delgado, Stephen P. Walborn, and Gustavo Lima. Experimental quantum state discrimination using the optimal fixed rate of inconclusive outcomes strategy. *Scientific Reports*, 12(1):17312, 2022.

[67] M. P. Hobson, G. P. Efstathiou, and A. N. Lasenby. *General Relativity: An Introduction for Physicists*. Cambridge University Press, 2006.

[68] O. Semerák. Stationary frames in the kerr field. *General Relativity and Gravitation*, 25:1041–1077, 1993.

[69] M. Zych, F. Costa, I. Pikovski, and Č. Brukner. Quantum interferometric visibility as a witness of general relativistic proper time. *Nature Communications*, 2:505, 2011.